1983

Sedimentation and self weight consolidation of dredge spoil

Tso-Wang Lin
Iowa State University

INFORMATION TO USERS

This reproduction was made from a copy of a document sent to us for microfilming. While the most advanced technology has been used to photograph and reproduce this document, the quality of the reproduction is heavily dependent upon the quality of the material submitted.

The following explanation of techniques is provided to help clarify markings or notations which may appear on this reproduction.

1. The sign or "target" for pages apparently lacking from the document photographed is "Missing Page(s)". If it was possible to obtain the missing page(s) or section, they are spliced into the film along with adjacent pages. This may have necessitated cutting through an image and duplicating adjacent pages to assure complete continuity.

2. When an image on the film is obliterated with a round black mark, it is an indication of either blurred copy because of movement during exposure, duplicate copy, or copyrighted materials that should not have been filmed. For blurred pages, a good image of the page can be found in the adjacent frame. If copyrighted materials were deleted, a target note will appear listing the pages in the adjacent frame.

3. When a map, drawing or chart, etc., is part of the material being photographed, a definite method of "sectioning" the material has been followed. It is customary to begin filming at the upper left hand corner of a large sheet and to continue from left to right in equal sections with small overlaps. If necessary, sectioning is continued again—beginning below the first row and continuing on until complete.

4. For illustrations that cannot be satisfactorily reproduced by xerographic means, photographic prints can be purchased at additional cost and inserted into your xerographic copy. These prints are available upon request from the Dissertations Customer Services Department.

5. Some pages in any document may have indistinct print. In all cases the best available copy has been filmed.

University
Microfilms
International
300 N. Zeeb Road
Ann Arbor, MI 48106

Lin, Tso-Wang

SEDIMENTATION AND SELF WEIGHT CONSOLIDATION OF DREDGE SPOIL

Iowa State University PH.D. 1983

PLEASE NOTE:

In all cases this material has been filmed in the best possible way from the available copy. Problems encountered with this document have been identified here with a check mark __√__.

1. Glossy photographs or pages ✓
2. Colored illustrations, paper or print ✓
3. Photographs with dark background _____
4. Illustrations are poor copy _____
5. Pages with black marks, not original copy _____
6. Print shows through as there is text on both sides of page _____
7. Indistinct, broken or small print on several pages ✓
8. Print exceeds margin requirements _____
9. Tightly bound copy with print lost in spine _____
10. Computer printout pages with indistinct print _____
11. Page(s) _____ lacking when material received, and not available from school or author.
12. Page(s) _____ seem to be missing in numbering only as text follows.
13. Two pages numbered _____. Text follows.
14. Curling and wrinkled pages _____
15. Other _____

Sedimentation and self weight consolidation of dredge spoil

by

Tso-Wang Lin

A Dissertation Submitted to the
Graduate Faculty in Partial Fulfillment of the
Requirements for the Degree of
DOCTOR OF PHILOSOPHY

Department: Civil Engineering
Major: Geotechnical Engineering

Approved:

Signature was redacted for privacy.

In Charge of Major Work

Signature was redacted for privacy.

For the Major Department

Signature was redacted for privacy.

For the Graduate College

Iowa State University
Ames, Iowa

1983

TABLE OF CONTENTS

CHAPTER I. INTRODUCTION

Problem Statement

In a hydraulic dredging project, the cost for disposing dredge material contributes a significant portion to the total cost. Dikes, grading, seeding and easements accounted for 19 to 25 percent of the total cost of recent western Iowa dredging projects. A nationwide survey showed that the disposal cost generally ranges from 15 to 20 percent of the total project cost; however, it may be as high as 35 percent if the dredging size is small (Gallagher and Company, 1978). This cost probably will go even higher in the future because of the increasing scarcity of disposal areas. The central issue is then on how to design an efficient, adequate containment for dredged materials.

Prior to 1970, the dredge spoil containments were sized assuming that the excavated material will occupy more space in a fill than in-situ because of the mechanical disturbance of dredging process and the removal of overburden pressure. Depending upon the texture of sediment to be dredged, bulking factors of 1.0 to 2.0 were applied to estimate the required volume of the facility. While this design approach was easy, uncertainty and dissatisfaction were associated with the use of these bulking factors because they depended heavily on practical experience and local conditions. It was observed that by using these factors some containments have been undersized by as much as 50 percent, and the others oversized by as much as 100 percent (Lacasse et al., 1977).

Because materials discharging into the disposal area are in a suspension of water, a scientific approach to the containment design problem requires study of the dredged materials' behavior. Sedimentation of particles has been studied for decades in many disciplines other than geotechnical engineering; these include mining and metallurgic engineering, chemical engineering and sanitary engineering. Some ideas from these other disciplines have been borrowed by geotechnical engineers and used in their containment designs. Unfortunately, most of the models proposed in these studies deal only with the "sedimentation" phenomenon in which the particle weight is solely supported by hydrodynamic forces and no effective stress exists. When the settling particles eventually come into contact to form a three-dimensional, interconnected lattice, effective stresses are developed and sedimentation models fail. Hence, studies on the settling behavior of suspensions should consider a model which includes consolidation as well as sedimentation.

Background on Dredge Slurries

Hydraulically dredged sediments are mixed with ambient water, sucked into a centrifugal pump, pushed through hundreds or even thousands of feet of pipe, and discharged into a containment at velocities of about 15 ft/sec. As a result of the mixing with water and the mechanical disturbance associated with the operations, the volume of the sediments increases; however, after sufficient time in the containment, it is possible that the materials will occupy less volume due to the disruption

of flocculent structure and consolidation.

Before 1970, the volume of dredge spoil was estimated largely by rule of thumb of multiplying a bulking factor with the volume of sediments being dredged. Generally, a value of 1.0 was assigned for sand, 1.25 for sandy clay, 1.45 for clay, 1.75 for gravel and rock, and 2.0 for silt as the bulking factor for immediate disposal (Huston, 1970). Later, the shrinkage of dredge materials due to long term settlement was considered in design, and a "settlement factor" was usually combined with the bulking factor to yield a sizing factor for the containment. According to the practice of several U.S. Army Corps of Engineers districts, the sizing factor ranges from 0.6 to 1.3 for sand and silt, and from 1.0 to 2.0 for clay (Lacasse et al., 1977). As for the determination of the detention time required to allow the solids to settle out of the water, the method employed was the same as the one used in sanitary engineering; i.e., assuming particles are spherical and settle according to Stokes' law.

This approach does not account for the fact that dredge materials will behave differently in different settling environments or under different operational concentrations. Also, clay particles are flake or plate shaped rather than spheres, and the material will eventually consolidate under its own weight. Recognizing the need for more scientific approaches to the problem of designing dredge spoil containment facilities, the U.S. Army Corps of Engineers sponsored research at Waterways Experiment Station (WES) in Vicksburg, Mississippi. Between 1975 and

1978, this research resulted in over 20 reports covering various aspects of dredge spoil containments and provided a major advance to state-of-the-art design. Palermo et al. (1978) summarized the results of the WES research and provided containment design and management guidelines.

The methodology developed by WES for design of dredge spoil containments requires both a sedimentation test and a consolidation test. Grab samples from the proposed dredge area are mixed mechanically with water to the operational concentration and pumped into a settling column. The mixing and pumping of the slurry is similar to the disturbance that the sediment experiences in the dredging operation, whereas the behavior of the slurry in the column simulates conditions in the containment area. The settlement of the slurry sample in the column is observed periodically, and after sedimentation has finished, samples are taken from slurry at the bottom of the column for a consolidation test.

To explain the sedimentation behavior, the WES has used the terminology from mining engineering (Fitch, 1962) in which the settling is classified into three categories according to the degree of solid concentration and interparticle cohesiveness: 1) discrete settling, 2) flocculent settling, and 3) zone settling. In discrete settling, particles settle individually with constant rate, whereas in flocculent settling particles agglomerate to form flocs and settling rate increases with time. In zone settling, particles agglomerate further and settle as a three-dimensional lattice. Because the concentration in most dredging operations average as high as 145 g/l (Montgomery, 1978), dis-

crete settling seldom occurs. According to the WES approach, if an interface between settling solids and the clear, supernatant water is formed during the test, the phenomenon is said to be in zone settling. The design criterion is then based on the work by Coe and Clevenger (1916). If no sharp interface is formed, the slurry is said to be in flocculent settling, and the design criterion is based upon the approach proposed by Mclaughlin (1959). Both criteria are used to design containments with sufficient areas and detention times to accommodate continuous dredge disposal activities and remove sufficient suspended solids. As for the consolidation analysis, the WES approach requires the sediment samples used in the settling tests also be subjected to consolidation tests. The test procedure is the same as the conventional consolidation test except that very low loading stresses are used. The results are interpreted according to one-dimensional consolidation theory (Terzaghi, 1925) to estimate the volume and time rate of the dredge material's consolidation under its own weight.

The development of self weight consolidation theory (Gibson et al., 1967; Lee and Sills, 1981) provides a refinement for describing the settlement mechanism and should result in a more rational containment design approach. The self weight consolidation theory differs from conventional one-dimensional consolidation theory in two distinct aspects: 1) no external load is applied to induce settlement; gravitation is the only driving force and 2) large strains occur in the process. Because the dredge material always experiences a large amount of strain during

consolidation, the assumption that the soil boundaries are fixed, as in the conventional consolidation theory, does not hold. Thus, the self weight consolidation theory should predict the material settling better if used in the WES approach.

Several researchers (Fitch, 1962; Gaudin and Fuerstenau, 1962; Michaels and Bolger, 1962) observed that in zone settling there was no jockeying for position by the particles, and the material settled as a plastic structure. If all the settling particles are locked into a three-dimensional lattice when zone settling starts, it is reasonable to conclude that consolidation process also begins at this moment. The existence of the lattice implies the existence of effective stresses. Although experimental proof of the existence of effective stress is quite difficult, the observed zone settling behavior is similar to that predicted by self weight consolidation theory. This suggests that the zone settling phenomenon can be described and analyzed according to the self weight consolidation theory which is in contrast to interpretations made in previous research. This alternative to the WES approach should put the settling column tests on a more rational basis and result in more accurate estimates of the time rate of settlement. Another implication of this hypothesis is that the results of the settling column tests can be directly used to predict the long term settlement behavior of the spoil thereby removing the need for conventional consolidation tests.

Literature Review

The sedimentation mechanism of a solid water system has been studied for more than a century since the pioneer work done by Stokes. Generally, the study has advanced in three major fields: mining and metallurgic engineering to treat ore pulp, chemical engineering to examine chemical precipitation, and sanitary engineering to handle sludge or solid waste. The developments in these disciplines are useful for studying the settling behavior of the dredge materials; therefore, pertinent literature from these three fields is reviewed and synthesized in the following paragraphs. The model for flocculent and zone settling deal only with the sedimentation process and fail to include the consolidation process. To provide a more complete study, literature on self weight consolidation theory is also incorporated in the review.

Coe and Clevenger (1916) were the first to describe the flocculent settling phenomenon. They assumed that shortly after a settling test starts, four distinct zones are formed as shown in Figure 1.1. From top to bottom they are:

A. Zone of clear water

B. Zone of constant concentration which settles at a constant rate

C. Transition zone with concentration decreasing from the bottom (top of zone D) to the top (bottom of zone B)

D. Compression zone in which the flocs are brought so close together that they rest directly upon one another, and further elimination of water is a function of time.

Figure 1.1 shows the development of these four zones at various stages of a settling test. Because of the marked concentration difference between A and B, an interface forms, as indicated in Figure 1.1 (II). The settling of the interface manifests the behavior of zone B until B diminishes (II, III, IV). After C has disappeared (V), the whole system undergoes a compression process (called "consolidation" elsewhere in this study), and eventually stops settling (VI). To explain this mechanism, Coe and Clevenger (1916) postulated that any layer has a capacity of discharging solids corresponding to its concentration and settling velocity. If the layer has a lower discharge capacity than the overlying layer, the layer will gain solids and expand its thickness and eventually dominate the settling behavior of the whole system unless the supply-discharge trend is changed. Coe and Clevenger prescribed a series of batch settling tests at various concentrations to obtain the concentration vs. settling rate relationship from which the solids discharging capacity could be calculated, and the design of an ore pulp thickener is to provide sufficient area to assure that the supply rate of solids is less than the discharge capacity of the limiting layer. Conceptually, the Coe and Clevenger approach is based upon the continuity equation. In a continuous pulp thickener, a steady state usually occurs, and different zones maintain constant positions and concentrations. In this type of thickener, the concept of solids discharging capacity is then suitable for describing the settling behavior of material. In a thickener where bottom withdrawal is not possible and concentration varies with

time and position, this approach is not useful.

A mathematical formulation for the thickening mechanism was derived by Kynch (1952) on the bases that the settling rate, v, of particles depends on the local concentration c, particles are of same size and shape, and no flocculation occurs. The concentration term, c, was defined as the number of particles per unit volume of the dispersion.

Using the continuity equation, Kynch (1952) mathematically showed that any concentration layer in the settling column can propagate upwards with a velocity, U, according to $U = -ds/dc$, where s is the particle flux, which is defined as the number of particles crossing a horizontal section per unit area per unit time, or $s = cv$. If the settling velocity of particles is a function of concentration, c, only, the particle flux, s, and therefore the propagating rate U, is also a function of c only. Because the original concentration is preserved when the layer propagates through the suspension, the resulting path will be linear in the height (H) - time (t) coordinates indicating a constant U (Figure 1.2).

During the settling test, both the particles and the interface are falling, while the concentration layers are moving upwards. Thus, all the particles, originally between the interface and a certain layer, will fall through that layer when the layer meets the interface. Using this concept, the settling behavior of the interface can be predicted. Kynch (1952) showed that if a settling column test starts out with a uniform initial concentration, c_i, all the upward propagating paths are

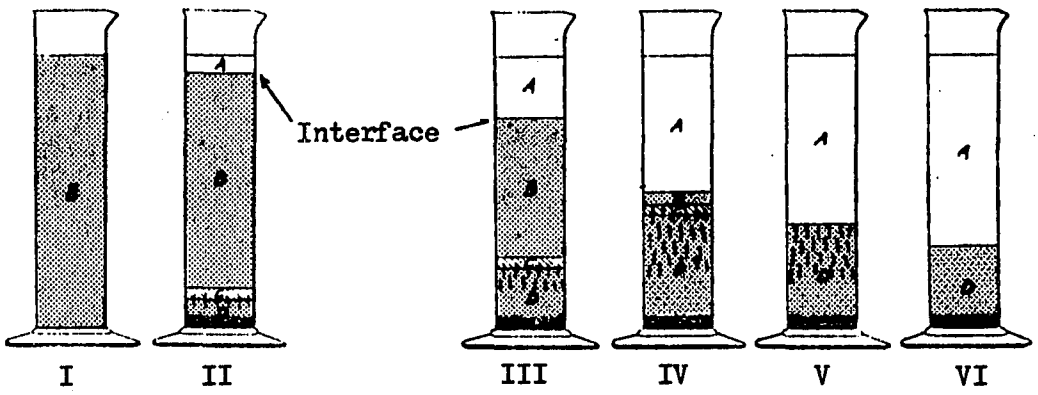

Figure 1.1. Four settling zones at various stages of a settling test (after Coe and Clevenger, 1916)

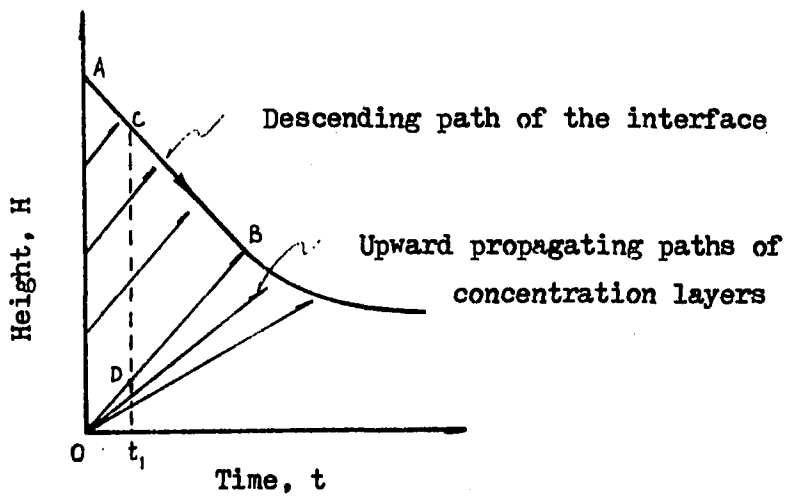

Figure 1.2. Motion of the interface and concentration layers in a uniform c_i test, according to Kynch theory

parallel, and the concentration in the sector AOB of Figure 1.2 is everywhere c_i, which results in a linear H vs. t plot AB of the falling interface. After point B, some higher concentration layer reaches the interface, the H vs. t plot then becomes curved, and the descent of the interface slows. Many researchers (Gaudin et al., 1959; Fitch, 1962), however, found that the H vs. t plots were strongly curved even at the beginning of the tests. In the author's study, a linear H vs. t relationship occurs only in the initial portion of some tests with low initial concentration of solids. This deficiency of the Kynch theory is that the theory works with the particle and layer velocities in a purely mathematical fashion and neglects physical phenomemon. For example, in Figure 1.2, the concentration profile at time t_1 is idealized as uniform from the interface, C, to certain depth, D, by the Kynch approach, whereas in real tests it seldom happens this way (e.g., see Been and Sills, 1981). Also, depending on the c_i, the dredge material will settle either as flocs or as a three-dimensional lattice structure, but not as individual particles. The applicability of Kynch theory seems rather doubtful.

Talmage and Fitch (1955) applied Kynch theory to the design of thickeners. For many years, this procedure has been used for thickener design in many disciplines. They assumed that a layer of any concentration, $c_1 > c_i$, is formed instantaneously at the bottom of the column at the onset of thickening. If the layer reaches the slurry-water interface, all solids in the column must have been "sieved" through this layer.

According to this argument, a simple material balance equation can be made, and from a single settling column test result, the c vs. v relationship can then be obtained, and the thickener design is possible. This approach implies that the settling curve is unique for a given material; i.e., the settling behavior of high c_i suspension can be obtained from the later portion of the low c_i test. As will be discussed in Chapter III, this is not supported by most of the author's tests on lake sediment. In addition, the concentration of the bottom layer gradually increases with time due to particle accumulation, instead of being instantly achieved.

Talmage and Fitch (1955) also compared the Kynch approach with the Coe and Clevenger method and found that the two methods agree in the low concentration range but diverge as concentration increases. This divergence, by their argument, was attributed to (Talmage and Fitch, 1955):

> The Coe and Clevenger test procedure, however, entails an additional assumption which is not necessarily valid and which is not contained in application of the Kynch analysis. The Coe and Clevenger test procedure ... assumes that the settling characteristics of the floc will be independent of the initial solids concentration in the pulp in which they are formed.

Therefore, Talmage and Fitch concluded that the Kynch approach is preferable. However, Coe and Clevenger prescribed a series of batch settling tests that result in an initial concentration vs. settling rate relationship. On the contrary, the Kynch approach inherits the assumption that

the settling characteristics of the floc are independent of the initial concentration because it generates the c vs. v relationship from only one settling column test result. The assertion and conclusion made by Talmage and Fitch does not seem correct.

Fitch (1962) classified the settling behavior of slurries into four categories according to the degree of solid concentration and interparticle cohesiveness:

A. Clarification, Class 1: is called discrete settling elsewhere. It occurs when no interparticle cohesiveness exists; e.g., sands and gravels, or cohesive particles at extremely low concentrations. Individual particles then settle independently at a constant rate.

B. Clarification, Class 2: is equivalent to the flocculent settling. It occurs when the interparticle agglomeration tendency is high, but the concentration is low. Particles agglomerate to form flocs during settling and the settling rate of flocs constantly changes.

C. Zone settling: occurs when both the concentration and the interparticle cohesiveness are high. Particles are locked into a plastic structure and subside at the same rate.

D. Compression: i.e., consolidation, occurs when the concentration is so high that the particle weight is no longer supported solely by hydrodynamic force, but by particles underneath as well, following the Coe and Clevenger's definition. The transmission of force through particle contacts in turn puts the solids structure in a compression state and causes settling.

The factors governing the removal of solids were also studied by Fitch. Using experimental evidence, he found that Kynch's assumption is not completely valid over the entire zone settling regime, and it is not valid at all in the consolidation regime. Therefore, Fitch (1962) concluded that the Coe and Clevenger approach seems preferable, although he did it

reversely in 1955.

The first nondestructive concentrations measuring device, named "Transviewer" was constructed by Gaudin and Fuerstenau (1958). This instrument enables researchers to more precisely measure the concentration at any specific time and location in the settling column test. The settling behavior of the material can then be studied without extracting any slurry for concentration measurements. The theory of the device is that when X-rays are sent through a suspension, part of their intensity will be lost due to the absorption of the suspension. A counter is used to pick up the quantity of X-rays transmitted, which theoretically is related to the density, γ, of the suspension as: $I = I_o \exp(-\mu_m \cdot \gamma \cdot d)$, where μ_m is the mass absorption coefficient which is a function of the atomic numbers of constituent elements of the solids, d the diameter of the column, I_o the reference intensity, I the intensity recorded. If the energy level of the incident X-rays is kept high and stable enough, the dependence on atomic number can be neglected. The transmitted X-ray intensity is then uniquely related to the density of the suspension, and the concentrations can be easily obtained by the readings recorded by the counter. A problem concerning the use of the X-ray Transviewer is that one has to compromise between the travelling speed of the X-ray and the time constant of the counter in order to obtain a satisfactory measuring accuracy and spatial resolution combination. Nevertheless, the settling mass in this case is not disturbed by the insertion of measuring device or by the removal of solution for concentration measurement as in conventional tests.

Using the Transviewer, Gaudin and Fuerstenau (1962) observed the zone settling of a thick suspension as:

> The mass is considered to be settling as an aggregate network or as one large floc,.... Furthermore, it seems that this single floc is in a state of compression from the beginning of settling, and that two phases of compression settling exist during sedimentation. The first occurs during the early stage of settling where liquid exudes easily and rapidly from the floc, while the second occurs in the compacting portion of the floc where water escapes more slowly and with much more difficulty.

This phenomenon is identical to what is called "consolidation" in soil mechanics. Hence, zone settling behavior may be alternatively described by consolidation theory. As will be discussed later in this chapter, the variation of escaping rate of fluid (called "permeability" in soil mechanics) during consolidation can also be included using self weight consolidation theory. However, Gaudin and Fuerstenau (1962) considered it as "a filtration phenomenon in which a pulp thickens by filtration of its contained liquor through the aggregate network of pulp above it." To model these behaviors, Gaudin and Fuerstenau assumed that the consolidating body is mechanically equivalent to a deformable solid containing numerous vertical tubes and tubules where tubules are conduits with much smaller diameter than the tubes. Filtration of water through tubes is completed at an early stage, whereas flow through tubulues continues indefinitely. Since the size of tubes and tubules varies randomly, a proper size distribution function must be assigned. For this, they accepted the Schuhmann size distribution. The Schuhmann distribution is

described by the equation: $y = (x/G)^m$, where x is the tube size, y the cumulative fraction of all tubes with size between 0 and x, and G the maximum tube size. The quantity of fluid flowing through tubes can be calculated from Poiseuille's law, i.e., if a fluid with viscosity μ flows through a tube having diameter of x, the average flow rate, q, can be expressed as:

$$q = \pi \frac{dp}{dl} \frac{x^4}{128\mu} \tag{1.1}$$

where dp/dl is the pressure gradient in direction 1. Gaudin and Fuerstenau defined it to be the excess weight of solids per unit area; i.e., $dp/dl = c(G_s - 1)\gamma_w$ where c is the concentration expressed in term of percent by volume, G_s the specific gravity of the solids, and γ_w the unit weight of water. Combining Equation 1.1 with the Schuhmann distribution then integrating q as a function of x from 0 to G, the whole size range of tube diameters, a theoretical expression for the filtration rate per unit area can be obtained as:

$$Q = \frac{c(G_s - 1)\gamma_w}{32\ \mu} \frac{m}{m + 2} G^2 \tag{1.2}$$

According to Gaudin and Fuerstenau, the filtration rate of water can also be determined experimentally by the following steps. From Transviewer records, the concentration readings at any time and location can be calculated. It is then possible to draw a family of contour lines of equal concentration on the height (H) - time (t) coordinates. Concentration profiles at different time periods are provided from the Transviewer data. Because no jockeying for position by particles occurs,

the descending path for a thin layer above which a certain percentage of the total solids remain can be traced on the H-t coordinates. By doing this repeatedly for various percentages, a system of settling curves can be drawn (Figure 1.3). The settling velocity or, equivalently, the filtration rate of water, at any point is simply the slope of the settling curve at that point. The corresponding concentration value can be read from the iso-concentration lines, and the Q versus c relationship is then established.

The main difficulty in applying the Gaudin and Fuerstenau's model is that neither m, nor G can be determined independently by these test results. Gaudin and Fuerstenau (1962) suggested that assuming if m = 1.0 the maximum tube sizes, and therefore the size distributions, under different concentrations can be obtained by putting the experimental Q vs. c relationship in the theoretical expression for Q, Equation 1.2. Using the obtained size distributions, they back calculated the filtration rates, Q, for several pulp concentrations and found that the Qs agreed well with the experimental ones. Gaudin and Fuersteanu then concluded that the Schuhmann function is proper for describing the size distribution of pores. However, it is the author's opinion that their conclusion is erroneous; because the experimental Q vs. c relationship is used to determine the size distribution, and therefore it should not be reused to check the suitability of the assumed size function. Nevertheless, the tube model provides an insight into the settling mechanism. The implication of this model will be discussed in the synthesis of the

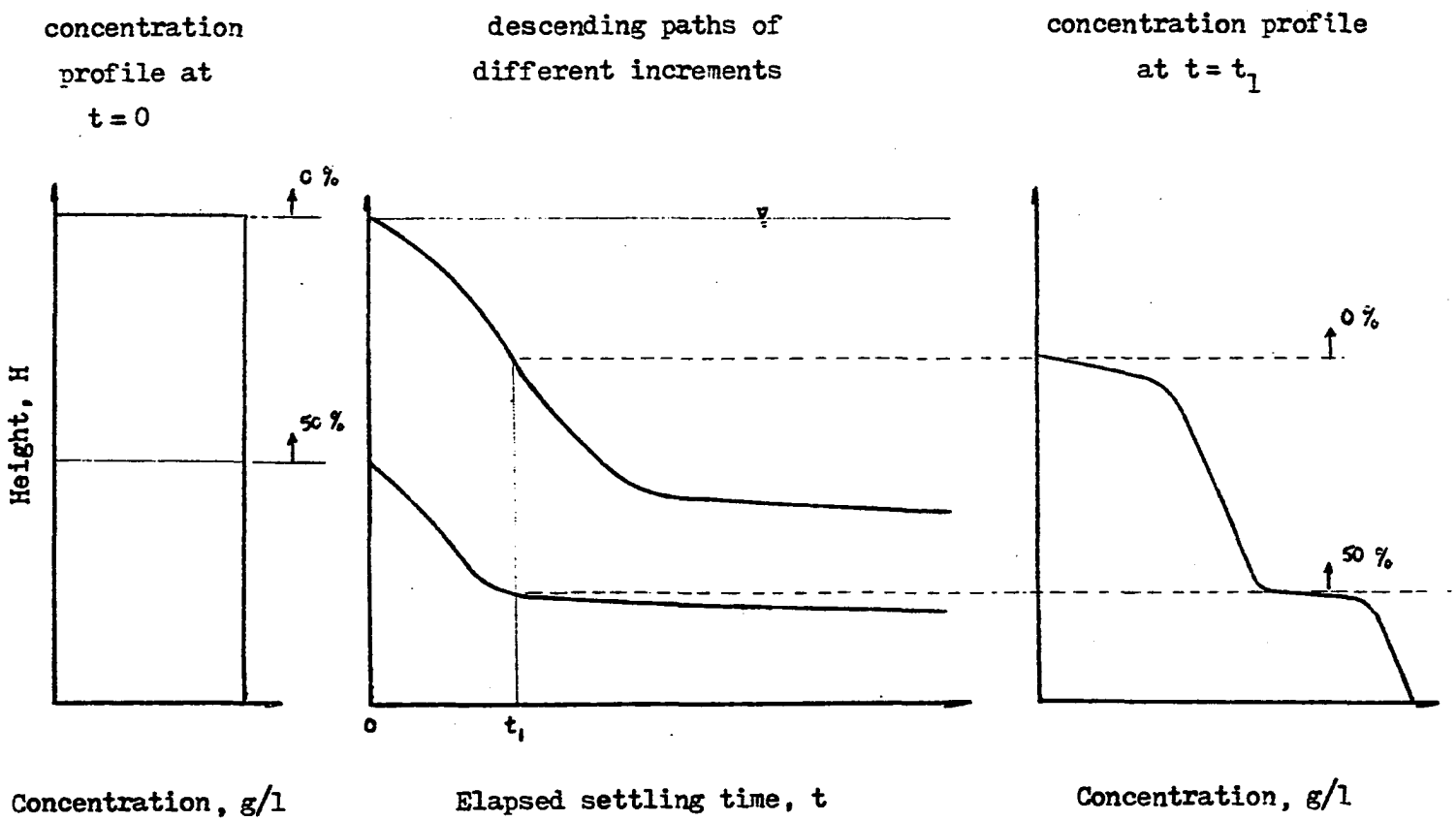

Index: ↥ a% — a% of total solid existing above this line

Figure 1.3. Construction of the descending paths for various increments

reviewed literature.

Michaels and Bolger (1962) interpreted the settling mechanism of clay minerals in terms of particle-particle interactions. Because the surface characteristics of kaolin and the microstructure it forms in a suspension have been frequently studied, flocculated kaolin suspensions were selected for their study. Michaels and Bolger postulated that the basic units in settling are not particles but flocs which have mechanical strength to resist the viscous shear and maintain their identity during settling. In a quiescent settling environment, clusters of flocs may agglomerate to form aggregates or even lattice structure depending on the local clay concentration. According to their test observations, the aggregates fall individually, roughly in spherical shape in low concentration suspension. The settling behavior can then be described by Stokes' law, but the size formed seems to be governed by two counteracting factors: the collision of aggregates which makes the size grow, and the viscous shear force in the fluid which breaks down the aggregates. Hence, it is a dynamic property, rather than a fundamental flocculation phenomenon. Using different mixing methods, they found that strong mixing usually produces large aggregates and yields higher settling rate.

Further, Michaels and Bolger tried to model the settling behavior of a high concentration suspension. They assumed that in the early settling period the concentration in the upper kaolin laden zone is constant, and the zone can be considered as a plug of slurry. The submerged

weight of the plug, F_p, is

$$F_p = \frac{\pi}{4} d^2 \Delta l \, g(\rho_s - \rho_w) \, c, \tag{1.3}$$

where d is the diameter of settling column, Δl the length of the plug, c the concentration in the plug, and F_p is supported by:

(A) resisting force of underlying material:

$$F_a = \frac{\pi}{4} d^2 \sigma_y \tag{1.4}$$

(B) shear forces at the wall:

$$F_b = \pi d \Delta l \tau_y \tag{1.5}$$

(C) force due to pressure gradient which generates the flow through plug:

$$F_c = \frac{\pi d^2}{4} \Delta l \frac{dp}{dl} \tag{1.6}$$

where σ_y and τ_y are the compressive and shear strength of the lattice structure respectively, and dp/dl is the pressure gradient. By Cozeny-Carman and Poiseuille Equations, the pressure gradient term can be expressed as:

$$\frac{dp}{dl} = C_s \mu v L_p^2 \frac{s^2}{n^3}, \tag{1.7}$$

where C_s is the shape factor of pores, L_p the tortuosity, s the specific area of pores, and n the porosity. At equilibrium condition, $F_p = F_a + F_b + F_c$. An expression for the settling velocity v can thus be obtained.

Basically, the working mechanism of the above model is similar to that of the Gaudin and Fuerstenau model, but the additional force terms, e.g., wall friction and under support, provides a means to account for the effect of column size and initial slurry height. The model predicts that the settling rate increases as the slurry height increases. The settling rate also increases with column size, though the effect is small. This, however, is contrary to the recent experimental results by Montgomery (1978). Montgomery observed that at high concentration in zone settling, column diameters less than 8 in. resulted in higher settling velocities than that in larger columns. This indicates that wall friction which retards the settling might be too small to be significant or that the wall slurry interface may provide less resistant passageways for pore water to escape. Because the rate of pore water dissipation is an indication of settling rate in the consolidation regime, the behavior observed by Montgomery suggests that zone settling is actually a self weight consolidation phenomenon.

Although some of the aforementioned researchers did notice the existence of consolidation, their models have no capability of describing it. Recently, this problem was studied by Hayden (1978) of WES. According to Hayden's argument, a high concentration suspension will pass through three distinct phases during the process of settling. The early phase is a period of agglomeration which results from particle flocculation. If the height of the slurry-supernatant water interface, H, in this period is plotted against time, t, with H as the ordinate and

t as the abscissa, a convex upward relationship will result, indicating an acceleration in the settling rate. The second phase consists of zone settling when the interface height varies linearly with time. The period of constant settling is then followed by a transition period. After that, the whole slurry enters into the last phase of consolidation. The settling behavior of the material in the last phase is governed by one-dimensional consolidation theory.

Hayden also proposed a method for calculating the volume change of slurry due to self weight consolidation. He assumed that the self weight consolidation of a layer with initial height H_o, and initial void ratio e_o will be caused by an effective stress of:

$$\bar{\sigma}_* = \gamma_w H_o \frac{G_s - 1}{2(1 + e_o)} \tag{1.8}$$

acting on the layer. $\bar{\sigma}_*$ in Equation (1.8) is the average effective stress acting at the midheight of the layer. A series of one-dimensional consolidation tests with a suitable range of loading stresses is performed to construct the experimental e-log $\bar{\sigma}$ curve. The void ratio at the end of primary consolidation, e_{100}, is obtained by interpolating $\bar{\sigma}_*$ in e-log $\bar{\sigma}$ curve. The final slurry height is calculated as:

$$H_{100} = \frac{(e_{100} + 1)(H_o P_w)}{P_w + G_s(1 - P_w)}, \tag{1.9}$$

where P_w is the percent solid by weight in the original suspension. The slurry height at the beginning of consolidation, H_a, can be obtained graphically from the settling curve of the interface by extending the

tangent to the zone settling portion of the curve to intersect the tangent to the consolidation portion of the curve. The slurry height corresponding to the point of intersection is H_a. The volume change of slurry in a disposal site which results from consolidation is then:

$$\Delta V = A\ (H_a - H_{100})\ , \tag{1.10}$$

where A is the area of the dispoal site. According to Hayden, this volume is the amount of containment capacity regained due to the long term settlement of the slurry.

Parallel to Hayden's work, Montgomery (1978) of WES studied the short term settling behaviors of the slurry and proposed a method for designing containments with sufficient areas and detention times to accommodate continuous dredge disposal activities and provide sufficient suspended solids removal. He suggested a settling column with 8 in. inside diameter and 6 ft. height, to be used for the sedimentation study. If a sharp interface is formed during the settling test, the slurry is said to be in zone settling. Although this phenomenon did sometimes occur in fresh water environment, Montgomery classified it as salt water settling. Design criterion in this case is based on the concept proposed by Coe and Clevenger (1916); i.e., to provide an adequate area so that the continuous discharging of slurry will not cause any concentration higher than the design concentration. If no sharp interface is observed, the slurry is in flocculent settling, and then design approach is that proposed by Mclaughlin (1959). First, concentration profiles at

several time periods after the test has started are plotted according to the concentration measurement data. Comparing these profiles with the initial one, a family of curves showing the relationship between percent solids removal and time at different depths can then be constructed. Knowing the requirement for returned water quality and the ponding depth, the detention time can then be obtained by interpolation.

The settling mechanism proposed by the WES studies separates the consolidation process from the sedimentation process. In reality, however, these two are quite inseparable. Usually, the bigger flocs may have already settled to the bottom of the column and started consolidating, while the smaller flocs are still settling in suspension. In addition, this long term settlement analysis inherits all the shortcomings of the conventional one-dimensional consolidation theory.

Because gravitation force is the sole agent which causes dredge material to settle, and the strain resulting from this settlement is generally very large, the volume change behavior of the dredge material ought to be best described by the self weight consolidation theory. The equation governing large strain consolidation behavior was formulated by Gibson et al. (1967). Consolidation parameters are considered to vary during consolidation, and void ratio, e, is not uniform throughout the sample thickness. The limitation of fixed soil boundaries as prescribed in conventional consolidation theory is removed. Because of the moving boundary, the Lagrangian coordinate system is convenient for describing the consolidation behavior.

Lagrangian coordinate system refers all events back to the initial t = 0 configuration. Consider a soil layer with a configuration as shown in Figure 1.4(a) before the consolidation starts. The position of material points within its domain is described by a space coordinate a. For example, the datum plane has a position of a = 0, which is assumed to be fixed. The top boundary is at a = a_o. A thin element of soil (A_o B_o C_o D_o) can be defined by its distance, a, from the datum plane and its thickness δ_a. After some time t, the soil layer has a new configuration as shown in Figure 1.4(b) due to consolidation. The top boundary has moved, and the element of soil occupies a new position (A B C D). A new position coordinate ξ, called convective coordinate, is then used to locate the material points [Figure 1.4(b)]. However, inconvenience arises from the use of ξ-coordinate because ξ itself is a function of the space coordinate, a, and time, t. If the element is labelled according to its initial position a, which is independent of time, throughout the consolidation process; e.g., the upper boundary is always considered as at a = a_o rather than at its current location, $\xi(a_o, t)$, the description of the system and the introduction of boundary conditions will be greatly facilitated. This labelling system is called the Lagrangian coordinate system.

Another coordinate z, called material coordinate or reduced coordinate, which labels only the particles, is defined as:

$$z(a) = \int_0^a \frac{da}{1 + e_o} \tag{1.11}$$

where e_o is the void ratio distribution at t = 0, which varies with position a. Equation 1.11 also implies:

$$\frac{dz}{da} = \frac{1}{1 + e_o} \tag{1.12}$$

If the permeability K is assumed to be a function of void ratio only, i.e., K = K(e), the generalized Darcy's law can be expressed as:

$$n(v_f - v_s) = - \frac{K}{\rho_f} \frac{\partial u}{\partial \xi} \tag{1.13}$$

where: n = porosity at time t

v_f = velocity of fluid

v_s = velocity of solid

u = excess pore pressure, can be expressed as $u = \sigma - \sigma' - u_h$ where σ is the total stress, σ' the effective stress, and u_h the hydrostatic pressure

To work with Equation 1.13, a transformation equation between the convective coordinate ξ and the Lagrangian coordinate a is needed. From Figure 1.4, the transformation can be expressed in a derivative form as:

$$\frac{\partial \xi}{\partial a} = \frac{1 + e}{1 + e_o} \tag{1.14}$$

If both fluid and solids are incompressible, the equilibrium in vertical direction requires:

$$\frac{\partial \sigma}{\partial z} + (e \rho_f + \rho_s) = 0 \tag{1.15}$$

where ρ_f and ρ_s are the unit weights of pore fluid and solids, respectively. To ensure the continuity of fluid flow, the following equation must be satisfied:

$$\frac{\partial}{\partial a}\left[\frac{e(v_f - v_s)}{1 + e}\right] + \frac{\partial e}{\partial t} = 0 \tag{1.16}$$

Combining Equations 1.13, 1.15 and 1.16 in terms of z-coordinate, it results:

$$\left(\frac{\rho_s}{\rho_f} - 1\right) \frac{d}{de}\left[\frac{K}{1 + e}\right] \cdot \frac{\partial e}{\partial z} + \frac{\partial}{\partial z}\left[\frac{K}{\rho_f(1 + e)} \cdot \frac{d\sigma'}{de} \cdot \frac{\partial e}{\partial z}\right] + \frac{\partial e}{\partial t} = 0 \tag{1.17}$$

Equation 1.17 is the general equation governing the large strain consolidation, which was derived by Gibson et al. (1967).

To obtain an analytical solution, Lee and Sills (1981) assumed that:

(A) the permeability K increases linearly with void ratio, or

$$K = \rho_f K_o(1 + e) \tag{1.18}$$

where K_o is constant.

(B) the coefficient of consolidation, C_F, defined as:

$$C_F = -\frac{K}{\rho_f(1 + e)} \frac{d\sigma'}{de} \tag{1.19}$$

is constant throughout the whole consolidation process.

Equation 1.17 then is reduced to:

$$C_F \frac{\partial^2 e}{\partial z^2} = \frac{\partial e}{\partial t} \tag{1.20}$$

In order to obtain Equation 1.20, the negative sign in Equation 1.19, which was not given in Lee and Sills' derivation, is required. The previous assumption implies that $d\sigma'/de$ is also constant. Lee and Sills assumed that σ' vs. e relationship to be: $\sigma' = A - \alpha e$, where A and α are constant. It should be noticed that both e and σ' are functions of material coordinate z and time t. To solve Equation 1.20, the following conditions are imposed:

(A) Initial conditions: Prior to self weight consolidation, the concentration, and therefore the void ratio, is uniform throughout the whole depth, and the effective stress is everywhere zero; i.e.,

$$e(z, 0) = e_i$$

$$\sigma'(z, 0) = 0 \qquad 0 \leq z \leq z_1 \tag{1.21}$$

where z_1 is the actual material height.

Equation 1.21 results in:

$$A = \alpha e_i, \text{ and}$$

$$\sigma'(z, t) = \alpha\left[e_i - e(z, t)\right] \tag{1.22}$$

(B) Final conditions: After the consolidation has ended, the effective stress is solely due to buoyant weight of solids because no excess pore pressure exists; i.e.,

$$\sigma'(z, \infty) = (\rho_s - \rho_f)(z_1 - z) \tag{1.23}$$

and

$$e(z, \infty) = e_i - \frac{\rho_s - \rho_f}{\alpha}(z_1 - z) = e_i - \beta(z_1 - z) \tag{1.24}$$

where $\beta = (\rho_s - \rho_f)/\alpha$.

Equation 1.24 indicates that after 100 percent primary consolidation the void ratio will distribute linearly from e_i at the material surface to $e_i - \beta z_1$ at the base, as shown in Figure 1.5.

(B) Boundary conditions: Since the effective stress is always zero at the material surface, the void ratio at there will then remain unchanged according to Equation 1.22; i.e.,

$$e(z_1, t) = e_i \tag{1.25}$$

In setting column tests or most of the disposal sites for dredge material, bottom drainage is not allowed. The condition at the lower boundary is then:

$$\frac{\partial u}{\partial z} = \frac{\partial}{\partial z}(\sigma - \sigma' - u_h) = 0$$

From Equation 1.15, $\frac{\partial \sigma}{\partial z} = -(e\,\rho_f + \rho_s)$. However,

$$\frac{\partial u_h}{\partial z} = \frac{\partial u_h}{\partial \xi}\frac{\partial \xi}{\partial z} = -\rho_f\left(\frac{\partial \xi}{\partial a} \cdot \frac{\partial a}{\partial z}\right) = -\rho_f(1 + e)$$

Hence,

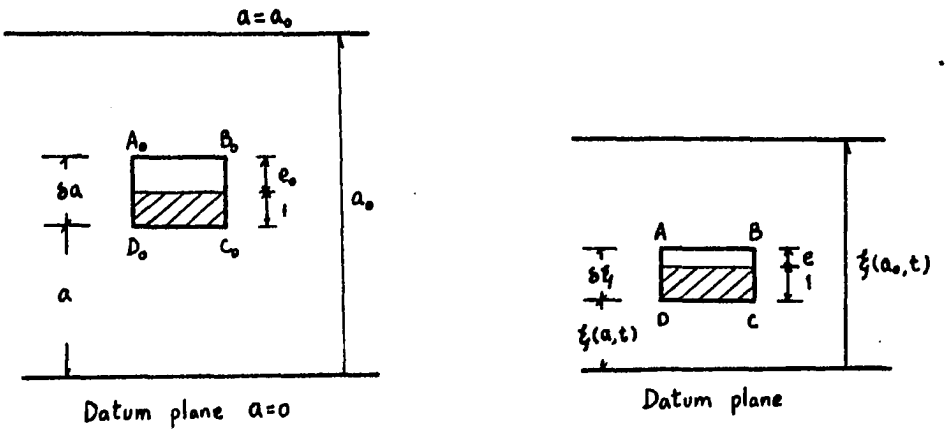

Figure 1.4. Lagrangian and convective coordinate: (a) initial configuration, t = 0, (b) configuration at time t

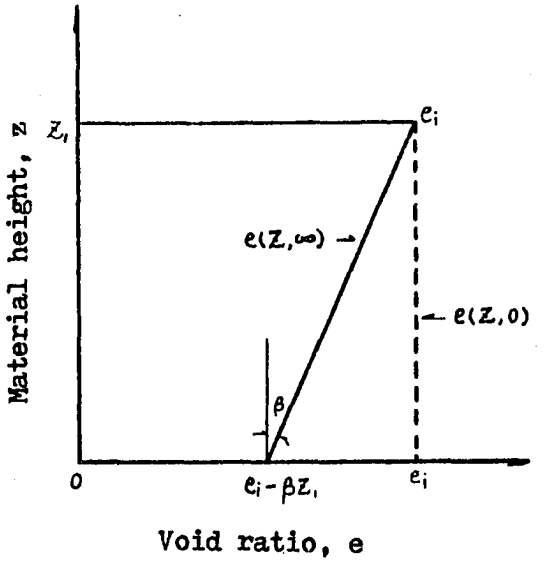

Figure 1.5. Assumed initial and final void ratio distributions by Lee and Sills (1981)

$$\frac{\partial}{\partial z}(\sigma - u_h) = -(e\rho_f + \rho_s) + \rho_f(1 + e) =$$

$$\rho_f - \rho_s = \frac{\partial \sigma'}{\partial z} = -\alpha \frac{\partial e}{\partial z}$$

Thus, the boundary condition at the impervious base is:

$$\frac{\partial e}{\partial z} = \frac{1}{\alpha}(\rho_s - \rho_f) = \beta \tag{1.26}$$

Utilizing these conditions together with Equation 1.20, Lee and Sills (1981) obtained an analytical solution for impervious base, which is:

$$e(z, t) = e_i - \beta\left[z_1 - z - 2z_1 \sum_n \frac{\cos(m\pi z/z_1)}{m^2\pi^2} \exp\left(-\frac{C_F m^2 \pi^2 t}{z_1^2}\right)\right] \tag{1.27}$$

where $m = \frac{1}{2}(2n + 1)$, $n = 0, 1, \ldots .$,

and the corresponding excess pore pressure distribution is:

$$u(z, t) = 2(\rho_s - \rho_f) \cdot z_1 \sum_n \frac{(-1)^n \sin[m\pi(1 - z/z_1)]}{m^2\pi^2} \cdot$$

$$\exp\left(-\frac{C_F m^2 \pi^2 t}{z_1^2}\right) \tag{1.28}$$

Slurry height at any time, h(t), can be expressed in terms of material coordinate z by integrating Equation 1.27 from 0 to the total material height z_1; i.e.,

$$h(t) = \int_0^{z_1} \left[1 + e(z, t) \right] dz$$

$$= (1 + e_i) z_1 - \tfrac{1}{2}\beta z_1^2 + 2\beta z_1^2 \sum_n \frac{(-1)^n}{m^3 \pi^3} \cdot$$

$$\exp\left(- \frac{C_F m^2 \pi^2 t}{z_1^2}\right) \qquad (1.29)$$

Final slurry height $h(\infty)$ is then obtained by letting $t \to \infty$ in Equation 1.29; i.e.,

$$h(\infty) = (1 + e_i) z_1 - \tfrac{1}{2}\beta z_1^2$$

Since the slurry height prior to consolidation is:

$$h(0) = \int_0^{z_1} (1 + e_i)\, dz = (1 + e_i)\, z_1,$$

the degree of self weight consolidation at time t, S(t), can be expressed as:

$$S(t) = \frac{h(0) - h(t)}{h(0) - h(\infty)} = \frac{\tfrac{1}{2}\beta z_1^2 - 2\beta z_1^2 \sum_n \frac{(-1)^n}{m^3 \pi^3} \exp\left(- \frac{C_F m^2 \pi^2 t}{z_1^2}\right)}{\tfrac{1}{2}\beta z_1^2}$$

$$= 1 - 4 \sum_n \frac{(-1)^n}{m^3 \pi^3} \exp\left(- \frac{C_F m^2 \pi^2 t}{z_1^2}\right) \qquad (1.30)$$

Time factor T can be defined as: $T = \frac{C_F t}{z_1^2}$, and $M = m\pi$. Equation 1.30 thus becomes:

for the impervious base,

$$S(T) = 1 - 4\sum_{n}\frac{(-1)^n}{M^3}\exp(-M^2T) \qquad (1.31)$$

where $M = m\pi = \frac{1}{2}(2n + 1)$. By the same approach except for different boundary condition at the base, Lee and Sills (1981) also obtained:

for the pervious base,

$$S'(T) = 1 - \sum_{n}\frac{2}{M^2}\exp(-4M^2T) \qquad (1.32)$$

Equation 1.28 indicates that at the onset of self weight consolidation the excess pore pressure distribution generated is triangular. In classical consolidation theory, the problem concerning triangular initial excess pore pressure distribution has also been studied by Terzaghi and Fröhlich (1936). In terms of time factor T, their solutions are:

for the pervious base,

$$S(T) = 1 - \frac{32}{\pi^3}\sum_{m=1}^{m=\infty}\frac{(-1)^{m+1}}{(2m-1)^3}e^{-(2m-1)^2\cdot\frac{\pi^2}{4}T}, \qquad (1.33)$$

and for the pervious base,

$$S(T) = 1 - \frac{8}{\pi^2}\sum_{m=1}^{m=\infty}\frac{1}{(2m-1)^2}e^{-(2m-1)^2\cdot\frac{\pi^2}{4}T}, \qquad (1.34)$$

where $T = c_v t/h^2$, and c_v is the coefficient of consolidation. According to their analysis, Equation 1.34 is also the solution for any linearly varied initial excess pore pressure distribution with pervious base, including the uniform one. It should be noticed that the term h in Equation

1.33 represents the total thickness of the soil layer, whereas that in Equation 1.34 only stands for half of the thickness.

Figure 1.6 compares the S(T) vs. $\sqrt{T}$ curves resulting from the classical consolidation theory with those from the self weight consolidation theory. An important feature is that in the case of the impervious base both theories predict the same consolidation behavior. This can also be verified by simplifying Equation 1.33, i.e., letting n = m - 1, and M = $\frac{\pi}{2}(2n + 1)$, Equation 1.33 becomes

$$S(T) = 1 - \frac{32}{\pi^3} \sum_{m=1}^{\infty} \frac{(-1)^{m+1}}{(2m-1)^3} \exp\left[-(2m-1)^2 \cdot \frac{\pi^2}{4} T\right]$$

$$= 1 - 4 \sum_{n=0}^{\infty} \frac{(-1)^{n+2}}{\left[\frac{\pi}{2}(2n+1)\right]^3} \exp\left[-\frac{\pi}{2}(2n+1)^2 T\right]$$

$$= 1 - 4 \sum_{n} \frac{(-1)^n}{M^3} \exp(-M^2 T) ,$$

which is identical to Equation 1.31. For the pervious base, however, self weight consolidation theory predicts a higher consolidation rate than the classical theory does, though both S(T) vs. $\sqrt{T}$ curves show an initially linear portion.

In the conventional consolidation test, the initial pore pressure distribution is assumed to be uniform throughout the whole sample depth, and drainage occurs at both top and bottom surfaces. The theoretical solution for this case is the curve (a) of the pervious base condition,

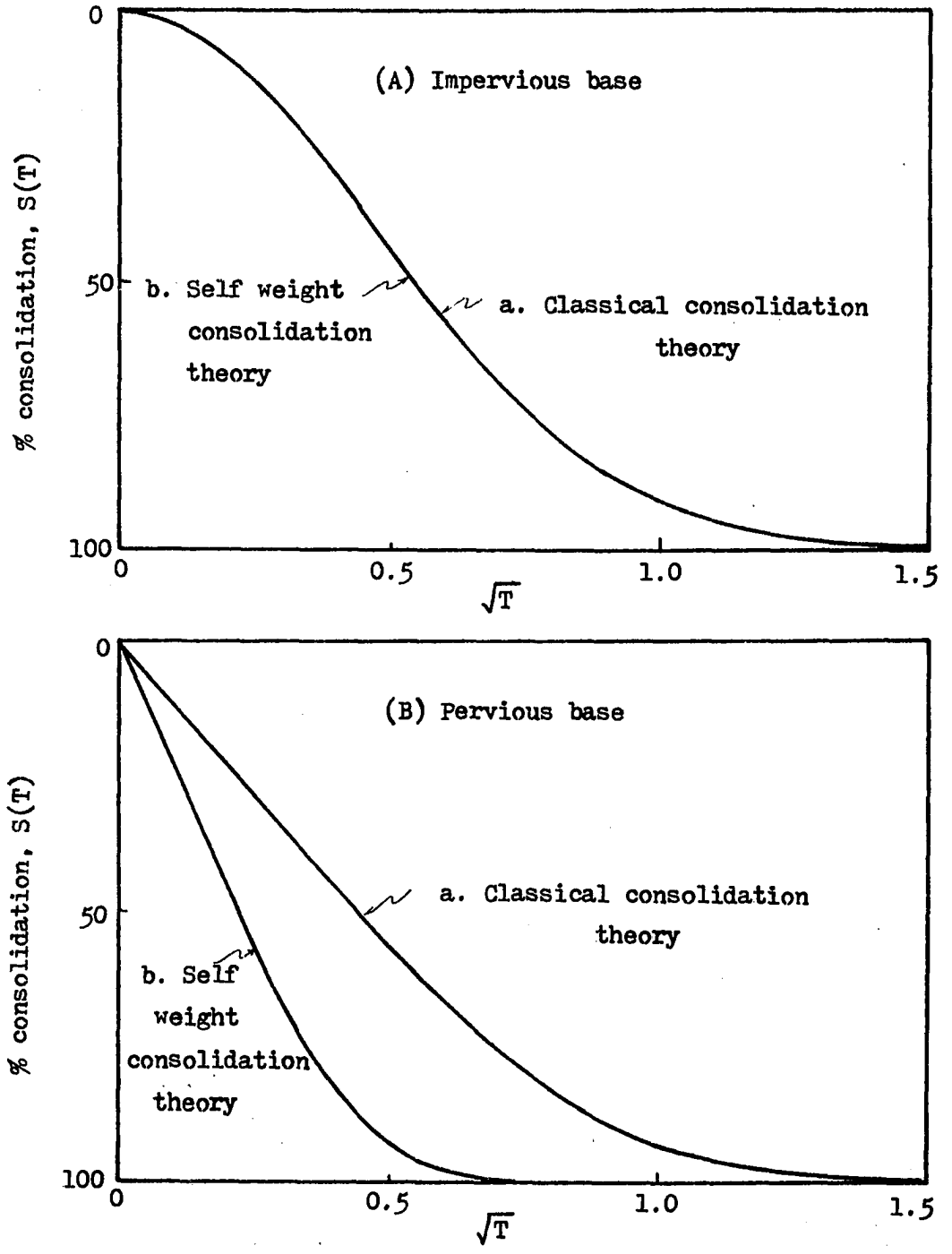

Figure 1.6. Comparison of S(T) vs. $\sqrt{T}$ curves for (a) classical consolidation theory, (b) self weight consolidation theory

i.e., case (B), in Figure 1.6. The WES study utilizes the test results to predict the time rate settlement of dredge material, which in essence is to simulate the consolidation behavior of case (A) by curve (a) of case (B) in Figure 1.6. An overestimation of settling rate in the early period of consolidation is expected.

The identical result yielded by these two consolidation theories in the impervious base case means that the error arising from the linear σ' vs. e and K vs. e assumptions in the self weight consolidation theory is probably compensated by the error of assuming small strain in conventional theory. They are, however, by no means identical. In fact, the self weight consolidation theory is different from the conventional theory by several distinct characteristics: 1) no external load, 2) the variation of soil parameters during consolidation can be accounted for, 3) large strain, and 4) moving boundaries. In addition, due to the buoyant effect of the submerged weight of solids, the excess pore pressure generated initially is always triangular in shape in self weight consolidation, whereas in conventional consolidation different external loading conditions may result in different excess pore pressure distributions. Furthermore, the self weight consolidation theory deals with the void ratio distribution and material coordinate. Thus, the slurry height (or solid boundary) at any time in the consolidation process can be predicated, e.g., by Equation 1.29, which can serve as a check of how well the theory can actually model the settlement behavior. The conventional theory, however, uses pore pressure dissipation as a basis for calculating degree

of consolidation and assumes the boundaries to be fixed. It is then not able to directly predict the slurry height h(t) by solution.

The validity of the Lee and Sills' solution was tested experimentally by Been and Sills (1981) using the X-ray Transviewer and pore pressure transducers. According to their observations, none of the assumptions made by Lee and Sills can be experimentally justified. For example, the permeability, K, is roughly proportional to the void ratio e in a semilogarithmic fashion, i.e., log $K \propto e$, instead of linear fashion as assumed by Lee and Sills. The relation between e and the effective stress, σ', is well defined when σ' is high, but it is poorly defined when σ' is low. In the extreme when $\sigma' = 0$, the σ' vs. e relationship is not unique because the bulk density at the top of the slurry, where $\sigma' = 0$, is observed to be increasing as the consolidation proceeds. Hence, after 100% primary consolidation the void ratio at the slurry surface will result in a value $e_o < e_i$, instead of maintaining at e_i. In order to accommodate this real situation to the Lee and Sills' solution, Been and Sills (1981) assumed that the void ratio difference which occurs at the slurry surface can be considered as the effect resulting from the addition of an imaginary overburden layer. The material thickness of this layer is so defined that the final void ratio still distributes linearly with material height and has same slope, i.e.,

$$\beta(z_o - z_1) = e_i - e_o, \tag{1.35}$$

where $z_o - z_1$ is the material thickness of the imaginary overburden layer

(Figure 1.7). The Lee and Sills' solution is still applicable by replacing z_o for z_1 as the total material height, but the excess pore pressure distribution as expressed in Equation 1.28 needs modification because there is no excess pore pressure at $z = z_1$ in reality. Thus,

$$u_1(z, t) = u(z, t) - u(z_1, t) \tag{1.36}$$

where $0 \leq z \leq z_1$, and $u_1(z, t)$ is the actual excess pore pressure distribution. Under these circumstances, three soil parameters are required to be able to describe the self weight consolidation of material: e_o, β and C_F.

From their tests, Been and Sills (1981) found that both e_o and β varied nonlinearly with the initial concentration, although the soils used were very similar. They argued that the variation was probably

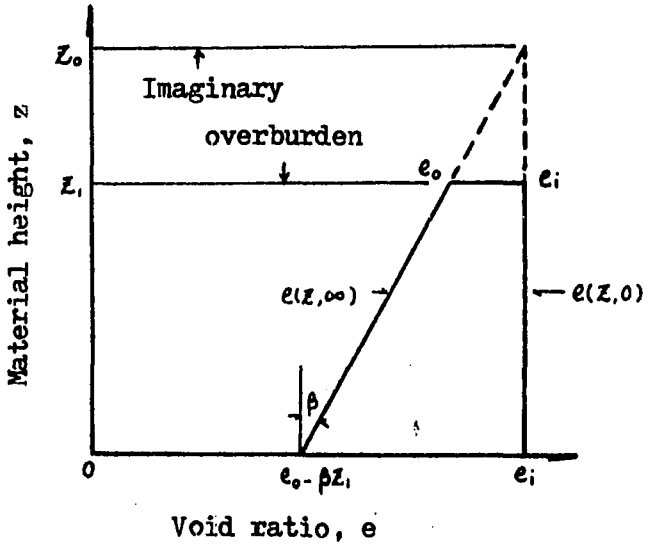

Figure 1.7. Modified initial and final void ratio distributions by Been and Sills (1981)

due to the flocculation and particle segregation in suspensions with low initial concentrations. However, the behaviors of e_o and β were not examined in detail by them, and both parameters were assumed constant in their calculations. To determine the coefficient of consolidation, C_F, Been and Sills used three different approaches:

(A) Direct calculation from measured soil properties

Since Darcy's law states that $n(v_f - v_s) = - Ki$, and continuity equation ensures that $v_s(1 - n) + v_f n = 0$, the permeability K can be expressed as: $K = -v_s/i$. The average fall velocity for an element of soil, v_s, is obtained by dividing the position change of the soil element between two concentration profiles by the time interval, and the pressure gradient, i, can be estimated from the excess pore pressure profiles constructed by transducer measurements. The corresponding void ratio, e, for the soil element is calculated from its concentration. Thus, the K vs. e relationship is obtained. Furthermore, the σ' vs. e relationship is constructed by concentration profiles and pore pressure measurement, which can generate the $d\sigma'/de$ value at any e. Finally, the coefficient of consolidation is calculated by:

$$C_F = \frac{K}{\rho_f(1 + e)} \frac{d\sigma'}{de} \tag{1.19}$$

(B) By comparison of pore pressure distributions.

Isochrones of excess pore pressure both from theoretical calculation and actual measurement are constructed and compared. A time factor, T, which corresponds to a certain real clock time, t, can be found. The C_F

is then calculated as:

$$C_F = \frac{Tz_o^2}{t} \tag{1.37}$$

(C) By comparison of settlement curves.

The experimental h(t) vs. t curve is compared with theoretical S(T) vs. T curve to find the T-t relation. Then, the C_F value is calculated as before.

They also compared the results from these three approaches and found that the C_F value estimated from the settlement curve is much higher than that given by the other two methods. The difference is expected because both (A) and (B) require an excess pore pressure distribution; whereas (C) doesn't. Been and Sills stated that the C_F value given by method (A) or (B) is not a good approximation to use.

There is another crucial problem in using the Lee and Sills' solution to interpret the consolidation behavior: how to determine the starting point of self weight consolidation? Theoretically, the consolidation process ought to begin at the onset of the development of the effective stress. However, to experimentally detect the existence of effective stress is rather difficult because it requires precise measurements of both density and excess pore pressure profiles. If particles are locked into a three dimensional lattice when zone settling starts, it is reasonable to conclude that consolidation process also starts from that moment. It is the author's opinion that Been and Sills failed to detect the early existence of effective stress, hence their

analysis was biased toward the later portion of the self weight consolidation.

Synthesis of Literature

This section compares the models reviewed in the preceding section and studies the similarities and relationships between them so that the existing models can be better understood and interpreted.

A consolidating soil body can be considered as a deformable solid containing numerous interconnected pores. Volume change of this body is then caused by the out flowing of pore water through these passageways. The seepage velocity $\bar{v}_a$ of water flowing through a channel can be described by Poiseuille's law:

$$\bar{v}_a = (C_s \frac{\gamma_w}{\mu} r_h^2) i \tag{1.38}$$

where $\bar{v}_a$ = average seepage velocity of water through channel

C_s = shape factor

r_h = hydraulic radius of channel section

i = hydraulic gradient

Because the apparent flow velocity $\bar{v} = n \bar{v}_a$, and the permeability $K = \bar{v}/i$, the equivalent permeability, K, for the channel is:

$$K = C_s \frac{\gamma_w}{\mu} r_h^2 n \tag{1.39}$$

where n is the porosity. Taylor (1948) suggested that in the soil system the hydraulic radius r_h could have a form as:

$$r_h = e \frac{V_s}{A_s} \tag{1.40}$$

where A_s is the solid surface exposed to flow, and V_s the volume of solid. Equation (1.39) thus becomes:

$$K = C_s \frac{\gamma_w}{\mu} \frac{e^3}{1 + e} \left(\frac{V_s}{A_s}\right)^2 \tag{1.41}$$

Therefore, the permeability of the soil should vary linearly with $e^3/1 + e$ rather than $1 + e$ (Equation 1.18). In addition, factors like the shape of the channel and the specific area of solids also influence the permeability.

Equation 1.41 also implies that the model using Poiseuille's law is physically equivalent to the model using Darcy's law as far as the mechanism of pore water flow is concerned. For example, the filtration (or seepage) rate per unit area obtained by the Gaudin and Fuerstenau's model is:

$$Q = \frac{c(G_s - 1)\gamma_w}{32\mu} \frac{m}{m + 2} G^2 \tag{1.2}$$

The hydraulic gradient i can be defined as:

$$i = \frac{1}{\gamma_w} \frac{dp}{dl} = c(G_s - 1),$$

thus the equivalent permeability K for this system is:

$$K = \frac{Q \cdot n}{i} = \frac{1}{32} \frac{\gamma_w}{\mu} \frac{m}{m + 2} G^2 \cdot n \tag{1.42}$$

Because Gaudin and Fuerstenau (1962) assumed that all the channels are

circular in shape, and the tube sizes follow the Schuhmann function, the expression for permeability K in Equation 1.42 is somewhat different from the general form, i.e., Equation 1.41.

In sedimentation, the submerged weight of solids is supported by hydrodynamic forces. However, once the three-dimensional lattice is formed, the weight of solids is supported initially by the pressure generated within pores and later is shared by the soil skeleton and the pore fluid. At the onset of consolidation, the excess pore pressure dp generated by a layer of suspension with thickness dl is:

$$dp = \frac{dW}{A} = \frac{c\ dV(G_s - 1)\gamma_w}{A} = c(G_s - 1)\ dl \cdot \gamma_w$$

where c is the solid concentration expressed in terms of percent by volume. The resulted pressure gradient is:

$$\frac{dp}{dl} = c(G_s - 1)\gamma_w, \tag{1.43}$$

which is exactly the same as that assumed by Gaudin and Fuerstenau (1962).

From the above discussions, it can be seen that Gaudin and Fuerstenau's model is similar to the self weight consolidation model. Nevertheless, when the consolidation process starts, and the effective stress begins to develop, Equation 1.43 no longer holds, and the settling behavior then can only be described by the self weight consolidation theory.

By assuming that both permeability K and effective stress σ' are

linear functions of void ratio e, Lee and Sills (1981) have solved the self weight consolidation problem. The solutions they obtained for the impervious base are Equations 1.27 and 1.28. Equation 1.27 indicates that at slurry surface, where $z = z_1$, the void ratio remains unchanged throughout the whole consolidation process. However, in reality the void ratio will reduce from e_i to e_o at the surface. In order to accommodate this real situation to the Lee and Sills' solutions, Been and Sills (1981) considered that the void ratio difference at the slurry surface is due to the effect of adding an imaginary overburden layer (Figure 1.8). By doing this, the Lee and Sills' solutions are still applicable if the actual material height z_1 is replaced by the modified material height z_o, where $z_o = z_1 + (e_i - e_o)/\beta$. Equation 1.27 then becomes:

$$e(y, T') = e_i - \beta\left[z_o - z - 2z_o \sum_n \frac{\cos(m\pi y)}{m^2\pi^2} \cdot \exp(-m^2\pi^2 T')\right] \quad (1.44)$$

for the void ratio distribution, and the corresponding pore pressure distribution, Equation 1.28, turns out to be:

$$u(y, T') = 2(\rho_s - \rho_f)\, z_o \sum_n \frac{\cos(m\pi y)}{m^2\pi^2} \exp(-m^2\pi^2 T'), \quad (1.45)$$

where $y = z/z_o$ and $T' = C_F \cdot t/z_o^2$. Equations 1.44 and 1.45 are graphically shown in Figure 1.8(a) and (b), respectively. Both equations are valid only for $0 \leq z \leq z_1$.

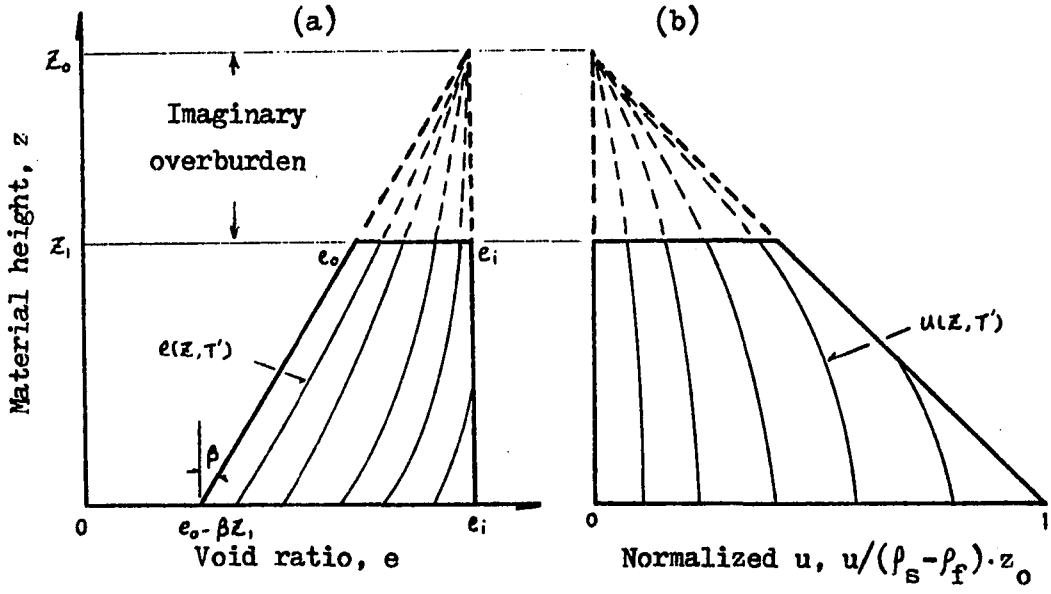

Figure 1.8. Modification of Lee and Sills' solution by Been and Sills (a) void ratio distributions (b) the corresponding excess pore pressure distributions

Either Equation 1.45 or Figure 1.8(b) shows that the excess pore pressure at $z = z_1$, i.e., the slurry surface, is $(\rho_s - \rho_f)\ (z_o - z_1)$ at the beginning of consolidation but reduces to zero after 100 percent of primary consolidation. In actual settling tests, however, there is no excess pore pressure existing on the surface at any time. Hence, Been and Sills further modified Equation 1.45 to be:

$$u_1(z, T') = u(z, T') - u(z_1, T') \tag{1.46}$$

where $0 \leq z \leq z_1$, or as:

$$u_1(y, T') = 2(\rho_s - \rho_f) z_o \sum_n \frac{\exp(-m^2\pi^2 T')}{m^2\pi^2} (\cos m\pi y - \cos m\pi r) \tag{1.47}$$

in which, $r = z_1/z_o$, $0 \leq y \leq r$ and $u_1(y, T')$ is the excess pore pressure distribution in real soil. Because of the additional modification, the function used to describe the void ratio distribution at any time, i.e., Equation 1.44, is not compatible with the function used to describe the excess pore pressure distribution, i.e., Equation 1.47. The degree of consolidation for the modified case, $S_m(T')$, however, should be calculated according to Equation 1.47 because it is close to the real situation. Thus,

$$S_m(T') = \frac{\int_0^r u_1(y, 0)dy - \int_0^r u_1(y, T')dy}{\int_0^r u_1(y, 0)dy}$$

$$= \frac{\sum_n \left\{ \left[\frac{\sin(m\pi r)}{m^3\pi^3} - \frac{r\cos(m\pi r)}{m^2\pi^2} \right] \cdot \left[1 - \exp(-m^2\pi^2 T') \right] \right\}}{\sum_n \left[\frac{\sin(m\pi r)}{m^3\pi^3} - \frac{r\cos(m\pi r)}{m^2\pi^2} \right]} \tag{1.48}$$

It is noticed that $S_m(T')$ varies with time factor T', as well as r, the ratio of the real material height z_1 to the modified material height z_o. Figure 1.9 shows the plots of $S_m(T')$ vs. $\sqrt{T'}$ relationship for different r values. For $r = 1.0$, i.e., no imaginary overburden layer exists, the consolidation behavior is identical to that obtained by Lee and Sills (1981). As r becomes smaller, the degree of consolidation gets higher for same T' value, which can be explained as the results of shorter

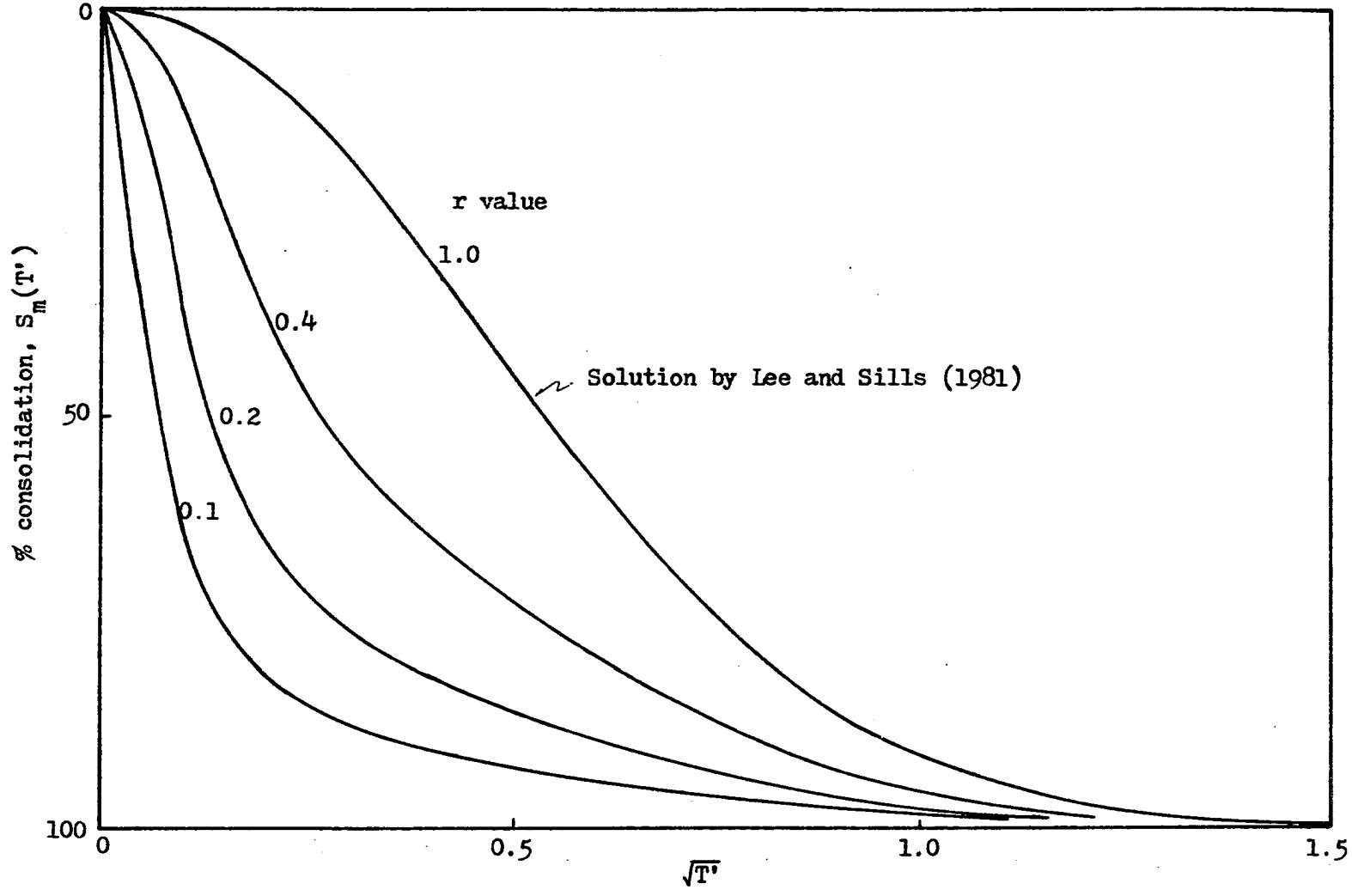

Figure 1.9. The Sm(T') vs. $\sqrt{T'}$ plots for different r values

drainage path for water to escape and thicker imaginary overburden layer exerting on the slurry layer.

Summary of Literature

Prior to 1960, the study of the settling behavior of materials was primarily based upon the hypotheses that materials fall through fluid medium as independent particles. No flocculation occurs, and the fall velocity of particles is a function of local concentration. Intuitively, that was an extension of Stokes' law. Using the concept of material continuity, simple equations relating concentration with either particle flux or fall velocity of particles resulted and provided the basis for thickener designs. These design criteria are not suitable for containment areas because dredge materials always settle as a mass or flocs. In addition, dredge spoil will accumulate and then gradually consolidate under its own weight instead of being constantly withdrawn from the bottom as in a thickener.

With the use of the Transviewer, the actual settling behavior of the material could be examined closely and researchers found that only in low concentration suspensions the material settled as individual flocs. Most of the time, it settled as a coherent mass because of particle agglomeration. The study of zone settling behavior thus emerged. Generally, the material was modelled as a porous plug containing channels through which water can flow as the material settles. However, these models could not account for the mechanism that as water

seeps through the solids, the particles are shoved closer together, and consoidation occurs. They only resulted in concentration vs. fall velocity relationships for thickener design. Nevertheless, these studies provide an insight into the actual settling mechanism.

The WES study combined sedimentation and consolidation in the settling mechanism, and the approach proposed by the WES researchers formed a rational basis for dredge spoil containment design. However, the way WES researchers interpreted the settling column test results is not satisfactory because the actual settling behavior in the consolidation regime bears little resemblance to the theoretical one-dimensional consolidation curve.

The mathematical formulation for large strain consolidation has been established. Lee and Sills (1981) applied self weight consolidation on the basis of two simple assumptions and their solution which describes consolidation of soil under its own weight is the most accurate one to date. Their solution can also serve as an alternative way of interpreting the zone settling phenomenon, which may put the settling column tests on a more rational basis and result in more accurate predictions of the time rate of settlement.

Objectives of Study

The purpose of this study was to examine the settling behavior of dredge materials for the design of containment areas. Specifically, the objectives are:

(A) to interpret the zone settling test results on the basis of self weight consolidation theory.

(B) to develop a practical approach to evaluate the apparent coefficient of consolidation, C_F, for self weight consolidation of dredge materials.

CHAPTER II. SETTLING COLUMN TESTS

This chapter is essentially a description of the laboratory test designed for the study of settling behavior of dredge materials, i.e., settling column test. Most of the test procedures follow those proposed by the WES. However, some modification is necessary because the WES distinction between flocculent settling and zone settling is somewhat arbitrary and can not suit the study well.

Background of the Area under Study

The sediment samples used in this study are all taken from Lake Panorama. Lake Panorama, located in Guthrie County, Iowa (Figure 2.1) is a long narrow impoundment, which was formed by damming a segment of the Middle Raccoon River in 1970. The watershed above Lake Panorama dam comprises about 440 square miles, with northeastern two-thirds of it composed of Wisconsin glacial till and the remaining areas of loess capped Kansan till (Schaefer, 1980). Because the lake is situated in an area of high sediment yields and intense cultivation, the problems associated with lake silting were recognized and studied.

The original capacity of Lake Panorama was calculated to be 19,345 acre-ft (Schaefer, 1980), whereas the hydrographic survey of 1980-81, conducted by USGS, resulted in a current lake volume of 14,019 acre-ft (Lin et al., 1981). Comparison of the capacities indicates that 5,326 acre-ft of storage capacity have been lost through sedimentation in the first 10-year period. Assuming a constant depositional rate of

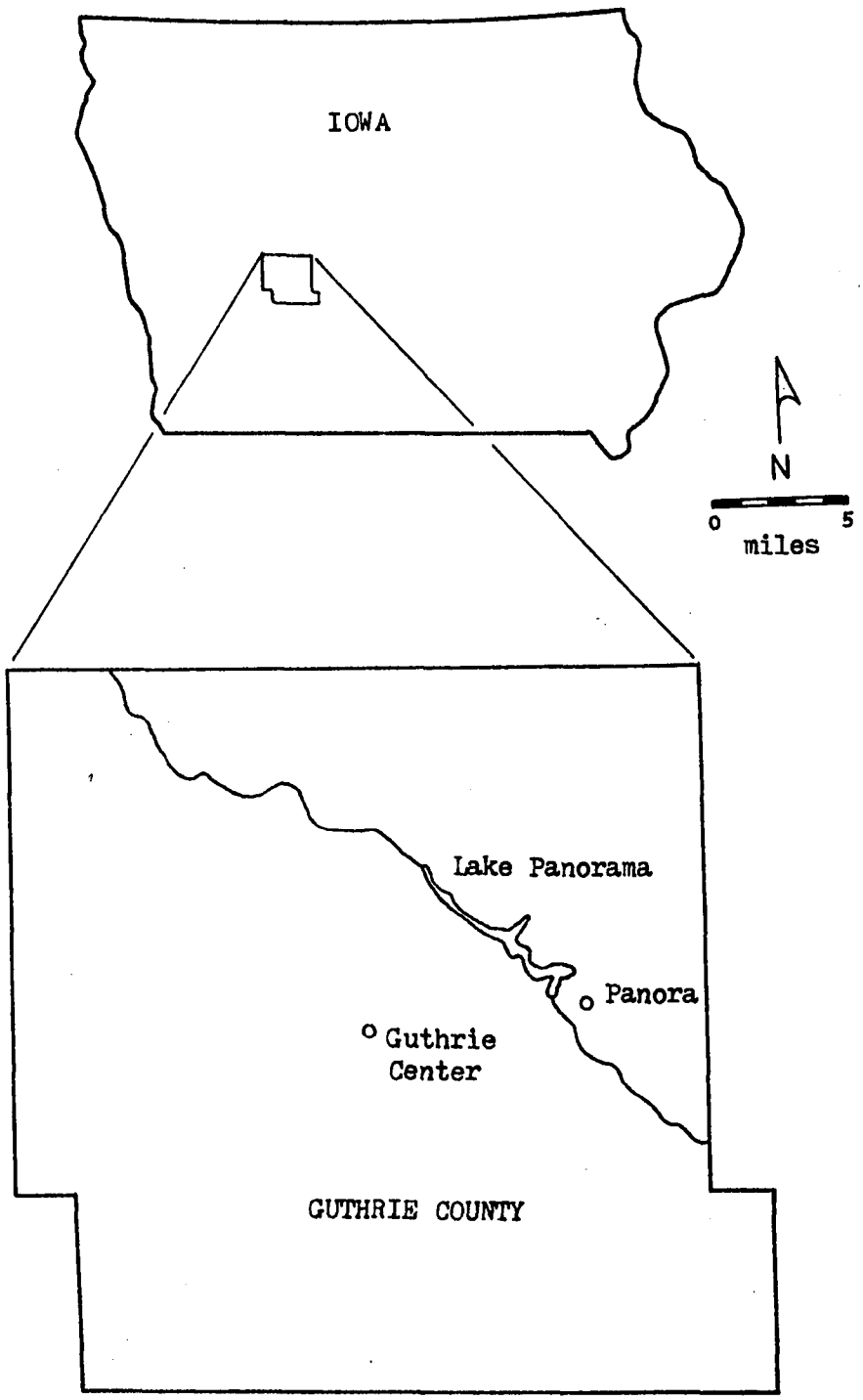

Figure 2.1. Location of Lake Panorama (after Schaefer, 1980)

sediment, the average annual silting rate of the lake is about 2.75% of the original capacity, which is high when compared to other lakes in Iowa. In order to prolong the useful life of the lake, some remedial measures have been proposed, including hydraulic dredging (Lin et al., 1981).

Sediment Properties

The physical properties of the lake sediments are useful in planning dredging operations; therefore, both disturbed and undisturbed samples were collected from Lake Panorama for laboratory testing. Generally, the disturbed samples were used for engineering index property determinations whereas the undisturbed samples were used to determine the dry unit weight. Engineering index tests included: Atterberg limits, natural water content, grain size distribution, and organic content.

Most of the tests were done by Schaefer (1980). Results of the Atterberg limit tests are plotted in Figure 2.2. It can be seen that most of the data points fall below the A-line. According to the Unified Soil Classification system, the sediment is classified as being in the ML or MH group, i.e., silts of both low and high plasticity. The organic content of the sediment ranges from 3 to 13 percent by weight and averages about 7.4 percent. Figure 2.3 shows the grain-size distribution range of the sediments taken from the central portion of the whole lake. Texturally, the soils are mostly silts and clays. Schaefer's

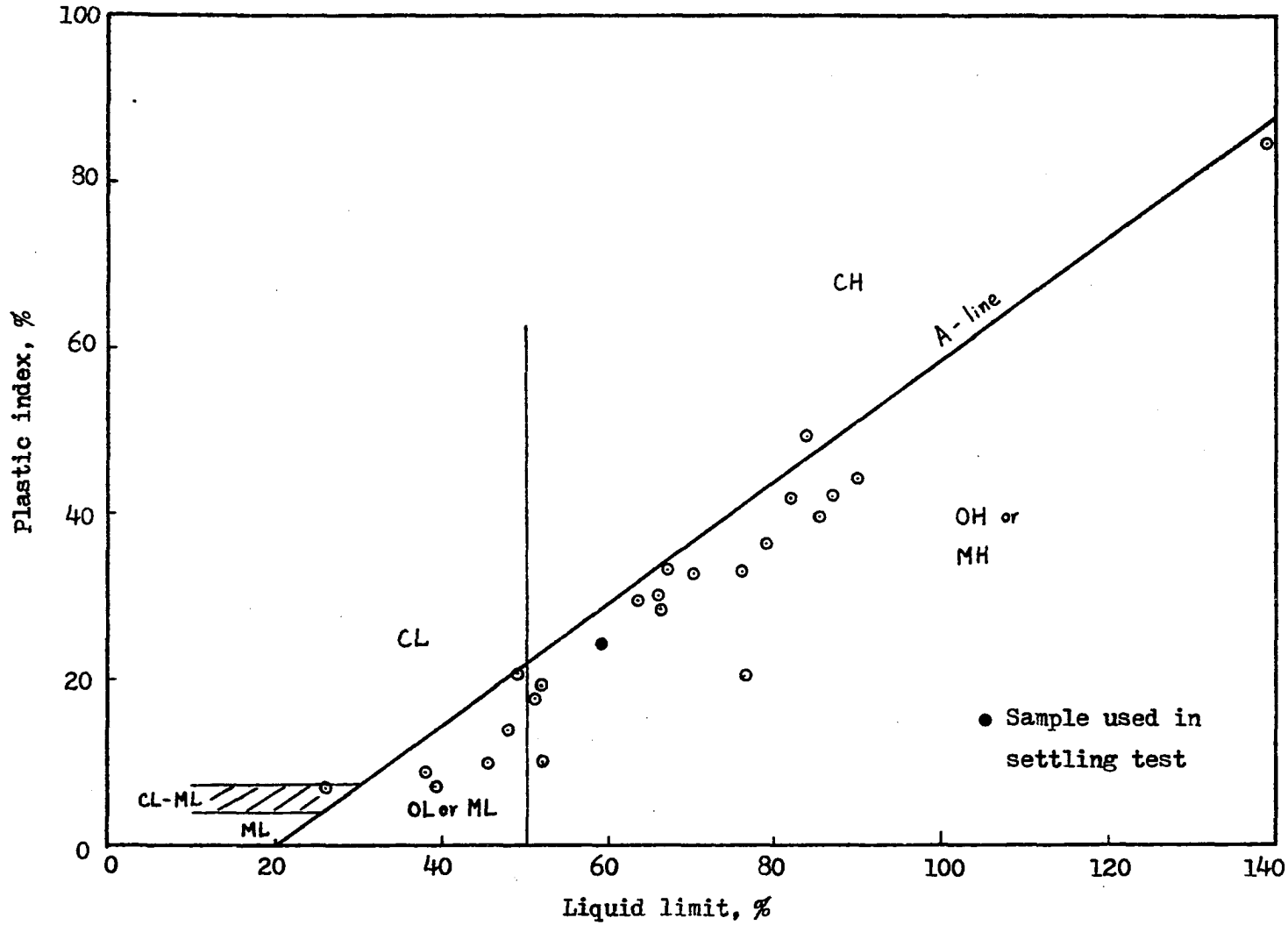

Figure 2.2. Classification of sediments from Lake Panorama

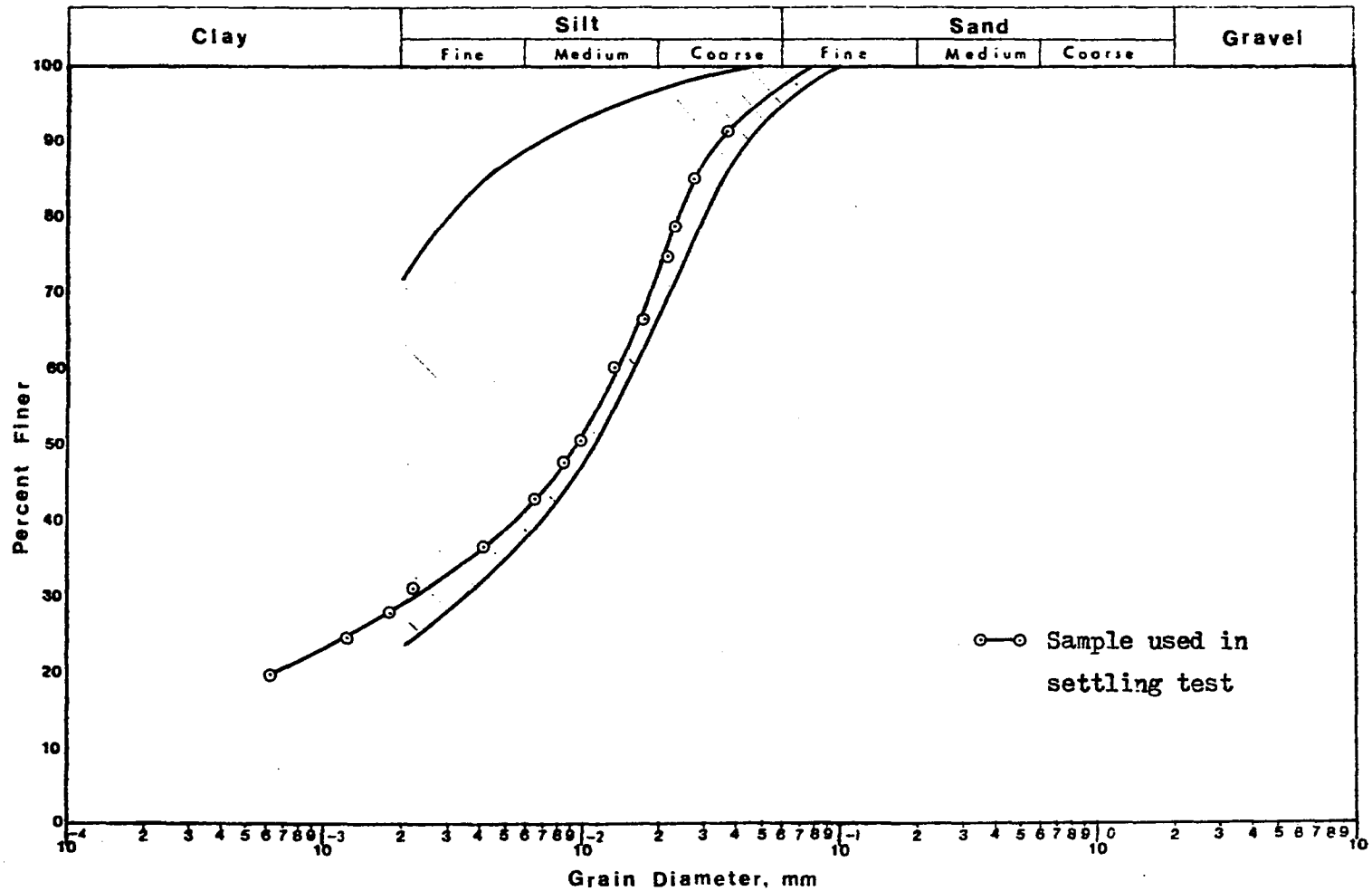

Figure 2.3. Grain-size distribution range of sediments from Lake Panorama

test on the undisturbed samples resulted in the dry unit weights of the sediment ranging from 55 pcf to 115 pcf.

The grab samples used in settling column tests were collected from the proposed dredging site, at about 5.2 miles upstream from Lake Panorama dam. The sample has the properties of:

Grain-size distribution:	37% clay and 63% silt
Natural water content:	78.9%
Dry unit weight:	50.2 pcf
Organic content:	5.6% by weight
Specific gravity:	2.74
Liquid limit:	59.4
Plasticity index:	24.7
Soil classification:	MH

which are comparable to the Schaefer results (Figures 2.2 and 2.3).

Test Equipment

The following equipment is necessary for performing the settling column test:

(A) Settling column - The WES study suggests that a plexiglass column, at least 8 in. inside diameter, and 6 ft. high should be used. However, in this study, a 5.5 in. diameter column was used because it is readily available. The column should have sample ports at 1 ft. intervals throughout the whole depth.

(B) Portable mixer - used to mix the sediment with water to form a uniform slurry with desired concentration.

(C) Positive displacement pump - used to discharge slurry into the settling column.

(D) Air supply - to keep the particles from settling during the column filling period.

(E) Concentration measurement devices - including hypodermic syringes to sample the slurry and a constant temperature oven to dry out the sample for concentration determination.

Figure 2.4 shows all the equipment except the constant temperature oven.

Test Procedures

Because the slurry discharged into a containment area usually has a rather high solid concentration, it will behave either as flocculent settling or as zone settling. In the WES guidelines (Palermo et al., 1978), the test procedures and design methods are different for these two types of settling behaviors, but the distinction between flocculent and zone settling is somewhat arbitrary. Generally, the WES researchers considered the formation of an interface during the test as evidence for zone settling (Palermo et al., 1978):

> Zone settling where the flocculent suspension forms a lattice structure and settles as a mass, exhibiting a distinct interface during the settling process.

Also, they found (Palermo et al., 1978):

> Sedimentation of freshwater sediments at slurry concentration 100 g/l can generally be characterized by flocculent settling properties. As slurry concentrations are increased, the sedimentation process may be characterized by zone settling properties ... the settling properties of saltwater dredged material can usually be characterized by zone settling tests.

Thus, roughly speaking, the freshwater sediments are classified as flocculent settling materials and the saltwater sediments are considered as zone settling materials by the WES study, and the containment design follows the test results accordingly. However, the author's tests on the freshwater lake sediments show that the interface always forms in the first hour of the test even at an initial concentration as low as 20 g/l. It is concluded that flocculent settling test alone does not provide enough information for the sedimentation study of the lake sediments. Hence, both the flocculent and the zone settling tests, prescribed by the WES study but with some modification, were performed on the lake sediments. Generally, procedures for the flocculent settling test are:

1. Prepare sufficient sediment for the settling test. Calculate the total volume of the column, V. In order to achieve a desired concentration c_i, the approximate weight of dry sample needed is $c_i V$, or the amount of wet sediment required is roughly $c_i V(1 + w)$, where w is the natural water content of the sediment.

2. The sediment is then mixed thoroughly with tap water to form a uniform slurry (Figure 2.5).

3. Pump the slurry into the settling column, while air is supplied from the bottom of the column to resuspend the falling particles.

4. When the filling process is finished, draw off samples at each sample port, using hypodermic syringes, for concentration determination. The initial concentration c_i is taken as the average of these concentration readings. After the samples are taken, stop the air supply and begin the settling test. The lineup of the apparatus for this test is shown schematically in Figure 2.6.

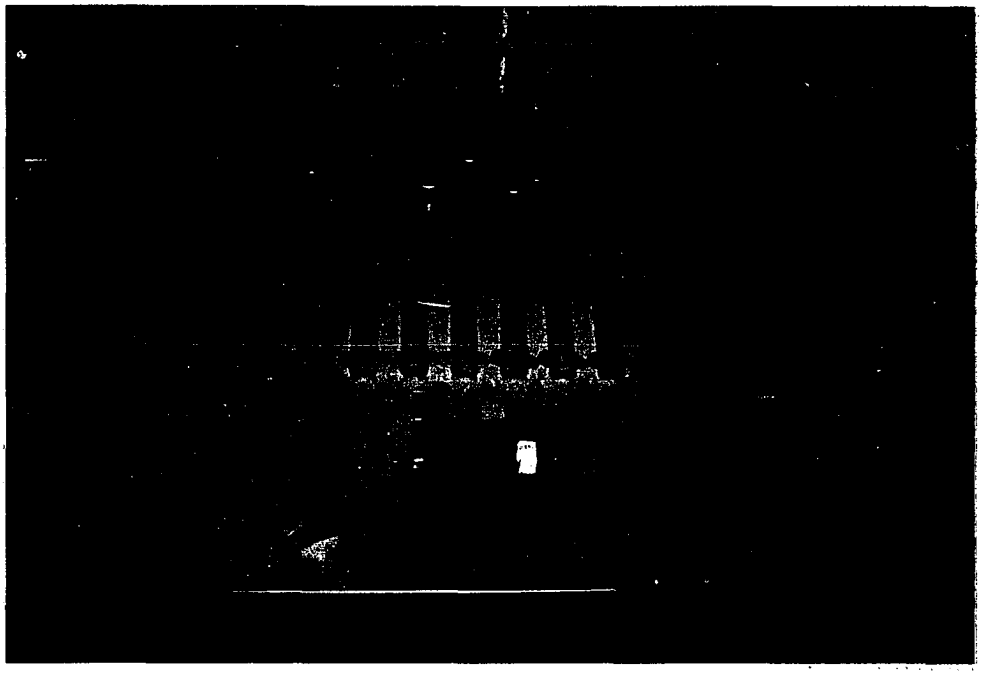

Figure 2.4. Equipment for performing settling column tests

Figure 2.5. Mixing to obtain a uniform slurry

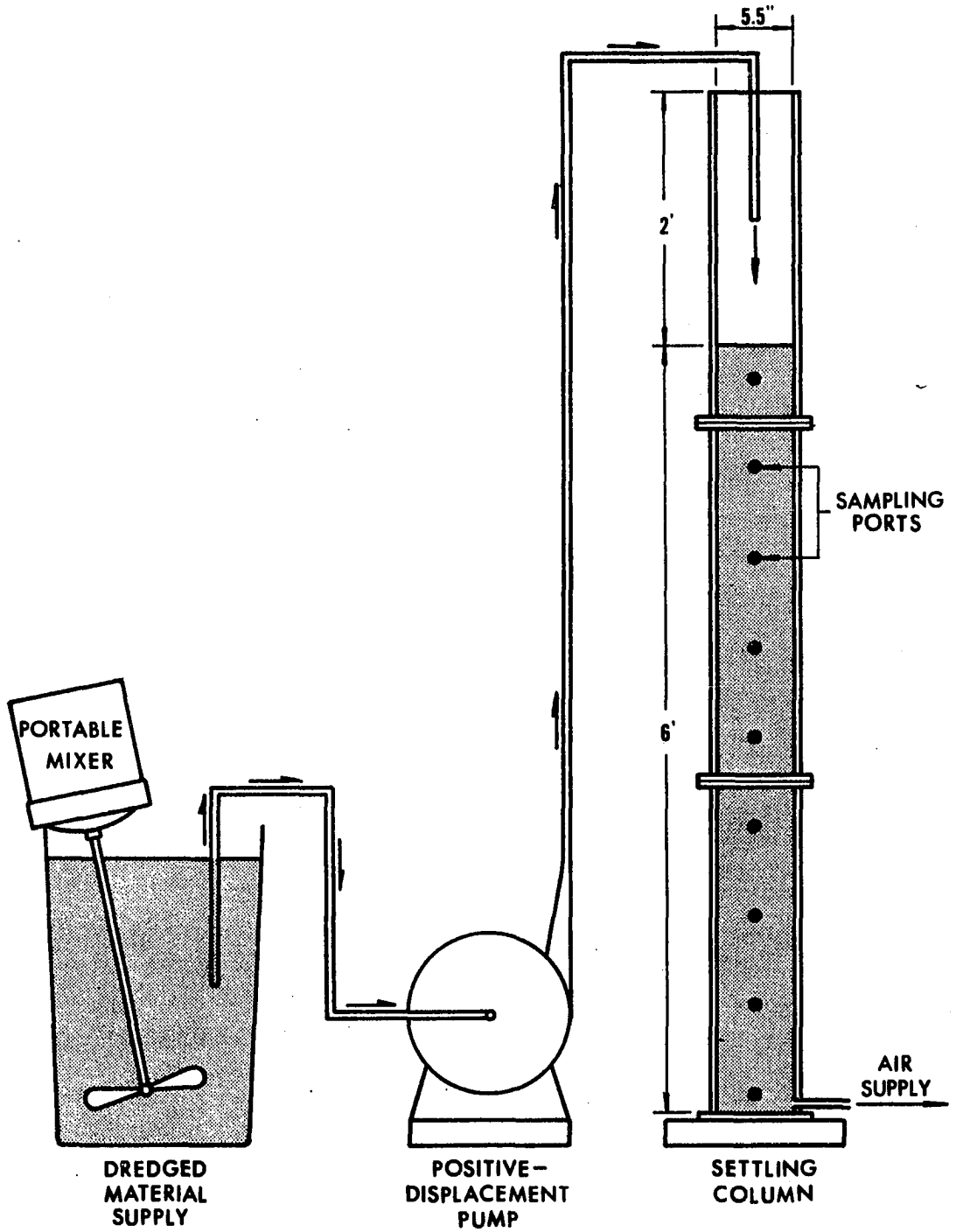

Figure 2.6. Schematic diagram of apparatus for settling column tests

5. At regular time intervals record the height of the interface if it has formed, and then withdraw samples from each sample port to determine the suspended solids concentration (Figure 2.7). Continue the test until the concentration above the interface is less than 1 g/l.

6. The above steps are repeated using different c_is ranging from 20 to 200 g/l. The WES researchers recommended that at least two tests should be performed at the proposed operational concentration. If the operational concentration is not available, a c_i = 145 g/l can be used.

The zone settling test is performed according to the following steps:

Steps 1, 2 and 3 are the same as those in flocculent settling test, except determine the c_i by drawing off three samples before the slurry is pumped into the settling column.

4. When the filling process is finished, shut off the air supply and start the test.

5. Observe the settling behavior of the slurry carefully. When a sharp interface between the sediment laden water and the clear supernatant water is formed, record its height and the time elapsed.

6. At regular time intervals record the height of the interface until the height vs. log (time) plot becomes almost linear.

7. Repeat the above procedures for different c_i values. For the purpose of comparison, at least two tests, one on the high c_i side and the other on the low c_i side, should be performed using the concentrations identical to those used in flocculent settling test.

The main difference between the two tests is that in flocculent settling test samples are regularly withdrawn from the column for the determination of the concentration profiles, but not in the zone settling test.

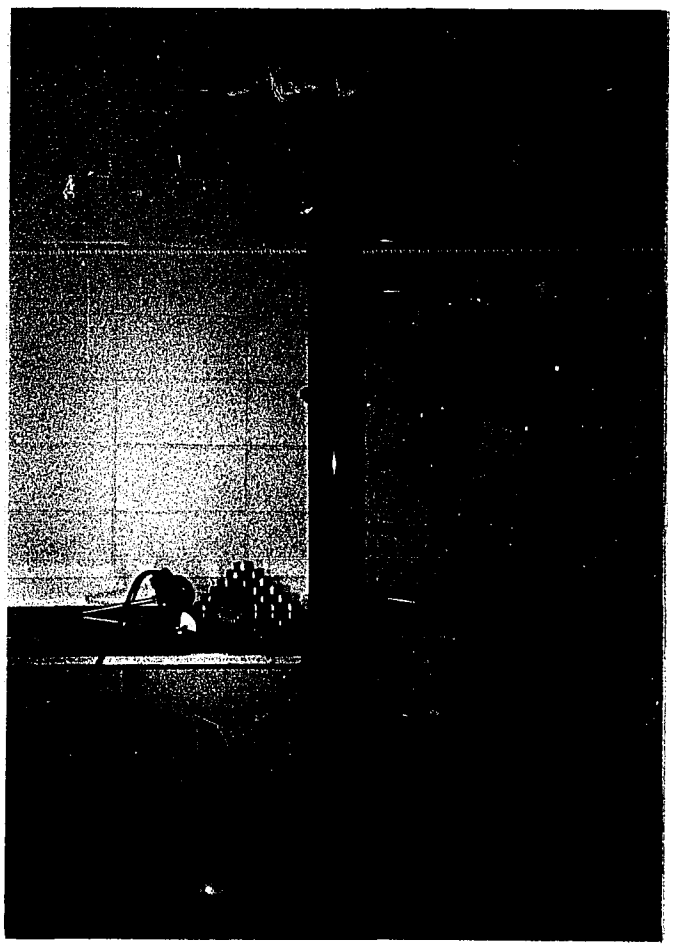

Figure 2.7. Sample withdrawal at regular time intervals

Test Program

All the tests in this study and their experimental conditions are listed in Table 2.1. The tests designated by "N" are performed according to the zone settling test procedures, i.e., no sample withdrawal, whereas the tests designated by "W" or "L" follow the flocculent settling test procedures in which samples are regularly taken. Tests L-1 and L-2 are low initial concentration tests. It can be seen that the initial concentration used in test W-1, W-2 and W-4 are very close to those for N-1, N-2 and N-4, respectively. The purpose is to examine the effect of sampling on the settling behavior of the slurry.

Table 2.1 Details of test conditions

Type of test	Experiment	Initial concentration g/l	Initial height in.	Duration hours
Zone settling test	N-1	75.3	70.75	125.0
	N-2	101.0	70.75	54.4
	N-3	147.0	70.75	56.0
	N-4	191.5	71.00	53.0
	N-5	226.5	71.25	70.3
Flocculent settling test	W-1	76.0	70.5	45.3
	W-2	99.1	70.5	119.2
	W-3	125.0	70.5	141.0
	W-4	190.0	70.5	53.3
	L-1	20.0	70.5	72.2
	L-2	30.0	70.5	124.3

CHAPTER III. PRESENTATION AND DISCUSSION OF TEST RESULTS

The settling behavior of the slurry under the condition of no sample extraction is characterized by observing the height of the interface at various times in a zone settling test. Alternately, the concentration profiles of the slurry at various times are obtained by performing the flocculent settling test procedures. The slurry height at various times is also observed in flocculent settling test. This chapter describes the observations in both zone settling and flocculent settling tests and discusses the implications of the test results. The settling curves and concentration plots resulting from both types of settling tests are summarized in the Appendix.

Concentration Profiles

To precisely and continuously measure the solid concentration along the settling column without disturbing the slurry requires elaborate testing equipment like the X-ray Transviewer. In this study, however, a crude method is employed, i.e., extracting samples from the settling column for concentration determination. Hence, the results are used only for qualitative analysis.

Figure 3.1 shows the concentration variation at various time intervals for a slurry with an initial concentration of 99.1 g/l and results are typical of most of the flocculent settling tests. The exceptions are

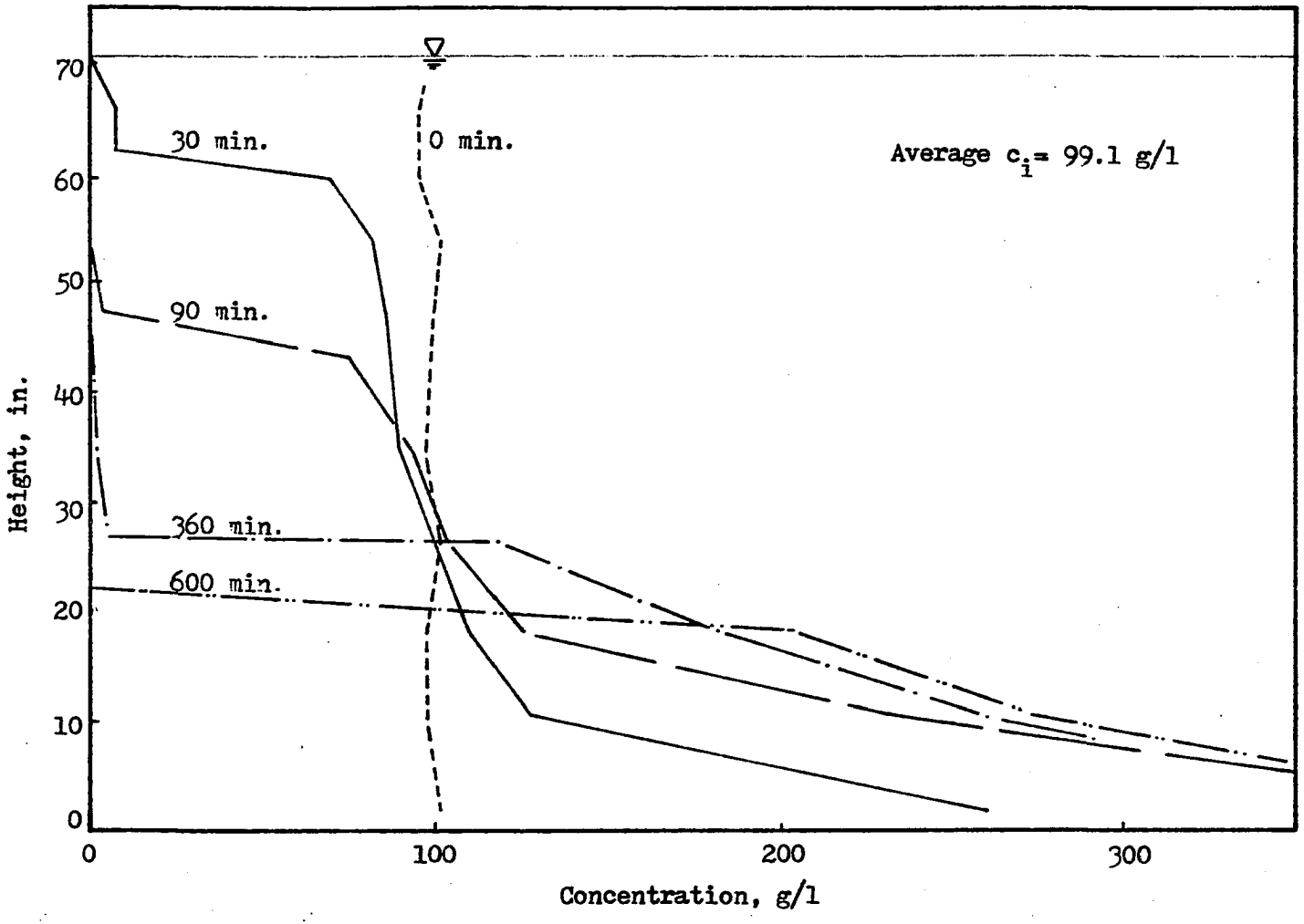

Figure 3.1. Typical concentration profiles resulting from settling test

tests with very low initial concentrations. Initially, the concentration is nearly uniform throughout the column, shown by the 0 min. profile, indicating that the air supply at the column base is able to prevent particles from accumulating during the column filling period. After the test begins, the suspension in the upper portion starts to settle and becomes less concentrated than the initial concentration, c_i. The supernatant water left above the falling suspension is turbid partly because the finer particles still suspend in water and partly as the result of the upward moving particle flux. No interface exists at this time. The jostling particle flux will eventually quiet down, the supernatant water clears up, and a sharp interface forms. From then on, all the particles seem to be locked into a three-dimensional lattice and settle as a mass.

At the column base, however, a high concentration zone is formed shortly after the test starts, which shows a high vertical concentration gradient. This zone results from the accumulation and consolidation of the fast settling flocs. As the test progresses, this zone increases in both thickness and concentration and finally meets the falling interface.

The test with low initial concentration, however, displays concentration profiles quite different from those discussed above. Figure 3.2 shows the results of a test in which c_i is equal to 30 g/l. The uniform concentration seems to decrease quickly while, at the column base, the high concentration zone forms. Then, the interface forms, and particles settle as a mass.

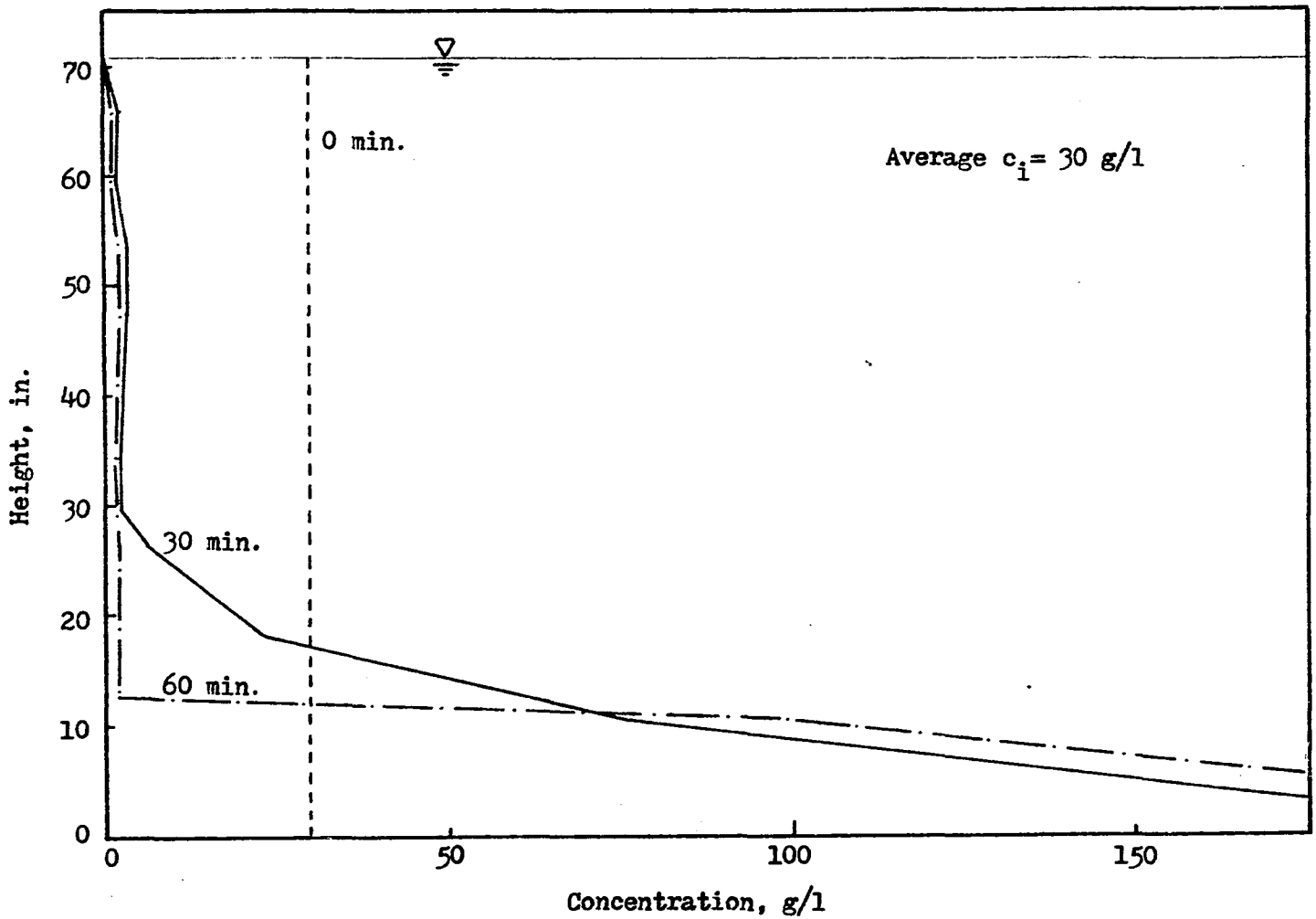

Figure 3.2. Concentration profiles for very low c_i test

Settling Behavior of Interface

Critical concentration, c_c

The zone settling test with low initial concentration, c_i, reveals that a relatively long period of time is required to form the interface. The time required to form the interface is inversely proportional to the c_i used. For example, Table 3.1 shows that the time required for the interface to form is 80 min. in test N-1 (c_i = 75.3 g/l) but 10 min. in test N-3 (c_i = 147 g/l). When c_i is higher than 147 g/l, the interface forms immediately after the test starts (N-4 and N-5). If self weight consolidation begins after the interface is formed, it is concluded that a critical concentration, c_c, exists in the settling process such that the slurry begins to consolidate under its own weight when its concentration is equal to or higher than c_c. The value of c_c depends on the

Table 3.1. Calculation of critical concentration c_c

Test	c_i g/l	H_i in.	t_c[a] min.	H_c in.	c_c[b] g/l
N-1	75.3	70.75	80	34.95	152.4
N-2	101.0	70.75	70	49.40	144.7
N-3	147.0	70.75	10	69.60	149.4
N-4	191.5	71.0			
N-5	226.5	71.25			

[a]Time required for the interface to form.

[b]Critical concentration, is calculated according to $c_c = c_i H_i / H_c$.

material being tested and the settling environment, e.g., column size and electrolyte concentration in the suspending medium.

The approximate value of c_c for a low c_i test can be obtained by the following steps. First, observe the slurry height, H_c, when the sharp interface is formed. Because the test starts with an initial concentration c_i and initial height H_i, the average concentration of the slurry is c_iH_i/H_c when the slurry height is H_c. Thus, the critical concentration c_c can be approximately taken as c_iH_i/H_c. Table 3.1 summarizes the calculation of c_cs for N-1, N-2 and N-3. The three c_c values are close and average about 148 g/l.

Observed settling behavior

Figure 3.3 shows the settling behaviors of tests N-1, N-3 and N-5, in which the observed slurry height, H, is plotted versus square root of time, $\sqrt{t}$. In general, the lower the initial concentration, the higher the settling rate. If the test starts with a high c_i (N-5), the interface immediately forms, and the settling curve shows an early convex upward portion. However, in the low c_i test (N-1), a period of time has elapsed before the interface forms, and the early convex portion is flattened. After passing the early settling period, all curves show a concave upward transition period and then become almost linear with $\sqrt{t}$.

When Figure 3.3 is compared to the theoretical S(T) vs. $\sqrt{T}$ curves for the modified self weight consolidation theory, i.e., Figure 1.9, it is observed that the shape of the settling curve resulting from the

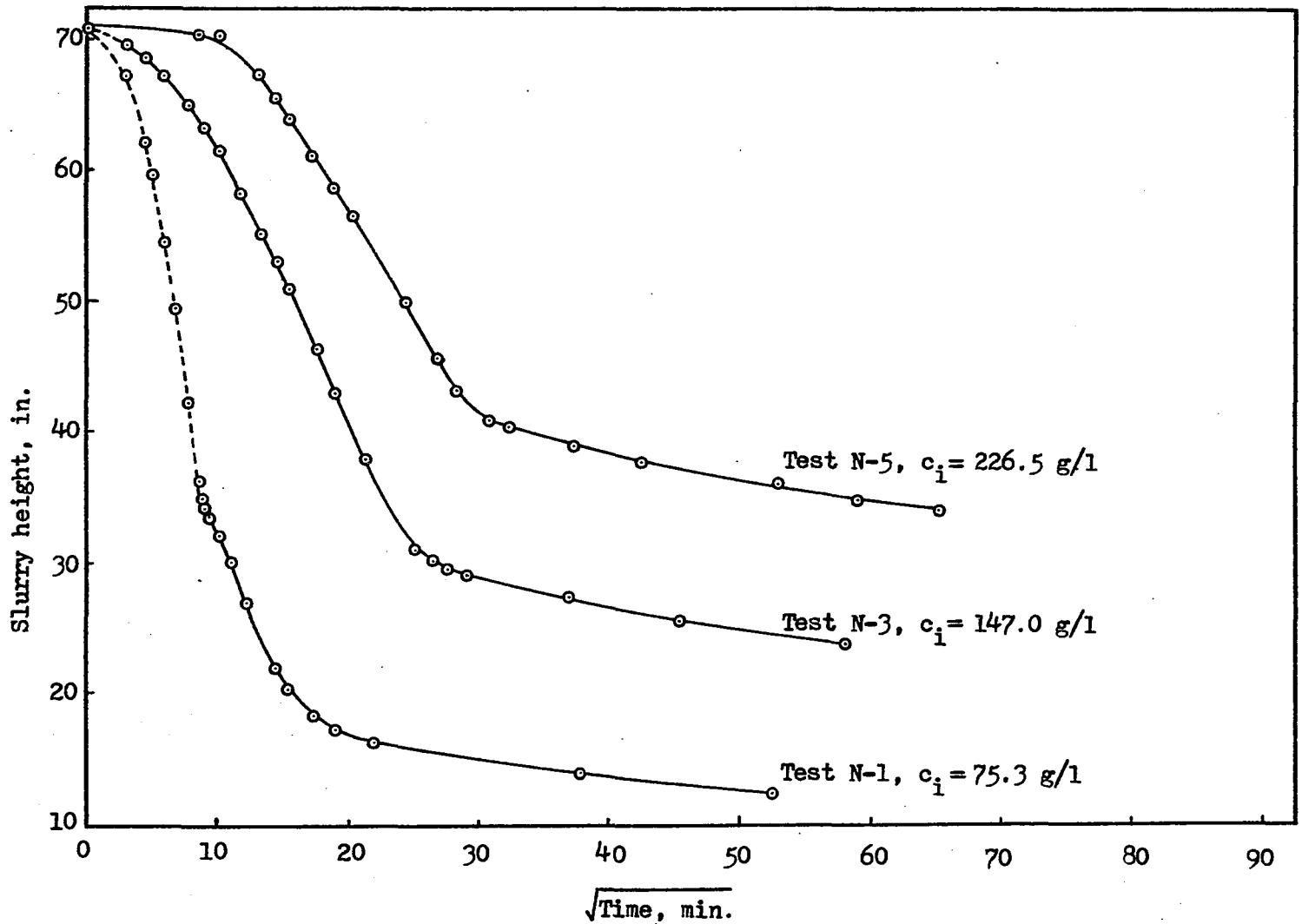

Figure 3.3. Comparison of settling behaviors of slurry at different initial concentrations

high c_i test is similar to the theoretical curve with high r value, whereas the experimental curve from the low c_i test is similar to the theoretical curve having low r value. This observation supports the hypothesis that the settling behavior of the slurry after the interface has formed can be described by the self weight consolidation theory.

If the slurry height in Figure 3.3 is plotted versus time, t, Figure 3.4 results. It is observed that the results of tests N-3 and N-5 do not show linear settling behavior in the beginning portion of the test, which is in contrast to what Kynch (1952) expected. Linear settling behavior only occurs in the early period of the c_i = 75.3 g/l (N-1) test before the interface has formed. Hence, Kynch theory is not capable of describing the zone settling behavior of the slurry.

From Figure 3.4, it is also observed that the settling behavior of the slurry depends very much on the initial concentration used, and it is impossible to obtain the settling behavior of the high c_i test from the later portion of the low c_i test because these curves are quite different in shape. Thus, the approach proposed by Talmage and Fitch (1955) does not seem correct.

Effect of Sampling on Settling Behavior

Low initial concentration test

The settling curves resulting from two c_i = 75 g/l tests, one with sample extraction (test W-1) and the other without (test N-1), are compared in Figure 3.5. Both curves show that a period of time has elapsed

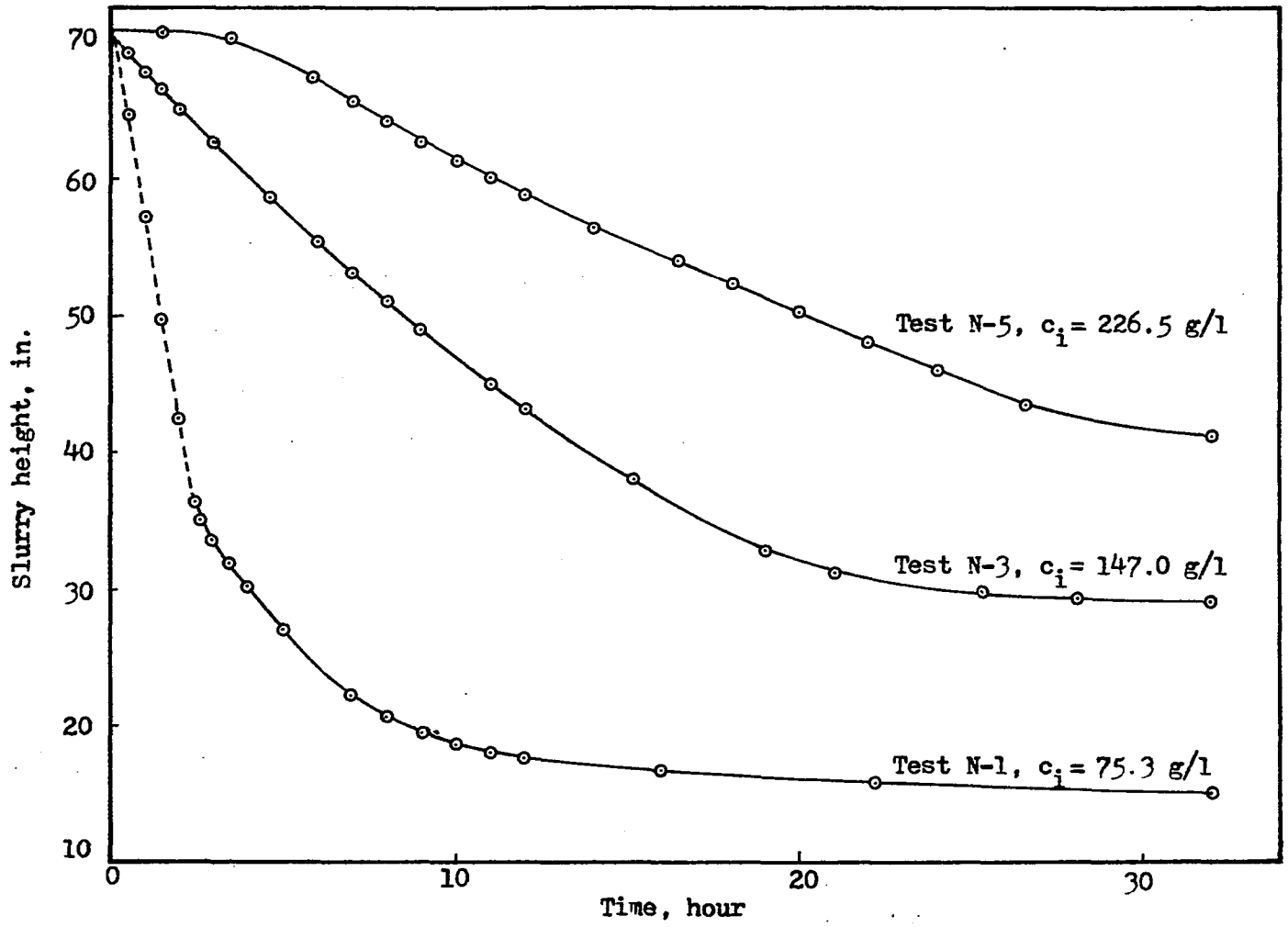

Figure 3.4. Comparison of settling behaviors of slurry at different initial concentrations

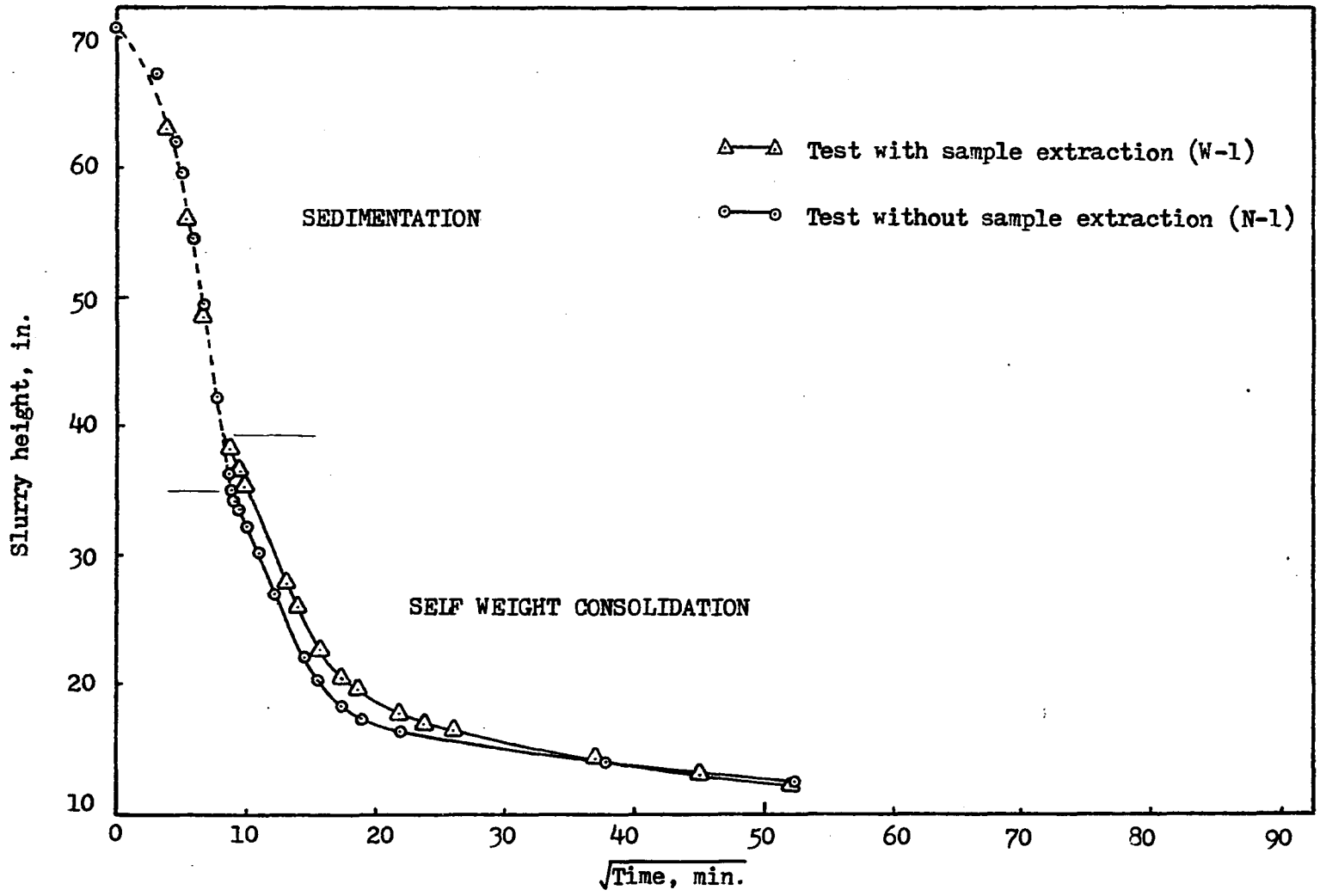

Figure 3.5. Comparison of tests with and without sample extraction (c_i = 75 g/l)

before the interface is formed. The settling behavior of the slurry in this period is obtained by observing the falling of the dark zone formed due to the concentration difference between the slurry and the turbid supernatant water. As can be seen in Figure 3.5, sample withdrawal does not produce a discernible effect on the settling behavior in this early period but slightly shortens the time required to form the interface, t_c. Due to the shorter t_c, the slurry in test W-1 lags behind in settling distance. However, after the interface has formed, sample extraction seems to accelerate the settling of the slurry because the slurry height of test W-1 eventually catches up to that of test N-1. This behavior is also observed in the comparison of tests N-2 and W-2, both having c_i = 100 g/l.

High initial concentration test

Tests N-4 and W-4, both with initial concentration about 190 g/l, are compared in Figure 3.6. Because the initial concentration is higher than the critical concentration (estimated to be about 148 g/l in previous section), the interface forms immediately after the test starts. It is noticed that the slurry in W-4, the test with regular sample extraction, shows a much higher settling rate than that in test without sample withdrawal, i.e., test N-4, indicating sample extraction increases the settling rate after the interface has formed.

Discussion

The above phenomena can be explained using a sedimentation consolidation mechanism. After the interface has formed, the system is said to

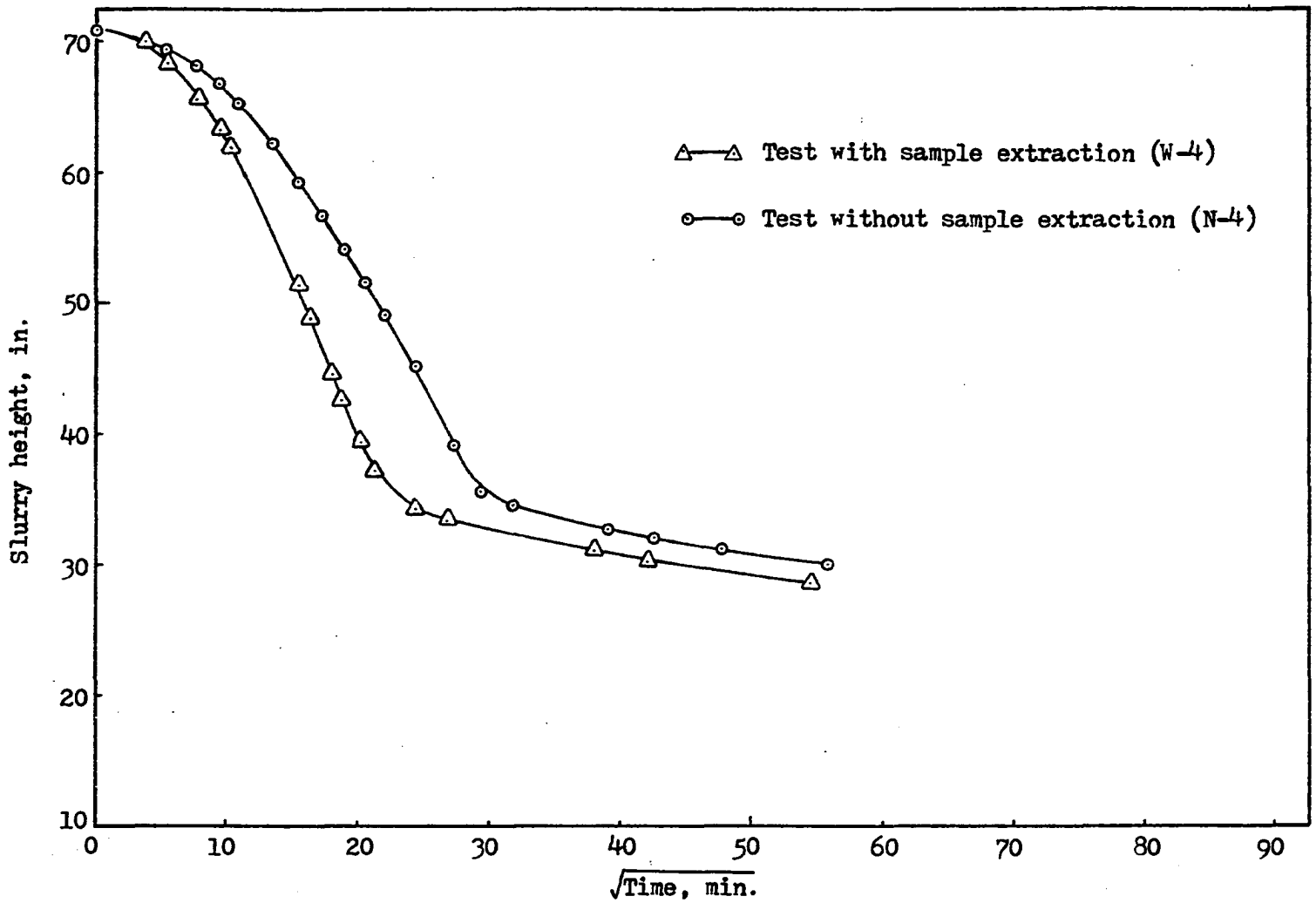

Figure 3.6. Comparison of tests with and without sample extraction (c_i = 190 g/1)

be in consolidation regime, where excess pore pressure has built up. The insertion of hypodermic needles at various depths creates many artificial passageways for pore fluid to escape, and the sample withdrawal aids the dissipation of excess pore pressure. Both accelerate the consolidation rate. However, before the interface forms, particles are in sedimentation, and no excess pore pressure exists. Thus, the sampling procedures cause only a minor influence on settling behavior. This explanation provides indirect evidence that zone settling can be considered as a self weight consolidation mechanism.

CHAPTER IV. EVALUATION OF COEFFICIENT OF CONSOLIDATION, C_F

In conventional consolidation theory, the prediction of time rate of settlement of a consolidating soil layer requires the determination of the coefficient of consolidation, c_v, for that soil. The coefficient of consolidation is a soil parameter which relates the theoretical time factor, T, to real time and the thickness of the soil layer, and thus applies the consolidation theory to prediction of the behavior of a specific soil layer. In self weight consolidation theory, the coefficient of consolidation is designated as C_F, but it is still the key parameter for describing the settling behavior of a slurry consolidating under its own weight.

As described in the previous chapter, the study by Been and Sills (1981) shows that the coefficient of consolidation can be measured using elaborate instrumentation in a settling column test. However, the equipment they used is costly, and the test procedures are time consuming and required skilled personnel to perform them. Hence, this approach is not suitable for conventional engineering design.

In this chapter, a simplified approach to evaluate the apparent coefficient of consolidation, C_F, is developed based upon the modified self weight consolidation theory by Been and Sills (1981). Because the C_F calculation in this approach requires only the zone settling test results, density and pore pressure measuring devices are not needed.

Development of Methodology

The coefficient of consolidation, C_F, is calculated according to Equation 1.37 as:

$$C_F = \frac{T\, z_o^2}{t} \tag{1.37}$$

where z_o = the modified material height to account for the void ratio change at the slurry surface

T = theoretical time factor of certain percentage of consolidation

t = real clock time corresponding to that percentage of consolidation

Usually, some curve fitting method is employed to relate the theoretical time factor T and the real time t. In this study, the square root of time fitting method is used. It should be noticed that the basic assumption for the curve fitting method is that the observed settling curves are similar in shape to the theoretical ones. Thus, it is necessary to check the validity of this assumption when the curve fitting method is applied. The following paragraphs describe the method for obtaining the necessary terms in Equation 1.37 to evaluate the C_F.

Modified material height, z_o

From Equation 1.35, the modified material height z_o can be expressed as:

$$z_o = z_1 + (e_i - e_o)/\beta \tag{4.1}$$

where z_1 = actual material height, which can be calculated as:

$$z_1 = \frac{c_i \cdot H_i}{G_s \cdot \gamma_w}$$

β = slope of final (i.e., after 100 percent primary consolidation) void ratio distribution

e_i = initial void ratio at the onset of self weight consolidation

e_o = final void ratio at the slurry surface

For clarification of each term, refer to Figure 1.7. The quantities z_1 and e_i are related to the initial test conditions; hence, they can easily be obtained. The parameters e_o and β, however, are used to describe the final void distribution and required more calculations.

Models for e_o and β Been and Sills (1981) plotted e_o and β versus the initial density of the slurry. Nevertheless, it seems more appropriate to relate e_o and β to the concentration at which self weight consolidation starts. All the settling column tests with initial concentration, c_i, lower than the critical concentration, c_c, will start the consolidation process at the critical concentration c_c and thus are assumed to result in only one set of e_o and β after 100 percent primary consolidation. Any test with c_i higher than c_c will result in a set of e_o and β values corresponding to its initial concentration because consolidation begins immediately after the test starts. Conceptually, there exists a limiting concentration, c_m, beyond which a normally consolidated soil stratum is formed, and no self weight consolidation occurs. Thus, if $c_i \geq c_m$, the uniform initial concentration profile is maintained

because of no self weight consolidation, or $\beta = 0$ and $e_o = e_i$. Between the two limits c_m and c_c, e_o and β are assumed to be functions of c_i only. Many simple functions satisfying the conditions at the limiting concentration c_m were evaluated, but it was found that only the logarithmic function can be successfully applied. Thus, the models for describing the variation of e_o and β between c_m and c_c are assumed to be:

$$e_o = e_m + k_2 \ln(c_m/c_i)$$

$$\beta = k_1 \ln(c_m/c_i) \qquad c_c \leq c_i \leq c_m \qquad (4.2)$$

where e_m = void ratio corresponding to the limiting concentration, c_m, can be calculated as:

$$e_m = (G_s \cdot \gamma_w/c_m) - 1$$

k_1 = proportional constant having a unit of 1/length in order to satisfy the dimension equality in Equation 1.35

k_2 = dimensionless constant

Slurry height after 100% primary consolidation, H_{100} The determination of the critical concentration c_c has been discussed in Chapter III, but to obtain the parameters c_m, k_1 and k_2 in Equation 4.2 it is necessary to introduce a quantity which can be measured in the settling column test and relates c_m with k_1 and k_2. For this, the slurry height after 100 percent self weight consolidation, H_{100}, is chosen. Theoretically, H_{100} is related to e_o and β as:

$$H_{100} = \int_0^{z_1} (1 + e_o - \beta z_1 + \beta z)dz = (1 + e_o)z_1 - \tfrac{1}{2}\beta z_1^2 \qquad (4.3)$$

Combining Equation 4.2 with 4.3, the expression for H_{100} becomes:

$$H_{100} = \left[k_2(\ln c_m - \ln c_i) + \frac{G_s \gamma_w}{c_m} \right] z_1 -$$

$$\tfrac{1}{2}k_1(\ln c_m - \ln c_i)\, z_1^2 \qquad (4.4)$$

The quantity H_{100} for a zone settling test can be estimated from the settling curve. First, the observed slurry height is plotted against $\sqrt{t}$. Usually, the later portion of the curve becomes approximately horizontal; therefore, the slurry height corresponding to this horizontal portion is taken as H_{100}. For example, Figure 4.1 shows the slurry height vs. $\sqrt{t}$ curve for test N-3(c_i = 147 g/l), and the H_{100} is estimated to be about 18.8 in.

In order to solve the three unknown quantities c_m, k_1 and k_2 in Equation 4.4, at least three zone settling tests on the same material should be performed. The e_o and β values for any specific test are then obtained by Equation 4.2, and the corresponding z_o is calculated by Equation 4.1.

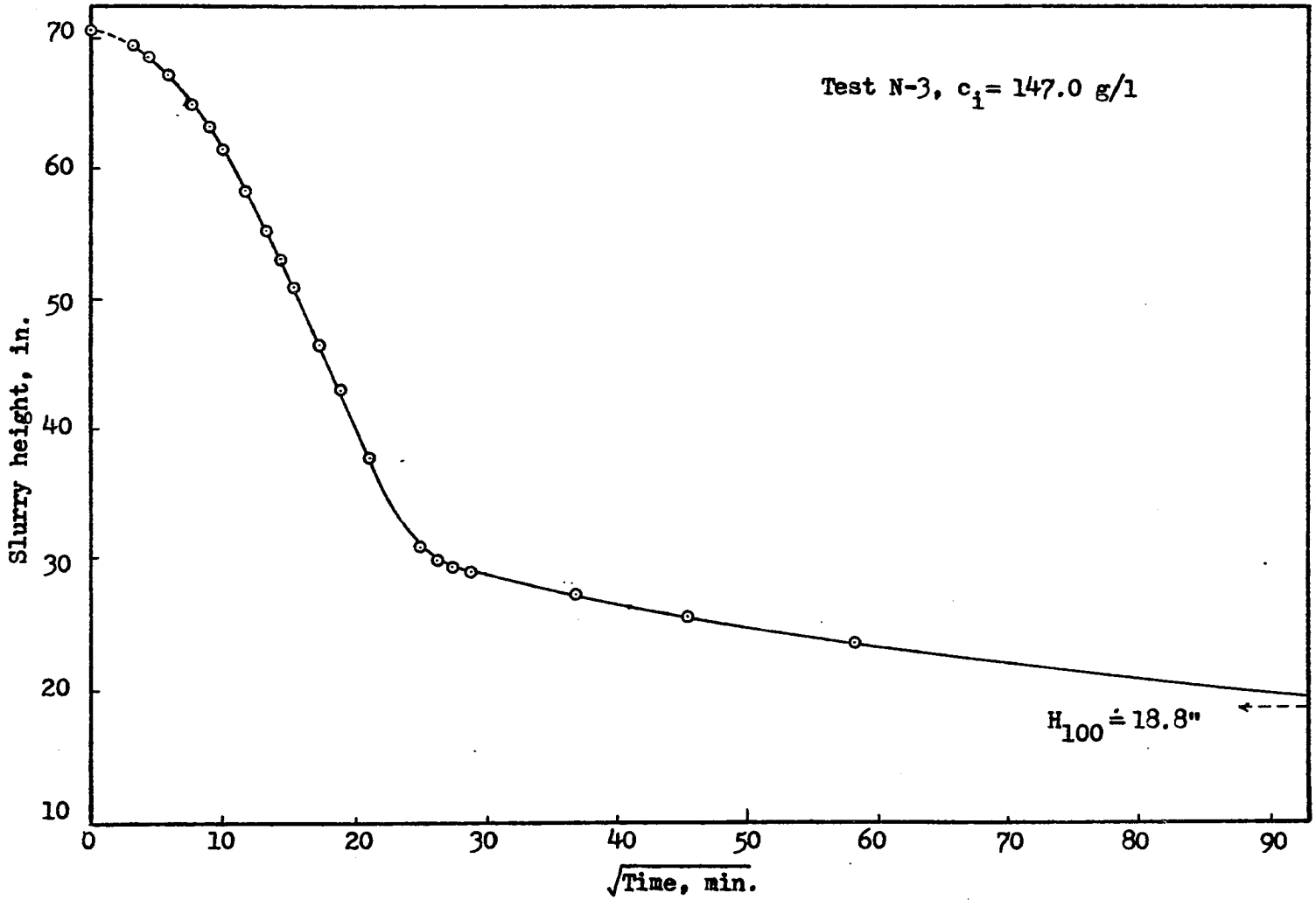

Figure 4.1. Estimation of the slurry height after 100% primary consolidation, H_{100}

Time factor, T, and real time, t

The degree of consolidation, $S_m(T)$, for the modified self weight consolidation theory is given by Equation 1.48 and can be simplified as:

$$S_m(T) = \frac{\sum_n \left\{ \left[\frac{\sin Mr}{M^3} - \frac{r \cos Mr}{M^2} \right] \cdot \left[1 - \exp(-M^2 T) \right] \right\}}{\sum_n \left[\frac{\sin Mr}{M^3} - \frac{r \cos Mr}{M^2} \right]} \qquad (4.5)$$

where $T = C_F \cdot t/z_o^2$

$M = m\pi = \frac{1}{2}(2n + 1)\pi \qquad n = 0, 1, 2 \ldots.$

$r = z_1/z_o$

Thus, $S_m(T)$ is a function of both time factor T and the ratio r. For a specific test, z_1 and z_o, and therefore r, can be obtained by the approach discussed in the previous section. Knowing the value of r, a theoretical $S_m(T)$ vs. $\sqrt{T}$ curve corresponding to this test results.

To illustrate $\sqrt{t}$ - fitting method, the results of test N-3 are used as an example. The observed slurry height for this test is plotted against $\sqrt{t}$ in Figure 4.2. Because r value for this test is about 0.22, the theoretical $S_m(T)$ vs. $\sqrt{T}$ curve for r = 0.22 is constructed from Equation 4.5 as in Figure 4.3. The following procedures are performed to obtain both T and t for 90 percent self weight consolidation of the slurry:

1. On the theoretical curve, e.g., Figure 4.3, locate the inflection point, B, and draw a tangent line through B to intersect the 0 percent horizontal line at point, A.

2. Find the 90 percent consolidation point, P, on the theoretical curve. The time factor for 90 percent

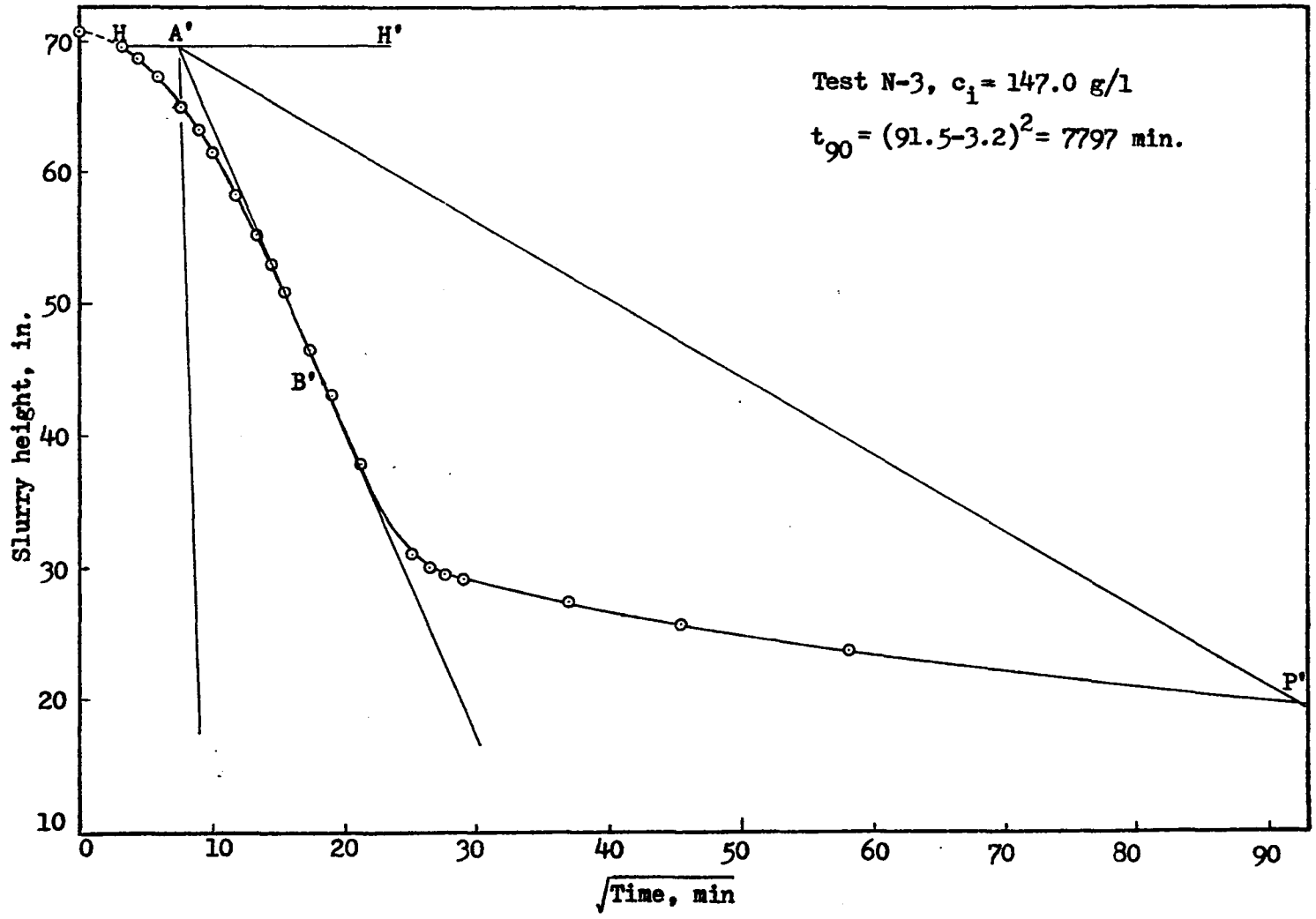

Figure 4.2. $\sqrt{t}$-fitting method applied on the settling curve of test N-3(r = 0.22)

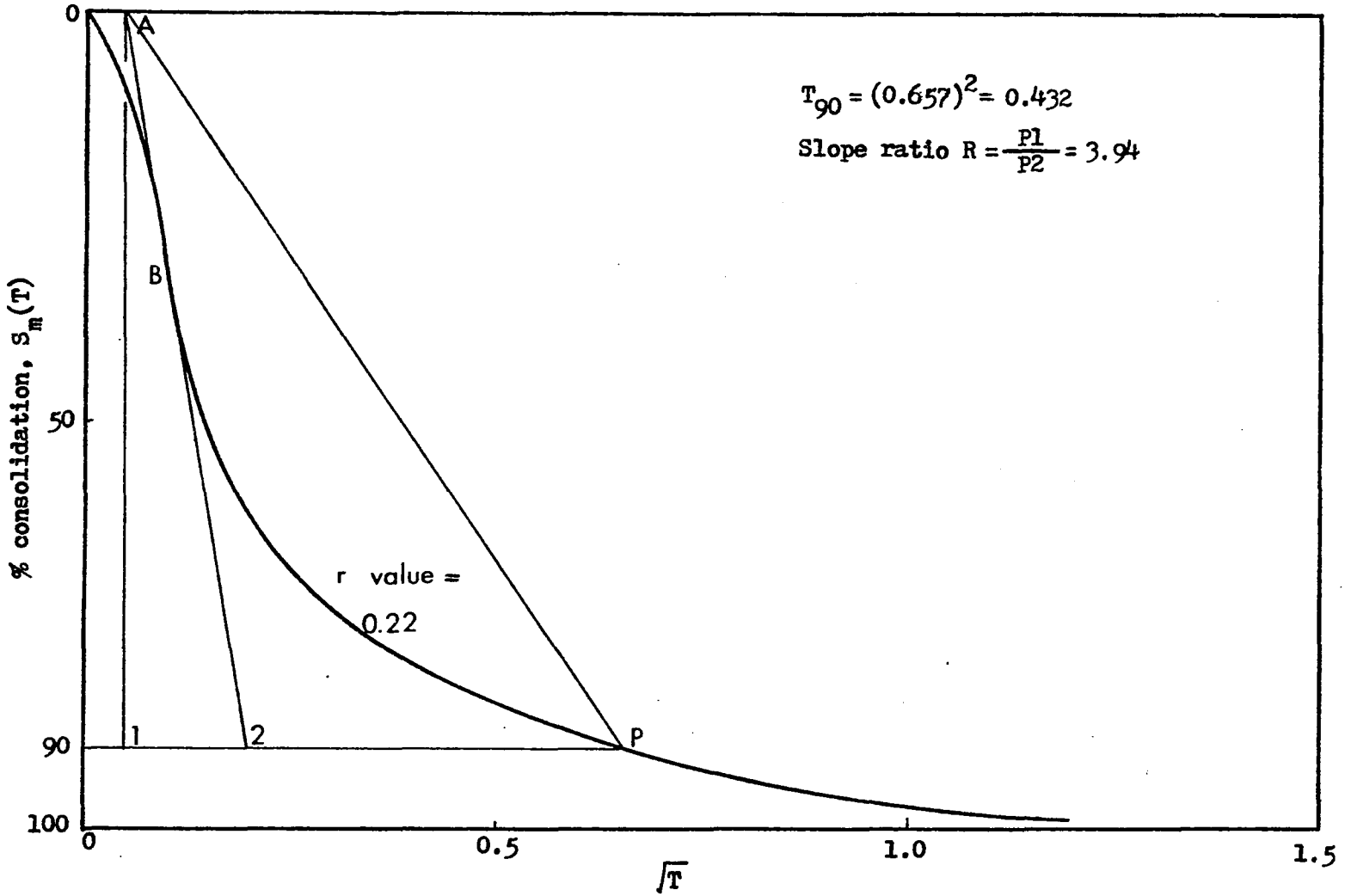

Figure 4.3. $\sqrt{t}$-fitting method applied on the theoretical $S_m(T)$ vs $\sqrt{T}$ curve with r = 0.22

consolidation is obtained by reading the T-coordinate for point P. For r = 0.22,

$$T_{90} = (0.657)^2 = 0.432$$

3. Connect points A and P, and estimate the ratio, R, of the slope of line AP to that of the tangent line AB. In this example, R = 3.94.

4. On the experimental zone settling curve, e.g., Figure 4.2, locate the starting point of self weight consolidation, H, i.e., the height at which the interface forms, and draw a horizontal line HH' through it. Line HH' is the experimental 0 percent consolidation line.

5. Draw a tangent line through the inflection point, B', of experimental settling curve to intersect line HH' at point A'.

6. From point A' on the experimental curve, draw a straight line A'P', having a slope R times the tangent line A'B' to intersect the settling curve at point P'. Experimental point P' corresponds to the theoretical time factor when the slurry reaches 90 percent self weight consolidation, and the corresponding time is t_{90}. In the low c_i test, the time required for slurry to reach the critical concentration should be subtracted from the obtained t_{90} to yield a modified one. In other words, the origin of the height vs. $\sqrt{t}$ plot needs to be adjusted to eliminate the time for sedimentation. In this example, the modified t_{90} = 7797 min.

After z_o, T_{90} and t_{90} are determined, the coefficient of consolidation C_F for the test can be calculated according to Equation 1.37. It is observed that the value of C_F varies with test conditions such as initial concentration, column size, initial slurry height, etc.

Summary of Procedures for Determining C_F

To evaluate the apparent coefficient of consolidation C_F, the following steps should be followed.

1. Perform zone settling tests at different selected initial concentrations, ranging from 20 g/l to 200 g/l. At least two low c_i tests are needed to obtain the critical concentration c_c, and additional three tests with $c_i > c_c$ are required to determine the three constants c_m, k_i and k_2.

2. Plot the observed slurry height, H, versus $\sqrt{t}$ curves separately for each test.

3. Estimate the quantity H_{100} for each test from the corresponding H vs. $\sqrt{t}$ curve.

4. Establish three experimental simultaneous, equations according to Equation 4.4 using three sets of z_1, c_i and H_{100} values, which are the results of three tests with $c_i > c_c$ and solve for c_m, k_1 and k_2.

5. The e_o and β values for any c_i between c_m and c_c can be obtained by Equation 4.2. It should be noticed that all the tests with c_i lower than c_c will start the consolidation process at the concentration c_c, and therefore result in only one set of e_o and β.

6. The modified material height z_o is determined from: $z_o = z_1 + (e_i - e_o)/\beta$, and $r = z_1/z_o$. For all the $c_i < c_c$ tests, e_i is considered as the average void at the onset of self weight consolidation, i.e., $e_i = (G_s \cdot \gamma_w/c_c) - 1$ for $c_i < c_c$ tests.

7. For each test, construct a theoretical $S_m(T)$ vs. $\sqrt{T}$ curve based on the appropriate r value, and determine T_{90} and t_{90} by the curve fitting procedures discussed in the previous section.

8. The apparent coefficient of consolidation C_F is calculated according to:

$$C_F = \frac{T_{90} \cdot z_o^2}{t_{90}} \qquad (4.6)$$

Sample Calculations

The test results of the five zone settling tests, N-1 to N-5, are used for C_F calculations. Test conditions and observations are listed in Table 4.1. Following the procedures prescribed for C_F determination, the results for each step are:

1. Three low c_i tests N-1, N-2 and N-3 result in a critical concentration about 148 g/l.

2. The slurry height vs. $\sqrt{t}$ plots for each test are shown in the Appendix.

3. The values of H_{100} resulting for each test are listed in Table 4.1.

4. Because the initial concentrations used in the tests N-1, N-2 and N-3 are all smaller than c_c, these three tests yield only one set of e_o and β values corresponding to c_c = 148 g/l. Three simultaneous equations can be set up by putting the H_{100} and z_1 of each of the three tests in Equation 4.3, i.e.,

$$\text{test N-1:} \quad 10.5 = (1 + e_o) \cdot 1.9443 - \tfrac{1}{2} \cdot \beta \cdot (1.9443)^2 \qquad (4.7a)$$

$$\text{test N-2:} \quad 13.3 = (1 + e_o) \cdot 2.6079 - \tfrac{1}{2} \cdot \beta \cdot (2.6079)^2 \qquad (4.7b)$$

$$\text{test N-3:} \quad 18.8 = (1 + e_o) \cdot 3.7957 - \tfrac{1}{2} \cdot \beta \cdot (3.7957)^2 \qquad (4.7c)$$

Only two of the above equations are needed to solve for e_o and β. The third equation, however, can serve as a check to see if the model is suitable. For example, Equations 4.7a and 4.7b yield:

$$e_o = 5.3$$

$$\beta = 0.91 \text{ in.}^{-1} \quad \text{for } c_c = 148 \text{ g/l}$$

If this set of values is used to predict the H_{100} for test N-3, the result is:

$$H_{100} = (1 + e_o) \cdot 3.7957 - \tfrac{1}{2} \cdot \beta \cdot (3.7957)^2 = 17.3 \text{ inch},$$

Table 4.1. Summary of the conditions and results of zone settling tests

Test	c_i g/l	H_i in.	z_1[a] in.	H_{100} in.	e_i	e_o	β in.$^{-1}$	z_o in.	r
N-1	75.3	70.75	1.9443	10.5	17.5	5.3	0.91	15.4	0.13
N-2	101.0	70.75	2.6079	13.3	17.5	5.3	0.91	16.1	0.16
N-3	147.0	70.75	3.7957	18.8	17.5	5.3	0.91	17.3	0.22
N-4	191.5	71.0	4.9622	26.0	13.3	5.7	0.64	16.8	0.30
N-5	226.5	71.25	5.8898	32.8	11.1	5.9	0.47	16.9	0.35

[a] z_1 is calculated using $G_s = 2.74$.

which is close to the observed value of 18.8 inch.

The obtained e_o and β values can then be used together with Equation 4.2, and two equations are generated:

$$5.3 = e_m + k_2(\ln c_m - \ln 148) \tag{4.8a}$$

$$0.91 = k_1(\ln c_m - \ln 148) \tag{4.8b}$$

An additional equation can be obtained using the results of test N-5 and Equation 4.4, i.e.,

$$32.8 = \left[k_2(\ln c_m - \ln 226.5) + \frac{2740}{c_m}\right] \cdot 5.8898 - \tfrac{1}{2} \cdot k_1(\ln c_m - \ln 226.5)(5.8898)^2, \tag{4.8c}$$

where $G_s = 2.74$ according to the result of specific test on the sediments used. Equations 4.8a, 4.8b and 4.8c yield the solutions of:

$$c_m = 360 \text{ g/l}$$

$$k_1 = 1.02 \text{ in.}^{-1}$$

$$k_2 = -1.50$$

The observed H_{100} of test N-4 has not been used in the above calculations; hence, it can serve as a check. Using the obtained constants, the H_{100} for test N-4 is predicted as:

$$H_{100} = \left[-1.50(\ln 360 - \ln 191.5) + \frac{2740}{360}\right] \cdot 4.9622 - \tfrac{1}{2} \cdot 1.02(\ln 360 - \ln 191.5) \cdot (4.9622)^2$$

$$= 25.1 \text{ in.}$$

which is close to the observed value of 26.0 in. with about 3.5 percent error. Hence, the logarithmic model used for describing the variation of e_o and β with concentration seems suitable.

5. The values of e_o and β for each test are calculated and listed in Table 4.1.

6. The modified material height z_o and ratio r are obtained and also listed in Table 4.1. It is noticed that as the c_i increases, the r value also increases.

7. Figure 4.4 shows the $S_m(T)$ vs. $\sqrt{T}$ curves for different r values corresponding to different tests. It is observed that when r becomes smaller, the initial convex upward portion of the theoretical curve gradually flattens. This trend is also observed in zone settling curves as c_i decreases (see Figure 3.3). Because the results in step 6 indicate that a lower c_i test results in a lower r value, it can then be concluded that the varying trend of the theoretical curves is identical to that of the settling curves. Thus, the assumption of the curve fitting method is approximately satisfied, and the method is appropriate for use. For each test, the $\sqrt{t}$ - fitting method yields a set of T_{90} and t_{90} values, which are listed in Table 4.2.

8. The apparent coefficient of consolidation C_F for each test is calculated, and the results are also listed in Table 4.2.

Table 4.2. Calculation of the coefficient of consolidation, C_F

Test	c_i g/l	z_o in.	t_{90} min.	T_{90}	C_F in.^{2}/min.
N-1	75.3	15.4	497	0.215	0.103
N-2	101.0	16.1	2052	0.298	0.038
N-3	147.0	17.3	7797	0.432	0.017
N-4	191.5	16.8	7744	0.545	0.020
N-5	226.5	16.9	5730	0.608	0.030

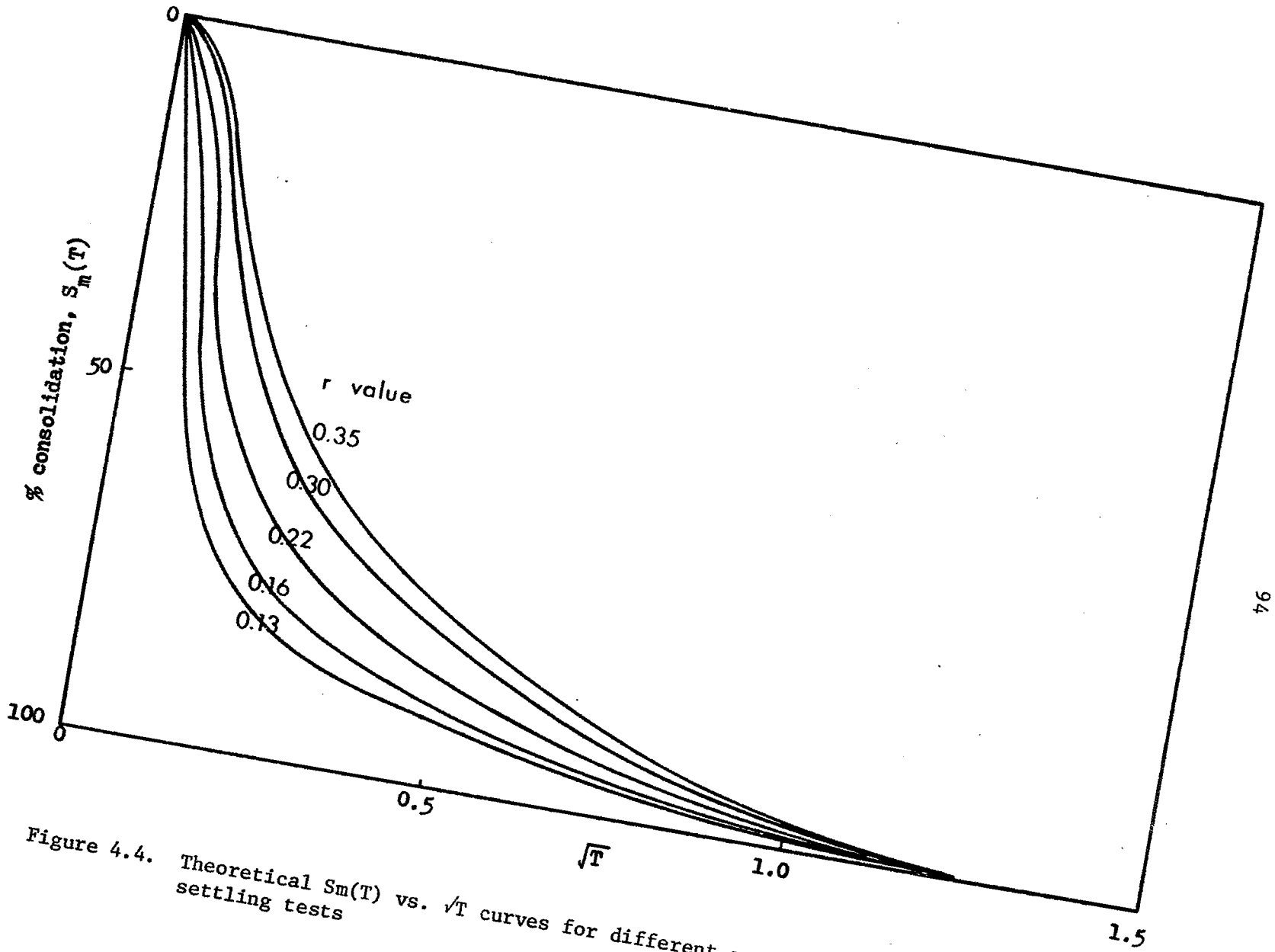

Figure 4.4. Theoretical Sm(T) vs. $\sqrt{T}$ curves for different r values obtained from the settling tests

CHAPTER V. CONCLUSIONS AND RECOMMENDATIONS

Conclusions

The findings of this study are the following:

1. The classical theories used by mining or chemical engineers for describing the settling mechanism of particles in a fluid emphasized entirely on the "sedimentation" phenomenon in which the weight of particles is solely supported by hydrodynamic forces, and neglected that particles will eventually come into contact, develop effective stresses and consolidate under their own weight. Hence, the theories are not adequate for studying the settling behavior of the slurry in a containment area.

2. The WES interpretation of the settling column test results separates zone settling behavior from consolidation processes. This study indicates that zone settling behavior of the slurry is the result of self weight consolidation. In addition, if the time rate settlement of dredge materials is predicted according to the one-dimensional consolidation theory, as in the WES approach, the settling rate in the early consolidation period will be overestimated.

3. The interface, separating the clear supernatant water from the particle laden water, will not form in the tests with low initial concentration unless the average concentration of the slurry has reached certain value, i.e., critical concentration.

4. The self weight consolidation theory, developed by Lee and Sills (1981) and modified by Been and Sills (1981), is used to describe the zone settling behavior in this study. This study shows that the ratio, r, of actual to modified material height relates the theoretical consolidation curves to corresponding zone settling curves.

5. Based on the modified self weight consolidation theory, an approach for estimating the apparent coefficient of consolidation C_F, utilizing primarily the results of the settling column test, is feasible. The method should not only facilitate the test procedures for estimating

the C_F, but also yield a better prediction of the C_F because the method precisely defines the point at which self weight consolidation begins.

Recommendations for Future Study

Successful application of the large strain consolidation theory, i.e., Equation 1.17, depends very much on the reasonable assumptions of the permeability, K, vs. the void ratio, e, and the effective stress, σ', vs. e relationships. Though the linear K vs. e and σ' vs. e relationships assumed by Lee and Sills (1981) facilitate the solving of the highly nonlinear differential equation (Equation 1.17), both assumptions can not be justified by the experimental results. Further study on these two relationships is needed. The following assumptions might make the model a better approximation of reality.

1. According to Equation 1.41, the permeability of soil seems to vary linearly with $e^3/1 + e$ instead of $1 + e$ as assumed by Lee and Sills.

2. Been and Sills (1981) found that when the effective stress σ' is very low, the σ' vs. e relationship is not unique. Because the behavior of e in low effective stress range associates with the phenomenon of creep or viscous flow, a thermodynamic model might be needed for the study of the σ' vs. e relationship.

REFERENCES

Been, K. and G. C. Sills. 1981. Self-Weight Consolidation of Soft Soils: An Experimental and Theoretical Study. Geotechnique 31, No. 4: 519-535.

Coe, H. S. and G. H. Clevenger. 1916. Methods for Determining the Capacities of Slime-Settling Tanks. American Institute of Mining Engineers Transactions 55, No. 9: 356-384.

Fitch, B. 1962. Sedimentation Process Fundamentals. American Institute of Mining Engineers Transactions 223: 129-137.

Gallagher, B. J. and Company. 1978. Investigation of Containment Area Design to Maximize Hydraulic Efficiency. U.S. Army Engineer Waterways Experiment Station, CE, Vicksburg, Miss., Technical Report D-78-12.

Gaudin, A. M. and M. C. Fuerstenau. 1958. The Transviewer - X Rays to Measure Suspended Solids Concentration. Engineering and Mining Journal 159, No. 9: 110-112.

Gaudin, A. M., M. C. Fuerstenau and S. R. Mitchell. 1959. Effect of Pulp Depth and Initial Pulp Density in Batch Thickening. American Institute of Mining Engineers Transactions 214: 613-616.

Gaudin, A. M. and M. C. Fuerstenau. 1962. Experimental and Mathematical Model of Thickening. American Institute of Mining Engineers Transactions 223: 122-129.

Gibson, R. E., G. L. England and M. J. L. Hussey. 1967. The Theory of One-Dimensional Consolidation of Saturated Clays. Geotechnique 17, No. 3: 261-273.

Hayden, M. L. 1978. Prediction of Volumetric Requirements for Dredged Material Containment Areas. U.S. Army Engineer Waterways Experiment Station, CE, Vicksburg, Miss., Technical Report D-78-41.

Huston, J. 1970. Hydraulic Dredging. Cambridge, MD, Cornell Maritime Press, Inc.

Kynch, C. J. 1952. A theory of Sedimentation. Faraday Society Transactions 48: 166-176.

Lacasse, S. E., T. W. Lambe and W. A. Marr. 1977. Sizing of Containment Areas for Dredged Material. U.S. Army Engineer Waterways Experiment Station, CE, Vicksburg, Miss., Technical Report D-77-21.

Lee, K. and G. C. Sills. 1981. The Consolidation of a Soil Stratum, Including Self-Weight Effects and Large Strains. International Journal for Numerical and Analytical Methods in Geomechanics 5: 405-428.

Lin, T. W., O. G. Lara, R. A. Lohnes, and M. D. Dougal. 1981. Study of Sedimentation in Lake Panorama. Progress Report submitted to Central Iowa Energy Cooperative, Cedar Rapids, Iowa.

Mclaughlin, R. T. 1959. The Settling Properties of Suspensions. American Society of Civil Engineers Proceedings 85, No. HY12: 9-41.

Michaels, A. S. and J. C. Bolger. 1962. Settling Rates and Sediment Volumes of Flocculated Kaolin Suspensions. Industrial and Engineering Chemistry Fundamentals 1: 24-33.

Montgomery, R. L. 1978. Methodology for Design of Fine-Grained Dredged Material Containment Areas for Solids Retention. U.S. Army Engineer Waterways Experiment Station, CE, Vicksburg, Miss., Technical Report D-78-56.

Palermo, M. R., R. L. Montgomery, and M. E. Poindexter. 1978. Guidelines for Designing, Operating, and Managing Dredged Material Containment Areas. U.S. Army Engineer Waterways Experiment Station, CE, Vicksburg, Miss., Technical Report DS-78-10.

Schaefer, V. R. 1980. Preliminary Investigation of Sedimentation in Lake Panorama, Iowa. Unpublished M.S. Thesis. Iowa State University Library, Ames.

Talmage, W. P. and E. B. Fitch. 1955. Determining Thickener Unit Areas. Industrial and Engineering Chemistry 47, No. 1: 38-41.

Taylor, D. W. 1948. Fundamentals of Soil Mechanics. New York, N.Y., John Wiley & Sons.

Terzaghi, K. 1925. Erdbaumechanik. Vienna, Franz Deuticke.

Terzaghi, K. and O. K. Fröhlich. 1936. Theorie der Setzung von Tonschichten. Vienna, Franz Deuticke.

ACKNOWLEDGMENTS

I wish to express my sincerest appreciation to Dr. Robert A. Lohnes for all the assistance and guidance he provided during my study at Iowa State University. His encouragement and discussions have made invaluable contributions to this dissertation.

My appreciation also goes to Drs. Richard L. Handy, Turgut Demirel, Ronald L. Rossmiller and Roger W. Bachmann for serving on my committee.

I thank my wife, Su-Men, who typed the original manuscript and endured many hardships during the thesis preparation period.

I gratefully acknowledge Central Iowa Energy Cooperative for funding this research project and the support of the Engineering Research Institute of Iowa State University.

APPENDIX. TEST RESULTS

Results of Zone Settling Tests

The slurry height at various times was observed during the settling column test without sample extraction. In Figures A-1 to A-5, the observed slurry height, H, is plotted versus $\sqrt{t}$, and the slurry height corresponding to 100 percent self weight consolidation, H_{100}, for each test is estimated. In addition, the t_{90} for each test results by applying the $\sqrt{t}$-fitting method.

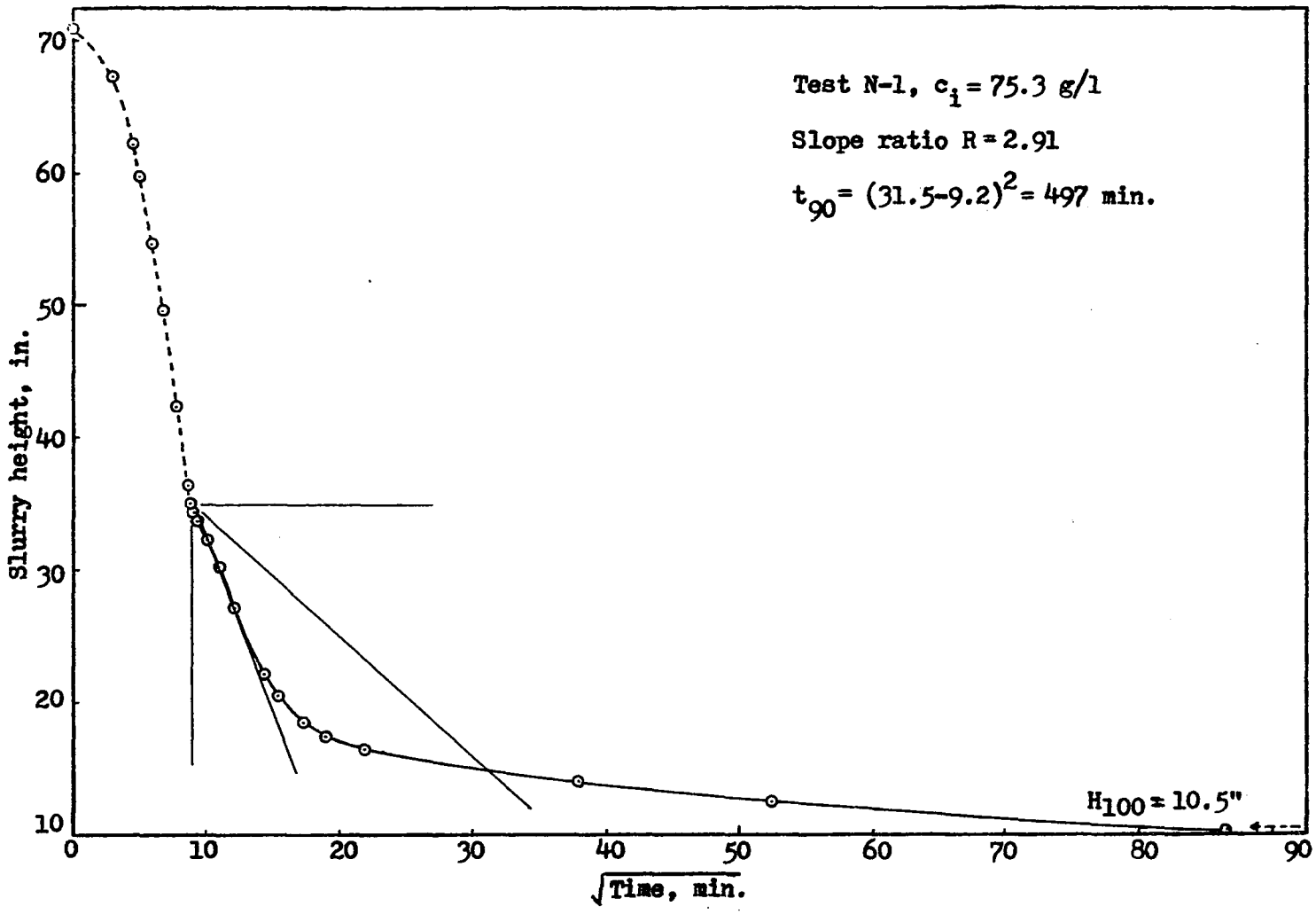

Figure A-1. The H vs. √t plot for test N-1

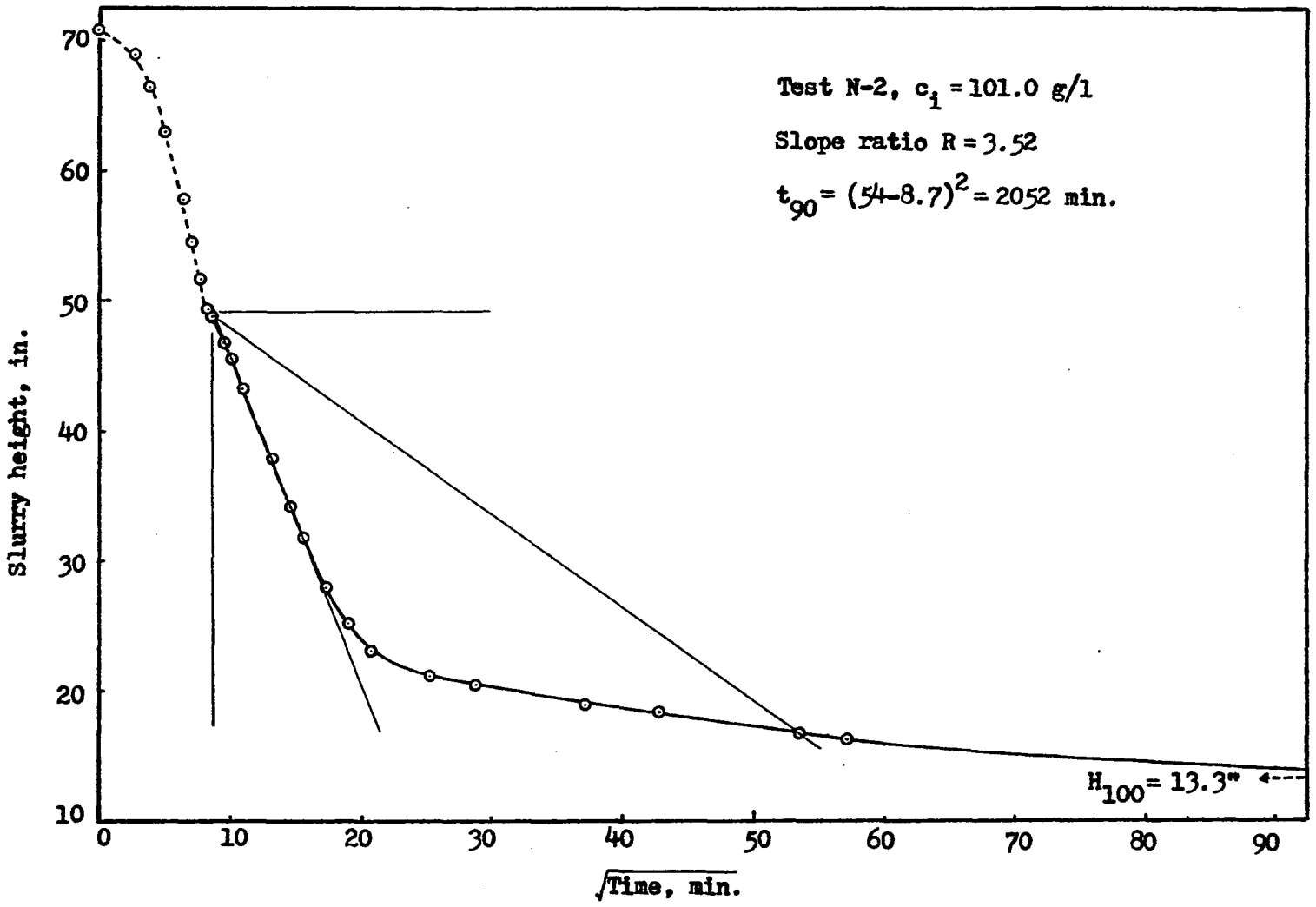

Figure A-2. The H vs. √t plot for test N-2

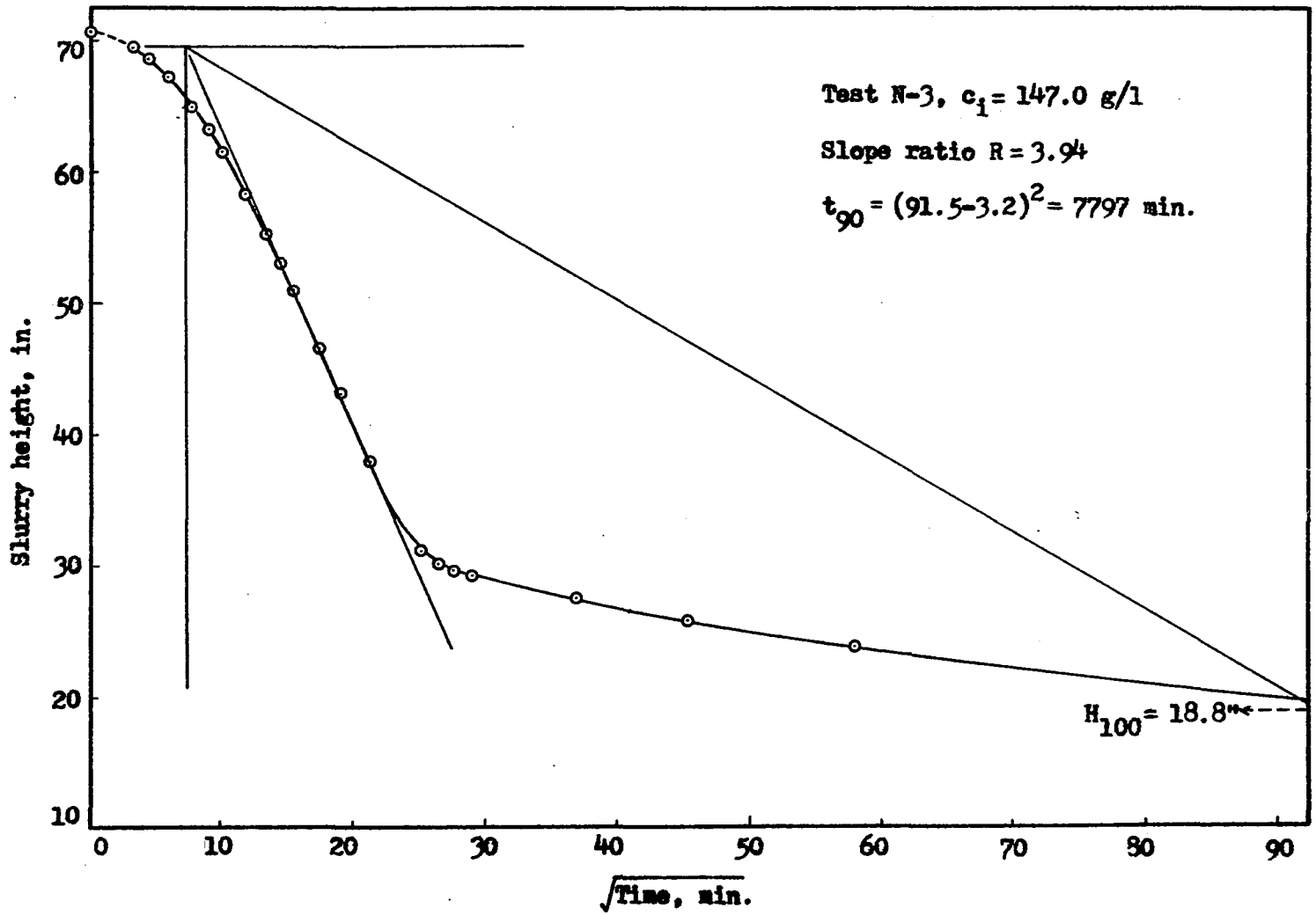

Figure A-3. The H vs. √t plot for test N-3

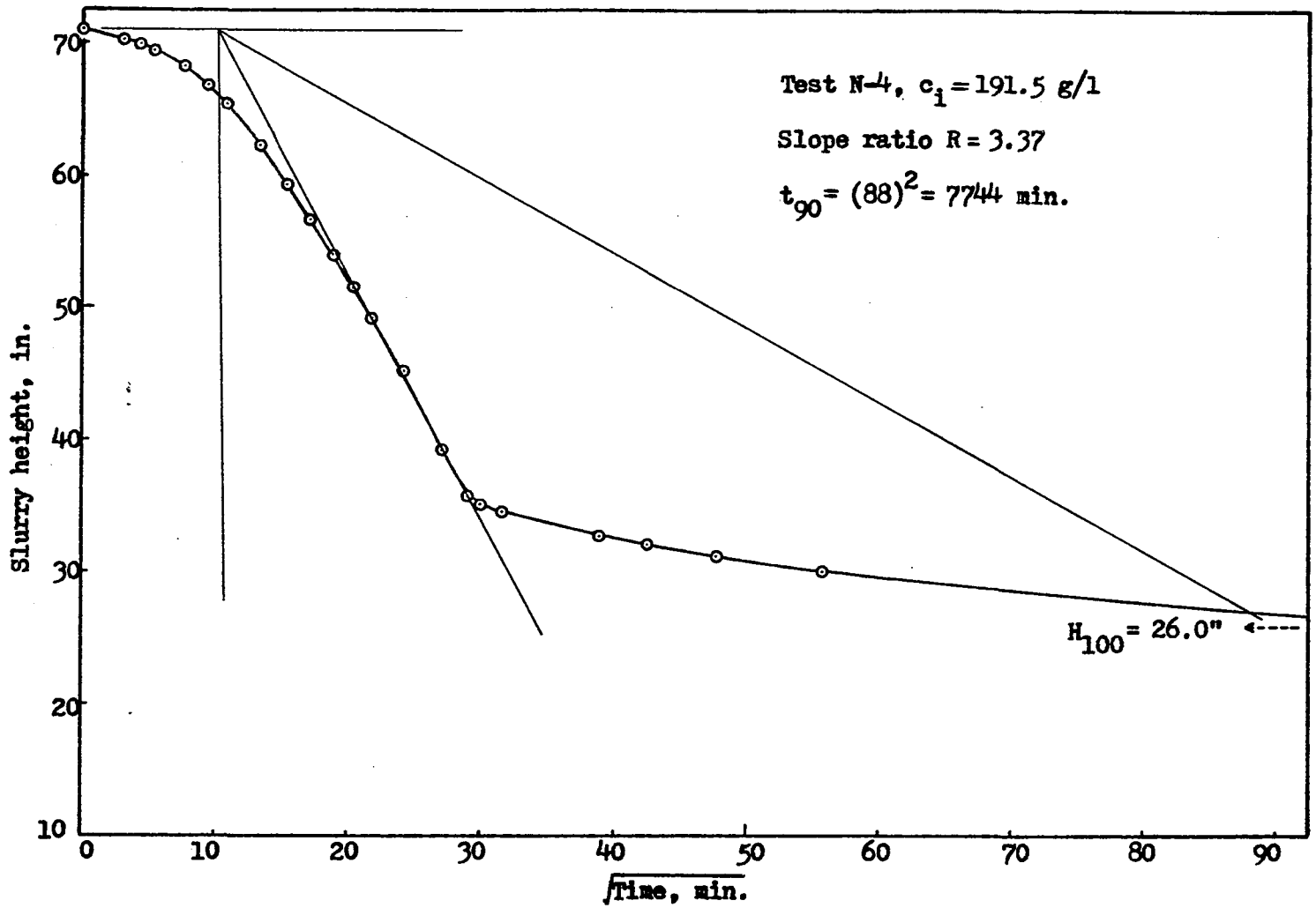

Figure A-4. The H vs. √t plot for test N-4

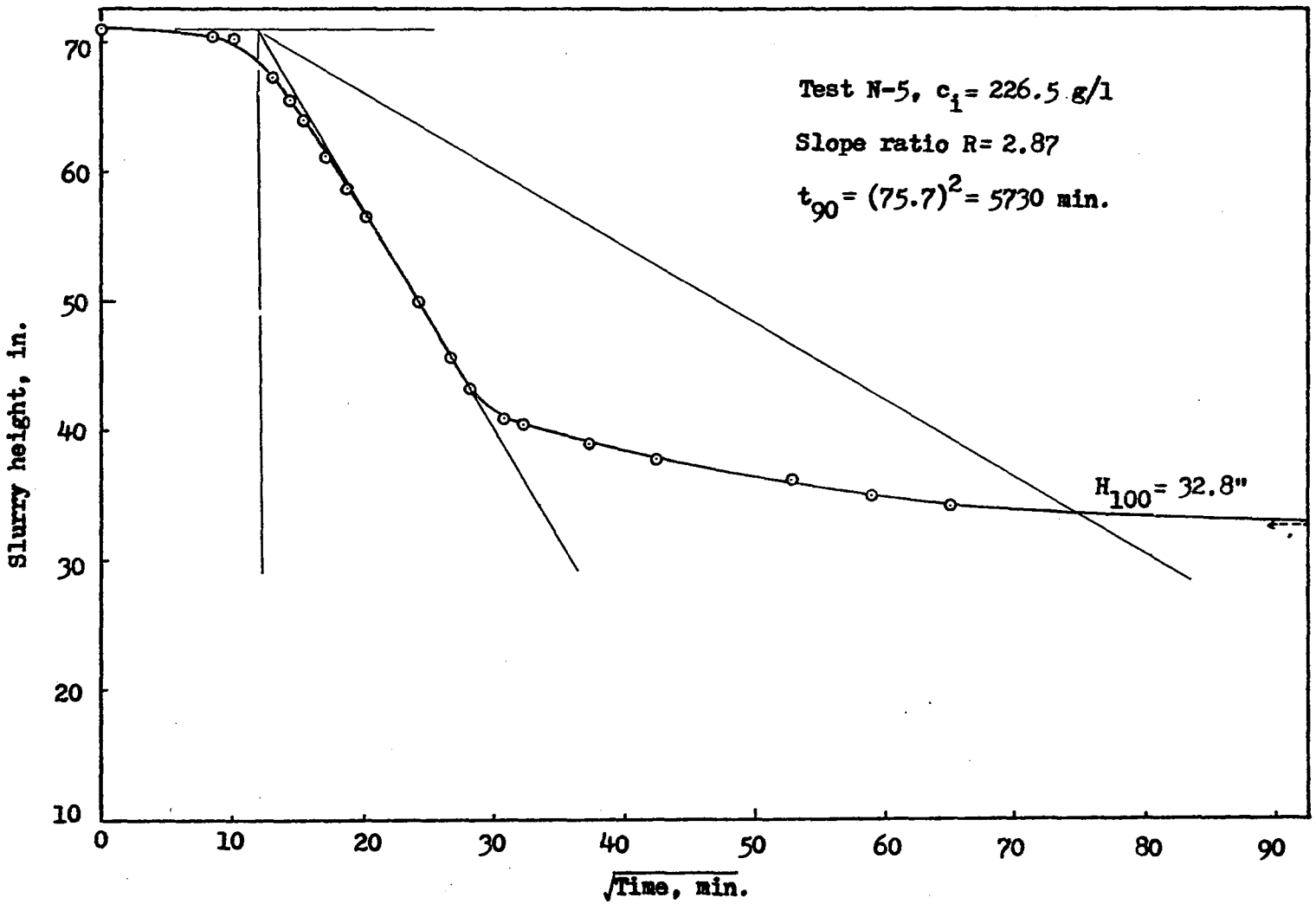

Figure A-5. The H vs. √t plot for test N-5

Results of Flocculent Settling Tests

Slurry samples were regularly withdrawn from the column for concentration determinations in flocculent settling tests. Figures A-6 to A-11 show the concentration profiles at various times for the settling tests with different initial concentrations. The slurry height, H, was also observed regularly in these tests, except for the two tests with very low initial concentration L-1 and L-2, and H is plotted versus $\sqrt{t}$ in Figures A-12 to A-15.

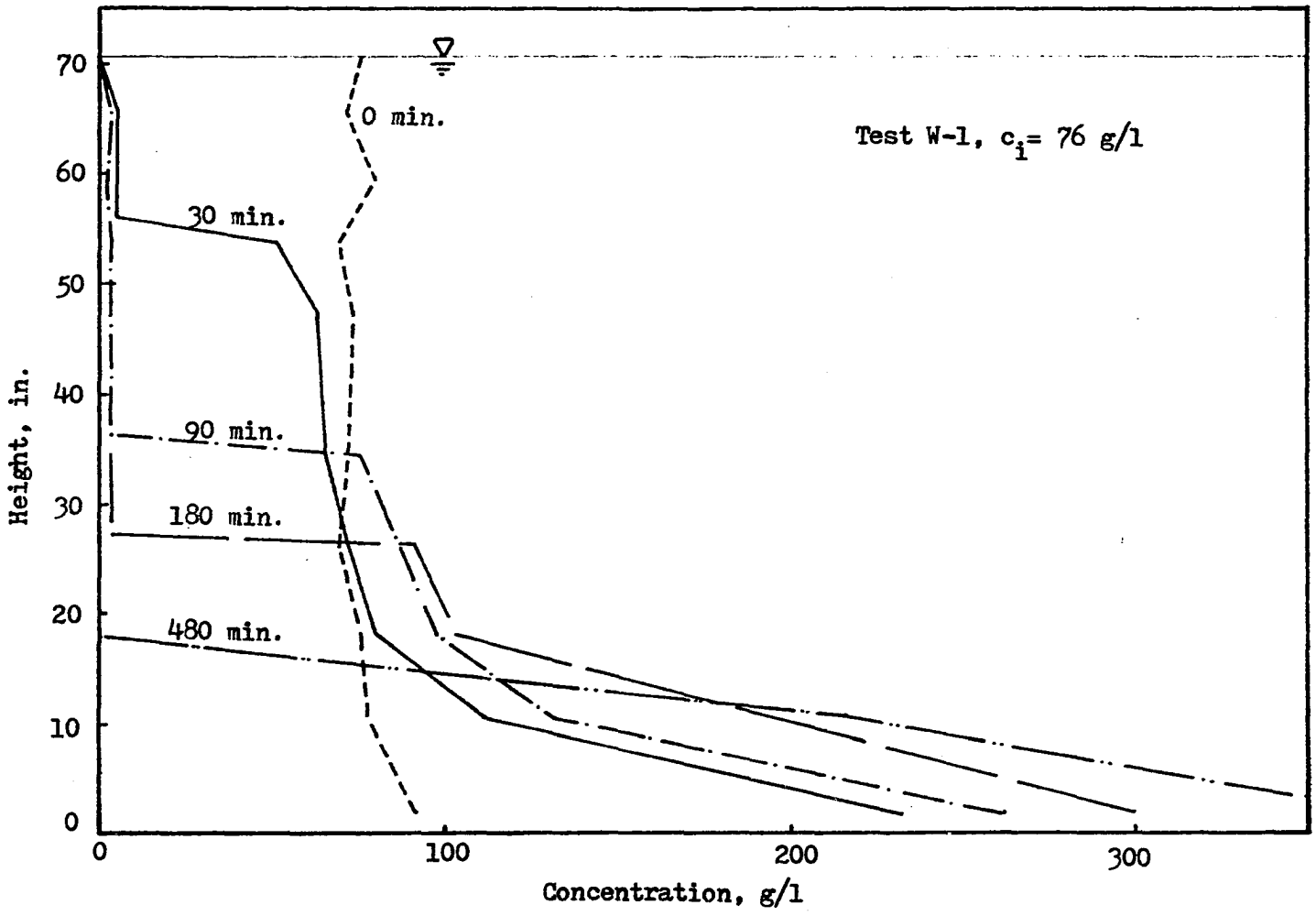

Figure A-6. The concentration profiles resulting from test W-1

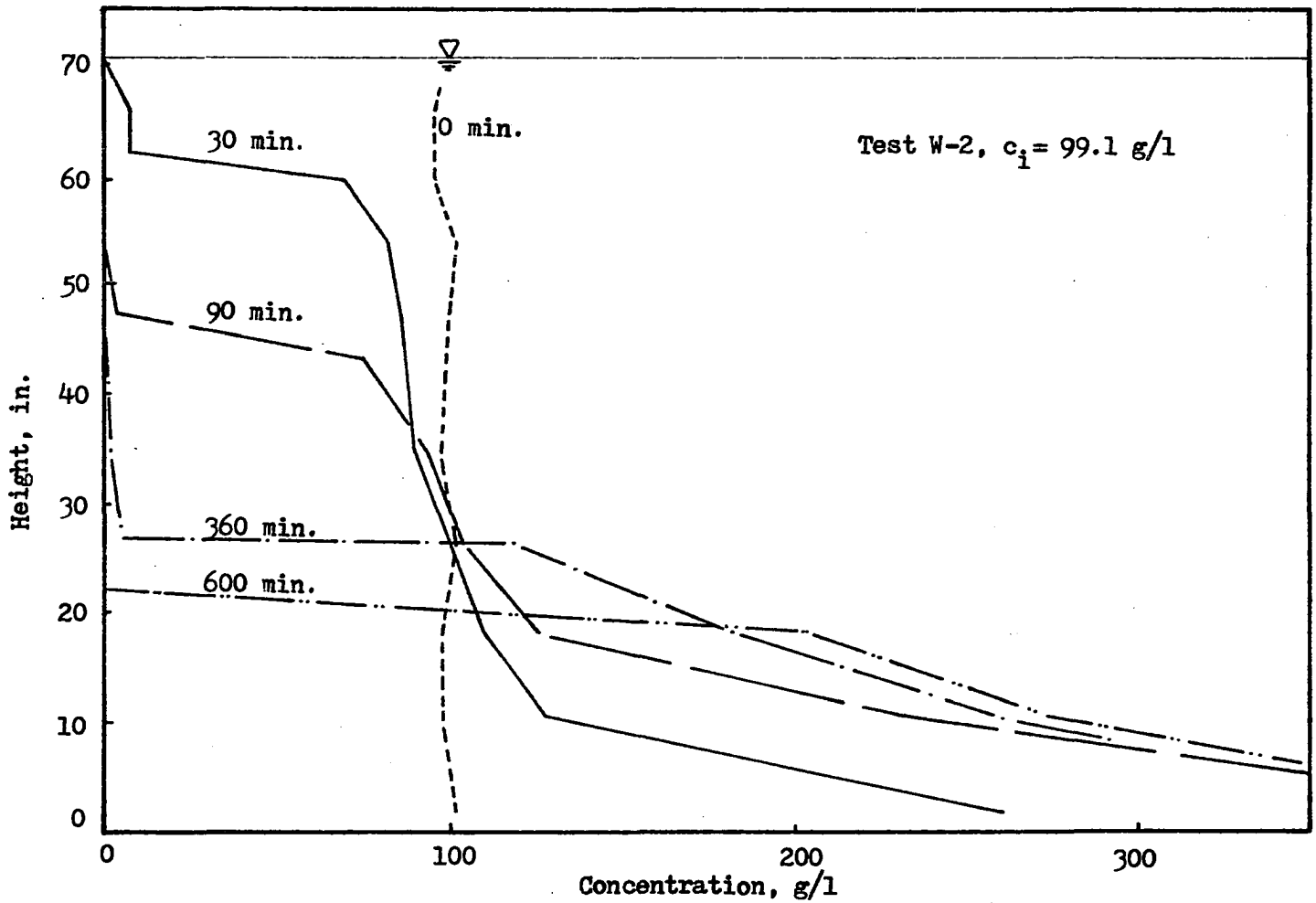

Figure A-7. The concentration profiles resulting from test W-2

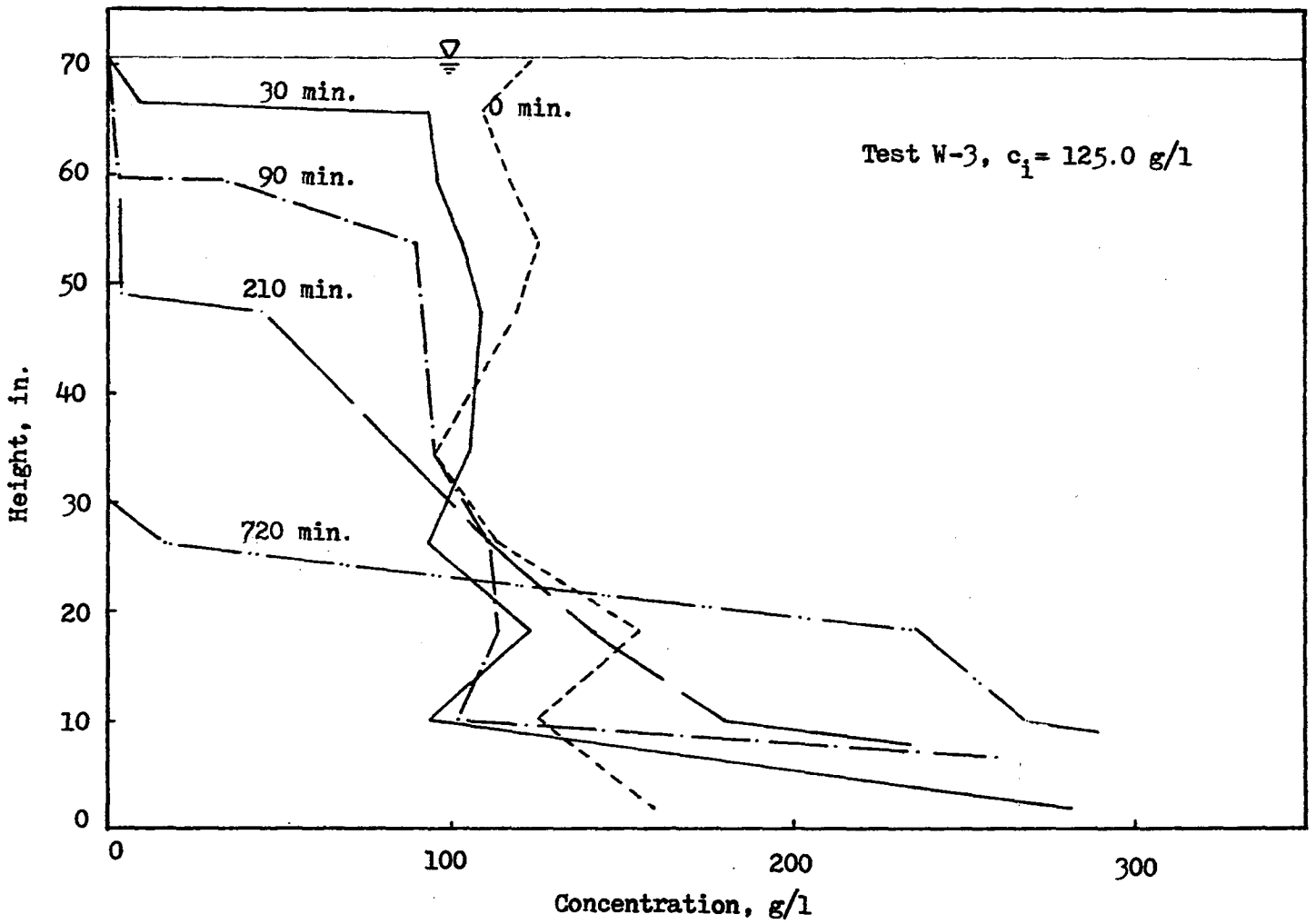

Figure A-8. The concentration profiles resulting from test W-3

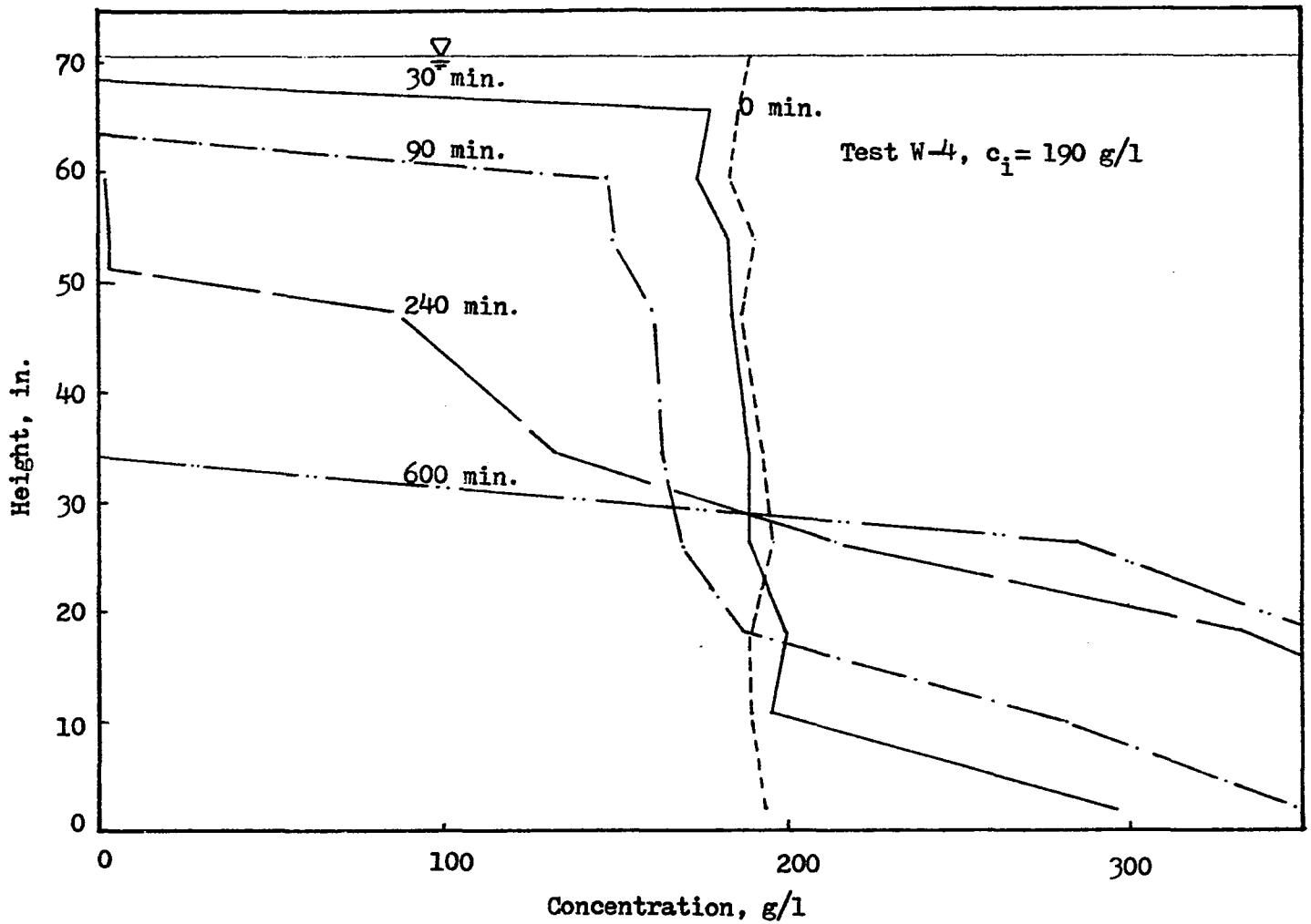

Figure A-9. The concentration profiles resulting from test W-4

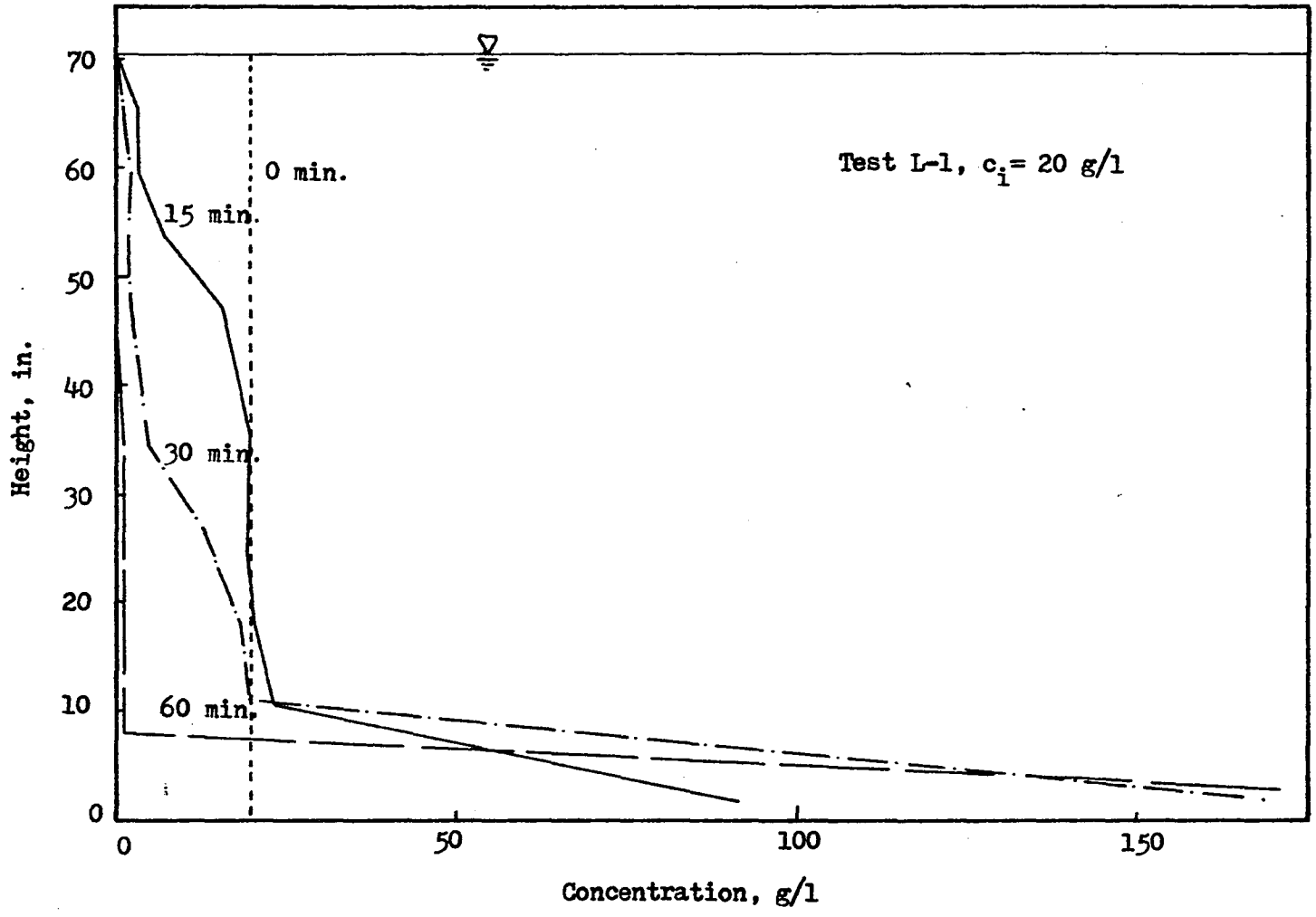

Figure A-10. The concentration profiles resulting from test L-1

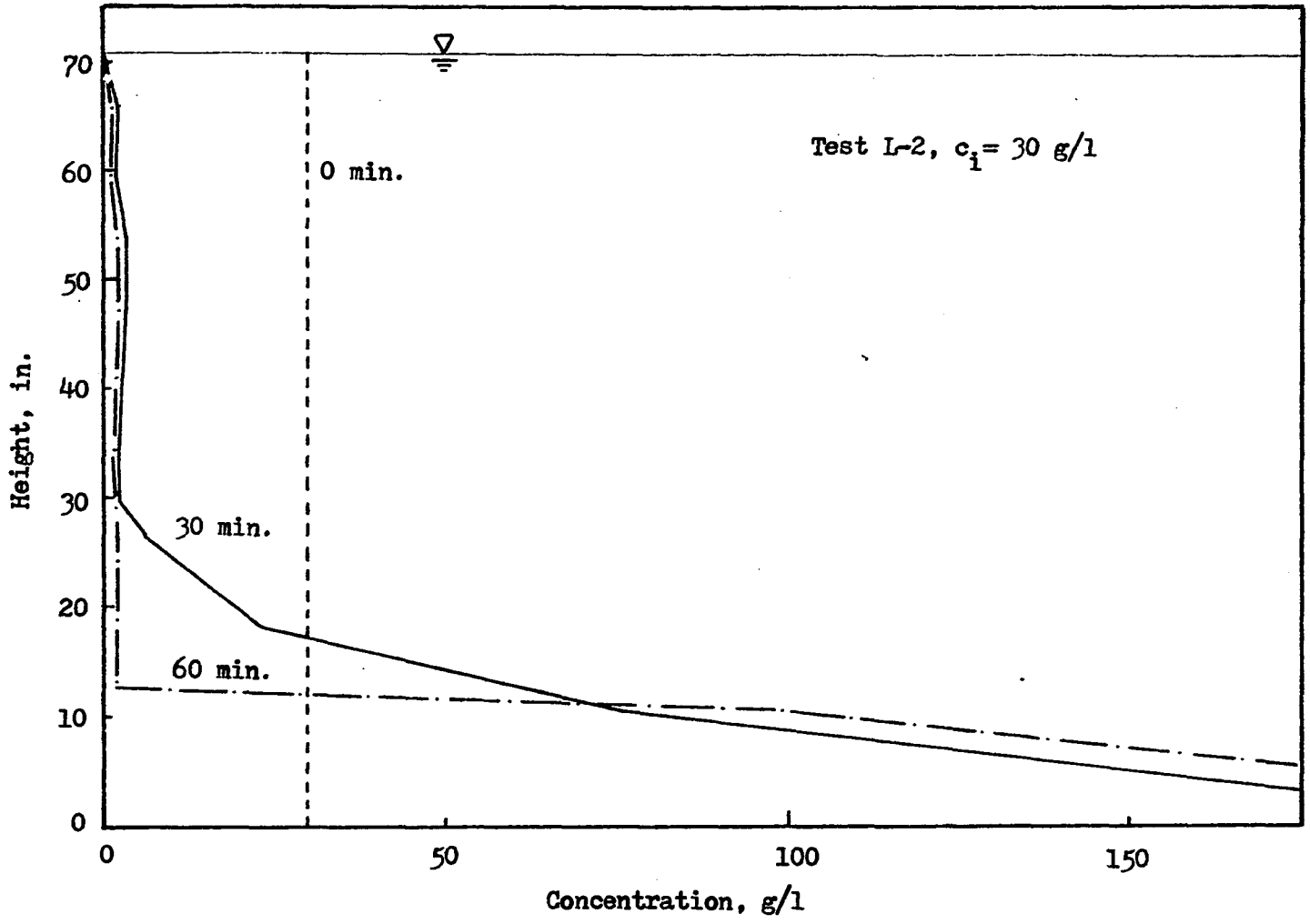

Figure A-11. The concentration profiles resulting from test L-2

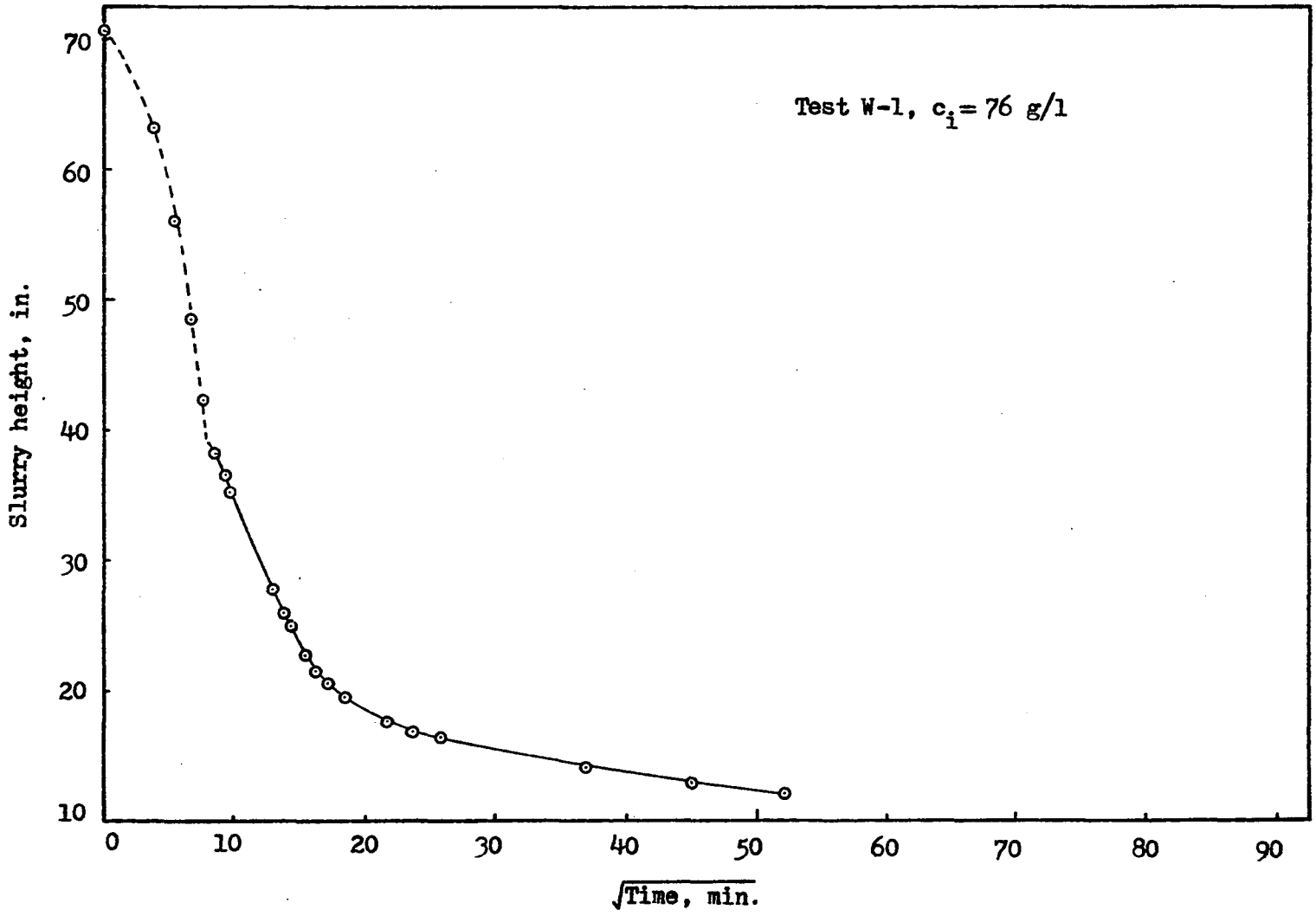

Figure A-12. The H vs. √t plot for test W-1

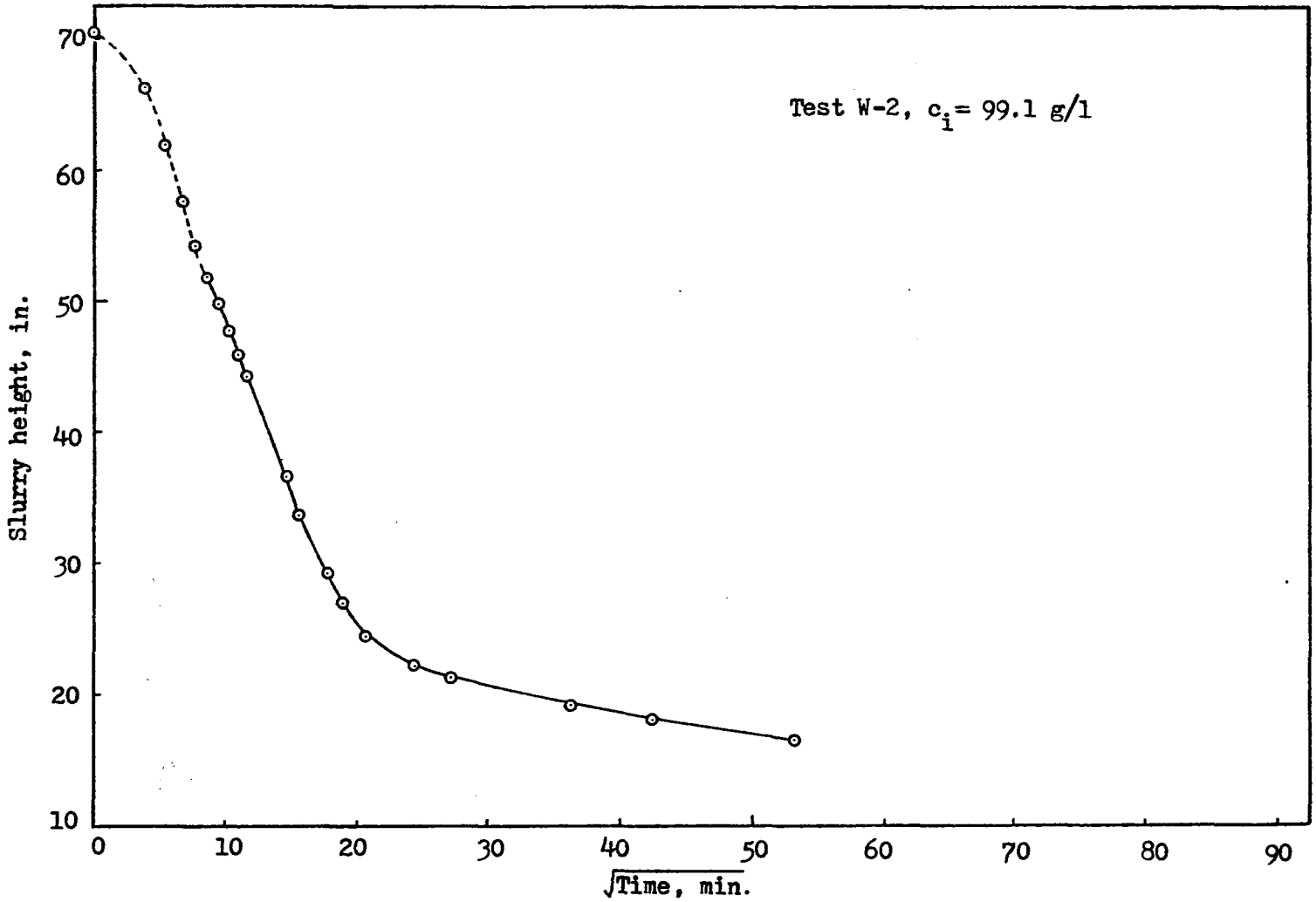

Figure A-13. The H vs. √t plot for test W-2

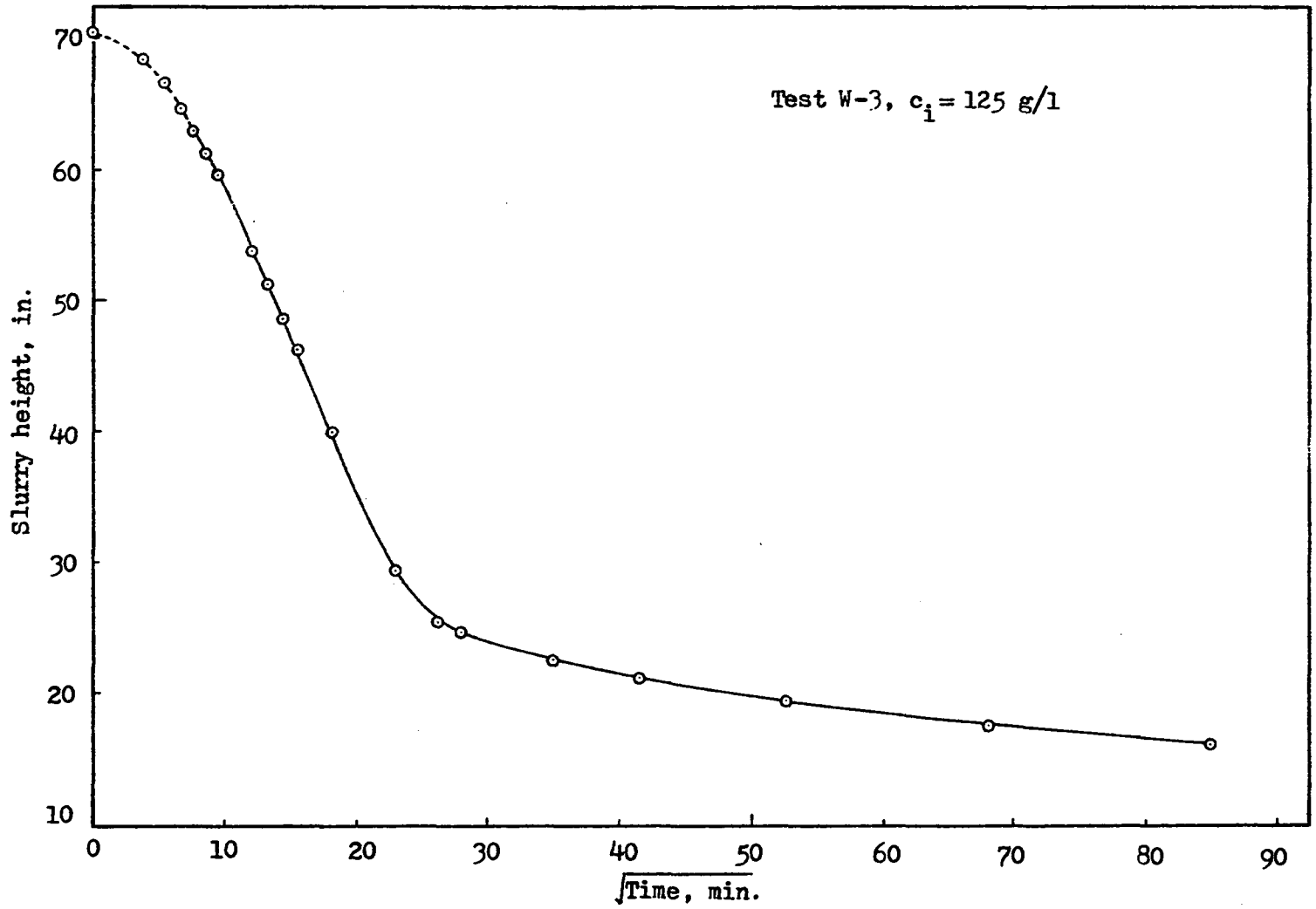

Figure A-14. The H vs. √t plot for test W-3

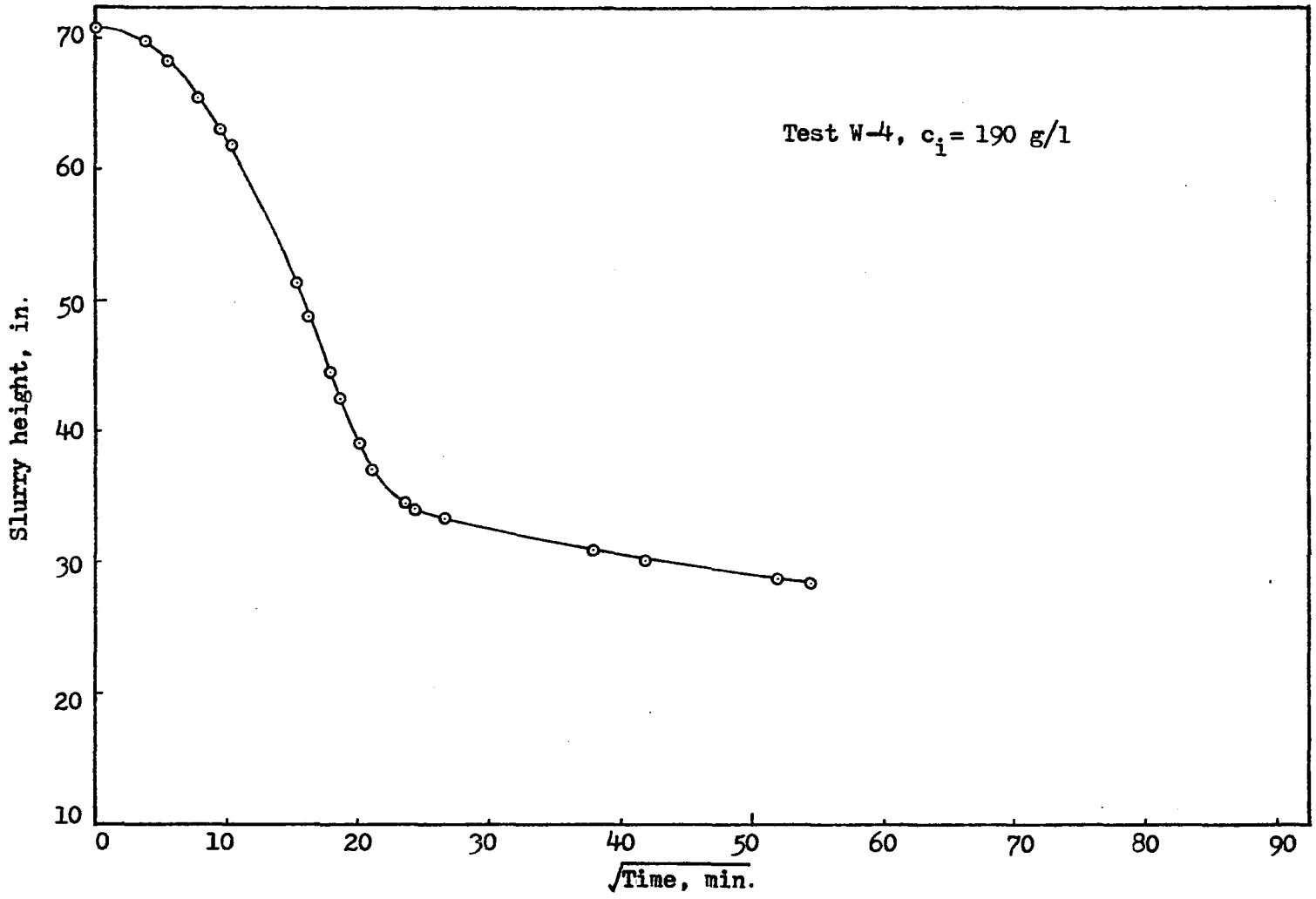

Figure A-15. The H vs. √t plot for test W-4